

Development of Lab-scale Forward Osmosis Membrane Bioreactor (FO-MBR) with Draw Solute Regeneration for Wastewater Treatment

Fozia Parveen

Jesus College

A thesis submitted for the degree of Doctor of Philosophy

Department of Engineering Science, University of Oxford

Michaelmas Term 2018

I dedicate this thesis to, my parents, for it was their dream

that I simply had to live

Acknowledgements

As tough as these five years have been, I only want to look back with gratitude for all the kind people I met in Oxford for their guidance and support.

First of all, **Professor Nick Hankins** and Dr Sher Jamal Khan for introducing me to this opportunity and for guiding me through my research in my DPhil and Masters respectively. My college Advisor, Stephen Morris for listening to me in moments of emotional crisis. Professor Ian, Helen and Wei for sitting through our Wednesday group presentations and providing useful feedback.

The list of people to thank is very long, five years after all. I would really like to thank the dearest of friends I have made in college. My super woman Vivi, and Pedro, Marein, Jess, Karan, Luigi, Vanessa, Angela, and Rachita for not giving up on me. My DPhil sisters, Rabia and 'the' Ping Shen for sharing the bench and stories. My office colleagues Bo (bro), Kim, Farrukh, Elias, Kat, Sihao and Ali for tolerating me through these years. My lab colleagues Shiv, Ana, Lakshmi, Gabi, Li, Yalda, Cordie and Marimar for letting me work in the lab with ever-growing mess and area claimed. Few families in Oxford for nearly adopting and feeding me like Awais bhai and Maria, Tia, and Sayrul bhai and family.

The many amazing people I got to know in Oxford such as Fouzia Farooq, Nabeel, Gustavo, Cheryl, Kokil, Salima, Rahim, Naeema, Zia, Catherine, Rafi, Lali, and so so many more. To Saqib bhai, Saman, Rizwana, Ainee, Mateen, Usman, Daniyal, for writing to me during this time and Ghalib bhai for his presence. My cousins Nahida, Rukhsana, Farzandu, Ashk, Nanu, KD, dadaq and Sania for keeping me in their thoughts. My uncles especially Bhuttu and Bakhtu mamu for all the silly things they do and say and Imtu mamu for keeping in touch. To my beautiful family and

friends from Pakistan for taking pride in me and my journey and for the love and prayers that I didn't deserve. Dearest Peru bhai for being so understanding. My sister in laws, Afshan and Salma for joining the gang. My Jimmy guru for all the moral and financial support, my selfless Tariq Jon, Aliya for being the best elder sister, Chimmu darling the commando with dagger of honour. For the ever growing family and new entrants Majeed and Sinnan, my handsome nephews whose smile let me get through a bad day especially the darkest days during the last two years.

Table of Contents

ACKNOWLEDGEMENTS III

LIST OF TABLES IX

LIST OF FIGURES XI

LIST OF ABBREVIATIONS XV

LIST OF SYMBOLS XIX

CHAPTER 1 1

INTRODUCTION 1

1.1BACKGROUND 1

1.2 RESEARCH OBJECTIVES 2

1.3 SIGNIFICANCE AND NOVELTY 3

1.4 CHAPTER SUMMARY 5

CHAPTER 2 7

LITERATURE REVIEW 7

2.1 FORWARD OSMOSIS SYSTEMS- THEORY AND PRINCIPLES 7

2.1.1. CONCENTRATION POLARIZATION 8

2.1.1.1 Internal Concentration Polarisation 13

2.1.1.2 External Concentration Polarisation 15

2.2 FORWARD OSMOSIS MEMBRANES 19

2.3 FORWARD OSMOSIS DRAW SOLUTIONS 27

2.3.1 Inorganic Solutes 30

2.3.2 Organic Draw Solutions 33

2.4 MEMBRANE DISTILLATION 41

2.4.1 MD Membrane Characteristics 43

2.4.2 Applications of Membrane Distillation 45

2.4.3 Heat and Mass Transfer in MD 47

2.4.4 Temperature Polarization (TP) 49

2.4.5 Fouling in MD 50

2.5 MEMBRANE BIOREACTORS (MBRS) 51

2.5.1 Forward Osmosis Membrane Bioreactor (FO-MBR) 55

2.6 THE FO-MD HYBRID 61

2.7 CONCLUSIONS 66

CHAPTER 3 67

COMPARATIVE PERFORMANCE OF A NANO FILTRATION (NF) MEMBRANE AND A TRADITIONAL FO MEMBRANE FOR USE IN A LAB SCALE FORWARD OSMOSIS MEMBRANE BIOREACTOR (FO-MBR) 67

3.1 INTRODUCTION 67

3.2 METHODOLOGY 68

3.2.1 Establishment of FO-MBR 68

3.2.2 Chemicals and Solutions 71

3.2.3. Toxicity 74

3.2.4. Viscosity 75

3.2.5 Membranes 75

3.3 RESULTS AND DISCUSSION 76

3.3.1 Osmotic Pressure as a Function of Concentration 76

3.3.2 Forward Osmosis Membrane versus Nanofiltration Membrane 82

3.3.3 Reverse Solute Transport *92*

3.3.4 Viscosity *95*

3.3.5 Toxicity *96*

3.4. CONCLUSIONS 98

CHAPTER 4 101

INTEGRATION OF FORWARD OSMOSIS AND MEMBRANE DISTILLATION UNITS FOR REGENERATION OF NOVEL DRAW SOLUTIONS AND WATER RECLAMATION 101

4.1 INTRODUCTION 101

4.2 METHODOLOGY 102

4.2.1 Chemicals and Membranes *102*

4.2.2 Benchscale Setup *103*

4.2.3 FO-MD Hybrid Experiments *104*

4.3 RESULTS AND DISCUSSION 105

4.3.1 Effect of Temperature on MD Flux *105*

4.3.2 Effect of Feed Flow on MD Flux *110*

4.3.3. Effect of Feed Type on MD Flux *112*

4.3.4 Performance of FO-MD Hybrids with Various Draw Solutions *115*

4.4 CONCLUSIONS 123

CHAPTER 5 127

OPTIMISING THE MEMBRANE CLEANING REGIME FOR THE FOMBR-MD LAB SCALE SYSTEM 127

5.1 INTRODUCTION 127

5.2 METHODOLOGY 129

5.2.1 Basic Cleaning of the Membranes 131

5.2.2 Acidic Cleaning of the Membranes 131

5.3 RESULTS AND DISCUSSION 132

5.3.1 FO-MBR Hybrid 132

5.3.2. Membrane cleaning-NaCl Draw Solution 135

5.3.3. Membrane cleaning-TEAB Draw Solution 138

5.3.4. Membrane Cleaning-PDAC Draw Solution 142

5.4 CONCLUSIONS 146

CHAPTER 6 148

CONCLUSIONS AND RECOMMENDATIONS FOR FUTURE WORK 148

6.1 SUMMARY OF WORK DONE 148

6.2 CONCLUSIONS 149

6.3 RECOMMENDATIONS FOR FUTURE WORK 152

APPENDIX I 156

FOMBR-MD Hybrid Scale up 156

APPENDIX II 165

FOMBR- MD bench-scale setup: installation cost 165

Appendix III 167

List of Journal Articles and Conference Presentations by the Author 167

KEYNOTE LECTURES 168

REFERENCES 170

List of Tables

Table 2.1 Summary of Operating conditions, performance, structural parameter, water and solute permeability for FO membranes 21

Table 2.2 Novel draw solutions studied by various research groups 28

Table 2.3 MNPs application for FO 37

Table 2.4 A summary of the removal efficiencies of FO-MBRs for organics, nitrogen and phosphorus. (Wang et al., 2016) 58

Table 2.5 Summary of forward osmosis membrane bioreactors (FO-MBRs) in literature (Wang et al., 2016) 59

Table 2.6. Summary of hybrid FO–MD processes with different draw solutes (Wang et al., 2015) 64

Table 3.1 Chemical composition of synthetic wastewater used in FO-MBR studies (Khan et al., 2013) 71

Table 3.2 Summary of the draw solutions used in the current study; * denotes Mol Wt of each monomeric unit, ** denotes average molecular weight of the polyelectrolyte solution 72

Table 3.3 Chemical composition of 2X M9 media for bacterial growth in microbroth dilution test with a final pH of 7.0 (Harwood & Cutting, 1990) 74

Table 3.4 Osmotic pressure for draw solutes determined using measured osmolality values. 80

Table 3.5 Flux with HTI CTA membrane at 1h and 8h time intervals with percentage decline in flux using DI water and FO-MBR as feed DI water (AL-DS mode) and FO-MBR as feed (AL-FS mode) at a CFV of 0.12m/s. 88

Table 3.6 Flux with NF membrane at 1h and 8h time interval with percentage decline in flux using DI water (AL-DS mode) and FO-MBR as feed (AL-FS mode) at a CFV of 0.12m/s. 90

Table 3.7 Reverse solute transport (GMH) for draw solutes used in the study after 24 hours of FO operation when run in the absence of a draw re-concentration system (AL-DS mode, CFV: 0.12m/s). 93

Table 3.8 Viscosities of draw solution at operational concentrations 96

Table 5.1 Summary of best cleaning procedures based on SEM imaging of membranes after cleaning. 145

Table 5.2 FO and MD flux for TEAB in the FOMBR-MD hybrid 145

Table 6.1 Draw solution RST loss in FOMBR-MD hybrid (see also Appendix I) 154

List of Figures

Figure 1.1 Thesis Summary and key decision.....4

Figure 2.1 Concentration polarisation in FO (Zhao et al., 2012). C_{feed}, C_{draw}, $\Delta\pi_{eff}$ and J_w represent the feed solution concentration, draw solution concentration, effective osmotic driving force and water flux, respectively. ICP represents the change in draw concentration across the support layer; ECP is that between the active layer surface and the bulk draw solution.....9

Figure 2.2 Dilutive (a) and concentrative (b) ICP across asymmetric membrane (Zhao et al., 2012). In both cases, ICP is the change in draw concentration across the support layer.....10

Figure 2.3 Relationship between FO, RO, and PRO (adapted from Lee et al., 1981) 12

Figure 2.4 Double-skinned forward osmosis membrane to reduce ICP and fouling in FO.....24

Figure 2.5 Graphene layer (left) on its own and rolled graphene as a nanotube (right).....27

Figure 2.6 Carboxyethyl amine sodium salts; (DDTP-Na) (n=1); (TTHP-Na) (n=2); (TPHP-Na) (n=3). 35

Figure 2.7 Hydrogel mechanical squeezing (Yu et al., 2016).....36

Figure 2.8 Hexa(4-ethylcarboxylatophenoxy)phosphazene salt structure (Stone et al., 2013) 40

Figure 2.9 Membrane distillation configurations: DCMD; AGMD; VMD; SGMD...43

Figure 2.10 Heat and mass transfer across a DCMD membrane (Adapted from Histove et al., 2015) 49

Figure 2.11 Temperature distribution in an MD process with a fouled layer 51

Figure 2.12 Development of the large-scale MBR plants around the world (the capacity of each plant > 100,000 m^3/d) (Meng et al., 2017).....54

Figure 2.13 A simple graphical demonstration of a submerged FO-MBR (with a continuous draw and feed solution loop).....55

Figure 2.14 Schematic diagram of FO-MD hybrid for desalination (Wang et al., 2015) 63

Figure 3.1 Schematic diagram for the external membrane cell: (a) Section of top and bottom plate; (b) Plan view of a single plate.....69

Figure 3.2 Forward osmosis (FO) bench scale setup showing a feed solution and draw solution loop, the tank for the latter being placed on a weighing balance 70

Figure 3.3 Molecular structure for polyelectrolytes used in the current study (a) PDAC ($C_8H_{16}Cl\ N)_{n\ ,}$ (b) PGBE ($CH_3(CH_2)_3(OCH_2CH_2)_nOH$).....73

Figure 3.4 SEM images of a flat sheet FO membrane (a) SL (b) AL (Blandin et al., 2014). 75

Figure 3.5 Plan view SEM image of NF membrane used in the study 76

Figure 3.6 Initial fluxes for polyelectrolytes PDAC and PGBE with NF and CTA membranes using both DI water as feed (AL-DS) and a live monoculture FO-MBR feed (denoted 'Bio', AL-FS mode) at 0.5M concentration (CFV: 0.12m/s).....83

Figure 3.7 Initial fluxes using SDS and TEAB as draw solutes against both DI water (AL-DS) as feed and a live monoculture FO-MBR feed (denoted 'Bio', AL-FS mode) for CTA and NF membranes at 0.05M surfactant concentration (CFV: 0.12m/s). 85

Figure 3.8 initial fluxes for NaCl and Na_3PO_4 as draw solutes using the CTA membrane and both DI water (AL-DS) as feed and a live monoculture FO-MBR feed (denoted 'Bio', AL-FS mode) at 0.5M concentration (CFV: 0.12m/s). 87

Figure 3.9 Optical density of bacterial solution using microbroth dilution test in minimal media with draw solutes 98

Figure 4.1 Membrane distillation setup established in the lab 102

Figure 4.2 Bench scale FO-MD hybrid established in the lab 103

Figure 4.3 MD water flux at different temperatures with CFV of 0.12 m/s at feed temperatures of 35, 45 and 55ºC and draw temperature of 20ºC respectively (AL-FS mode). 107

Figure 4.4 Heat and mass transfer profiles during membrane distillation 107

Figure 4.5 Effect of Feed cross flow velocity on flux performance with the feed temperature at 35°C using PDAC as MD feed (AL-FS mode) 111

Figure 4.6 MD and FO flux over three days with NaCl as a draw solution and DI water as a feed at a CFV of 0.12m/s (FO: AL-DS, MD: AL-FS) 117

Figure 4.7 MD and FO flux over three days with TEAB as a draw solution and DI water as a feed at a CFV of 0.12m/s (FO: AL-DS, MD: AL-FS) 120

Figure 4.8 MD and FO flux over three days with PDAC as a draw solution and DI water as a feed at a CFV of 0.12m/s (FO: AL-DS, MD: AL-FS). 121

Figure 4.9 RST in FO feed (DI water) and MD permeate (DI water) in a continuous setup at a CFV of 0.12m/s (FO: AL-DS, MD: AL-FS) 123

Figure 5.1 SEM images for a nascent forward osmosis cellulose triacetate membrane (a) Active layer (b) Support layer, and a PTFE MD membrane (c) Support layer (d) Active layer 130

Figure 5.2 MD and FO flux over three days with NaCl, TEAB and PDAC as the FO draw solution and synthetic wastewater with bacterial inoculum as the FO feed in an FOMBR-MD hybrid at a CFV of 0.12m/s (FO: AL-FS, MD: AL-FS)..... 134

Figure 5.3 SEM image when NaCl was used as a draw solute after basic cleaning at two different magnifications (a) SL-DS, FO (b) AL-FS, FO (c) AL-FS, MD 136

..... 138

Figure 5.6 SEM image when TEAB was used as a draw solute after basic cleaning (a) AL-FS MD (b) AL-FS FO (c) SL-DS FO 141

Figure 5.7 SEM image when PDAC was used as a draw solute after basic cleaning (a) AL-FS MD (b) AL-FS FO (c) SL-DS FO 143

Figure 5.8 SEM image when PDAC was used as a draw solute after acidic cleaning (a) AL-FS MD (b) SL-DS FO (c) AL-FS FO 144

List of Abbreviations

A	Water permeability coefficient
AFM	Atomic force microscopy
AGMD	Air Gap Membrane Distillation
AITC	Allyl isothyocyanate
AL	Active layer
AL-DS	Active later facing draw solute
AL-FS	Active layer facing feed solute
B	Solute permeability coefficient
CECP	Cake enhanced concentration polarization
CFV	Crossflow velocity
CMC	Critical micelle concentration
CNF	Carbon nanofiber
CNT	Carbon nanotube
CP	Concentration polarization
CTA	Cellulose triacetate
CTB	Cooling tower blowdown water
DAP	di-ammonium phosphate
DCMD	Direct Contact Membrane Distillation

DS	Draw solute
ECP	External Concentration polarization
ED	Electrodialysis
EDTA	Ethylenediaminetetraacetic acid
EDTP-Na	Ethylenimine pentapropionic acid sodium
FO	Forward osmosis
FO-MBR	Forward Osmosis membrane bioreactor
FS	Feed Solution
GO	Graphene oxide
HRT	Hydraulic retention time
HTI	Hydration technology inc.
ICP	Internal concentration polarization
J_s	Solute flux (GMH)
LBL	Layer by layer
MBR	Membrane bioreactor
MD	Membrane distillation
MF	Microfiltration
MFC	Magnetic field control
Na-CQDs	Na^+-functionalized carbon quantum dots
NF	Nanofiltration

PAA-Na	Polyacrylic acid-sodium salt
PAI	Polyamide-imide
PAM	Polyacrylamide
PBI	Polybenzimidazole
PDAC	Polydiallyldimethylammonium chloride
PEGDA	Polyethylene glycol diacrylate
PEI	Polyethyleneimine
PES	Polyethersulfone
PGBE	Poly (ethylene glycol) butyl ether
PP	Polypropylene
PRO	Pressure retarded osmosis
PSA	Poly (sodium acrylate)
PSA-NIPAM	Poly (sodium acrylate)-poly(*N*-isopropylacrylamide)
PTFE	Polytetrafluoroethylene
PVDF	Polyvinylidene fluoride
RO	Reverse osmosis
RST	Reverse solute transport
SDS	Sodium dodecyl sulphate
SEM	Scanning electron microscopy
SGMD	Sweeping Gas Membrane Distillation

SL	Support layer
SND	Simultaneous nitrification and denitrification
SRT	Sludge retention time
SSM	Stainless steel mesh
TDS	Total dissolved solid
TEAB	Tetraethyl ammonium bromide
TMC	Trimesoyl chloride
TMP	Transmembrane pressure
TOC	Total organic carbon
UF	Ultrafiltration
VMD	Vacuum Membrane Distillation

List of Symbols

A	Membrane area (m^2)
C	Concentration (M)
C_{bf}	Feed concentration in the bulk (M)
C_{mf}	Feed concentration at the membrane surface (M)
D	Diffusion coefficient
d_h	Hydraulic diameter
F	Force (N)
J_s	Reverse solute transport (GMH)
J_w	Water flux (LMH)
k	Mass transfer coefficient
K	Solute resistivity
k_D	Mass transfer coefficient at the draw side
k_F	Mass transfer coefficient at the feed side
L	Length (m)
n	number of solute molecules
P	Pressure (atm)
P_f	Hydraulic pressure on the feed side (atm)
P_p	Hydraulic pressure on the permeate side (atm)

Q	Heat flux (subscripts f,m,p for feed, permeate and membrane respectively)
R	Ideal gas constant (m^3atm/K mol)
Re	Reynolds number
S	Membrane structure (m)
Sh	Sherwood number
T	Temperature (K; ºC)
T_{bb}	Temperature in the permeate bulk (K; ºC)
T_{bf}	Temperature in the feed (K; ºC)
T_{mb}	Temperatures at the cold membrane surfaces (K; ºC)
T_{mf}	Temperature at the hot membrane surfaces (K; ºC)
V	Velocity (m/s)
V	Volume (m^3)
x	Thickness of support layer
X	Mole fraction
η	Coefficient of viscosity (N/m^2)
Φ	Osmotic coefficient
i	Dimensionless Vant Hoff's factor
π	Osmotic pressure (atm; Pa)
τ	Tortuosity

τ	Temperature Polarization
τ	Thermal boundary layer
φ	Porosity of the membrane
δ	Boundary layer thickness (FO), Membrane thickness (MD)
α_w	Coefficient of water
π_{Db}	Osmotic pressure of bulk draw solution
π_{Dm}	Osmotic pressure at the membrane surface, draw side
π_{Fb}	Osmotic pressure of bulk draw solution
π_{Fm}	Osmotic pressure at the membrane surface, feed side
ρ_m	Density of the membrane (kg/m^3)
ρ_{pol}	Density of the polymer
$\Delta\pi$	Osmotic pressure gradient

Development of Lab-scale Forward Osmosis Membrane Bioreactor (FO-MBR) with Draw Solute Regeneration for Wastewater Treatment

Fozia Parveen, Jesus College, Michaelmas Term 2018

Abstract

The overall aim of the current work was to perform a practical, lab-scale study to examine the component parts and integrated operation of a continuous and feasible FOMBR-MD hybrid system, for the treatment and recycle of wastewater. This was achieved by comparison of the performance of a commercial Cellulose triacetate (CTA) FO membrane with that of a single layer nanofiltration (NF) membrane when used with novel and conventional draw solutions.

Higher flux and a higher decline in flux were observed for simple inorganic draw solutions compared to higher molecular weight draw solutions e.g. for CTA FO membrane in an MBR configuration, the flux (5.3 LMH) and the percentage decline in flux (43%) were highest for NaCl and lower for SDS (2.3LMH and 14.2% respectively) in MBR configuration (AL-FS).

The fluxes as well as RSTs were higher for the NF membrane in comparison to the CTA FO membrane. In the absence of a reconcentration system in place after 24 hours of operation, the highest RST was observed for NaCl (9.33 GMH) and the lowest for higher molecular weight draw solutes (Poly ethylene glycol butyl ether (PGBE): 1.2 GMH) for the CTA FO membrane. Similar results were observed in the NF membrane.

In the toxicity test, *B.subtilis* was still able to grow at the highest draw solution concentration (0.5M). The highest percentage growth was observed for Na_3PO_4 (53% compared to that of the control) and the lowest growth was observed for SDS (16%), proving their non-toxicity even at such a higher concentration.

For MD optimisation, a temperature difference of 15ºC was chosen with a low feed temperature of 35ºC and a permeate temperature of 20ºC. An increase in cross flow velocity (CFV) decreased the temperature and concentration polarization and increased the flux for MD. An optimum CFV of 0.17 m/s was selected. The MD feed concentration also affected the flux when all other conditions were similar; slightly lower fluxes for feed (which was the diluted draw solutions) with higher molecular weight solutes (Polydiallyldimethylammonium chloride (PDAC): 1.8 LMH) were observed than with lower molecular weight solutes (NaCl: 2.1 LMH). When MD was combined in a hybrid system with FO, steadier fluxes were observed for the FO compared to FO run on its own, and the RST was lower. Due to a higher FO flux, a more balanced system was achieved for NaCl compared to that of TEAB (Tetraethylammonium bromide) and PDAC. The FO-MD hybrid enabled pure water production and a non-volatile component rejection of nearly 99%.

Cleaning tests were performed on the membranes which were employed throughout this study, using both acidic (2% HNO_3 with 2% H_3PO_4) and basic (0.5 mM EDTA with 0.5g/L NaOH) cleaning solutions. Observation of SEM images of the membrane surfaces revealed that the low molecular weight (NaCl) and high molecular weight (PAC) draw solutes exhibited a lower residual fouling after cleaning than the medium molecular weight (TEAB) draw solute. The level of residual fouling also seemed consistent with earlier observations of flux decline. Apart from the case of the NaCl draw solute, acidic cleaning was generally more

effective than basic cleaning for both sides of the FO membrane. The two cleaning methods were equally effective for the MD membrane active layer

Chapter 1

Introduction

1.1Background

Globally, water demand is predicted to increase significantly over the coming decades. Two thirds of the world's population currently live in areas that experience water scarcity for at least one month a year. About 500 million people live in areas where water consumption exceeds the locally renewable water resources by a factor of two (WWAP, 2017). Alongside efficient use of water resources, two strategies to combat water scarcity are; (1) Water reuse and recycling through wastewater treatment; (2) Desalination of seawater and brackish water. Membrane technology plays a vital role in both of these processes (Wachinski, 2013). Thus, water scarcity is a major driver for the treatment of domestic and municipal secondary effluent water for reuse and recycling. Methods of wastewater treatment were initially developed in response to public health issues and the adverse conditions caused by the discharge of wastewater to the environment (Tchobanoglous et al., 2014).

In this thesis, a niche membrane technology applicable to water and wastewater treatment known as forward osmosis (FO) has been used. FO has been combined with membrane distillation (MD) to create an integrated, hybrid treatment process at laboratory scale which yields clean water. This hybrid process will be evaluated in detail in the chapters to follow.

1.2 Research Objectives

The work reported in this thesis represents one of the first engineering-oriented studies to examine the component parts and integrated operation of a continuous FOMBR-MD system for the treatment and recycle of wastewater. The specific objectives of the study are:

- To investigate the feasibility of a range of novel draw solutions for use in FO, when applied to waste water treatment and recycle.
- To thus develop a continuous FO-MBR hybrid for the treatment of wastewater, and achieve fouling control such that continuous operation is feasible, and thence:
- To investigate the possibility of achieving a stable and acceptable MD flux for the recycle of wastewater, using the FOMBR-MD Hybrid;

All of these objectives are to be achieved using a system developed at the laboratory-scale. At the end of the thesis, the future work which must be addressed to allow running of a full-scale, engineered system will be discussed.

Based on the objectives stated, two key research questions were established;

1. Would using a higher pore-size Nano-filtration (NF) membrane in combination with high molecular weight novel draw solutions for forward osmosis improve the overall performance of FO-MBR systems by improving flux without excessive reverse solute transport?
2. Can FO-MBR systems with novel high molecular weight draw solutions be used in combination with MD for continuous draw regeneration and water reclamation?

1.3 Significance and Novelty

The present study has attempted to explore a range of novel draw solutions in both the FO-MBR, and in an FOMBR-MD hybrid. Most of the studies in the literature are focused on simple inorganic draw solutions such as NaCl and $MgCl_2$ (Table 2.1, Table 2.5). The present study also includes micellar draw solutions that have been previously explored by our research group in simple FO systems but have not been integrated into a full and continuous FOMBR-MD process. Their application was further built upon here by evaluating their use in the FO-MBR, particularly in relation to their potential toxicity, and the FO-MD hybrid systems for practical, continuous application in which the FO and MD fluxes can be maintained and balanced. Similarly, polyelectrolytes have been tested in continuous, hybrid systems. These polyelectrolytes have not previously been studied in either FO, FO-MBR or FOMBR-MD hybrid systems. To complete the picture alongside flux performance, reverse solute transport (RST), toxicity and membrane cleaning performances were studied. Indeed, unlike all the studies that are specifically focused on either the membrane, the type of draw solution or water reclamation from the draw solution, the present work conducts a complete study by considering all these aspects in an integrated fashion, and thus examines the feasibility of long term, continuous application of the system.

The topics of each chapter and their interrelationship have been summarised in Figure 1.1 and section 1.4 of this chapter, and these topics are then explored in greater detail in the individual chapters which follow.

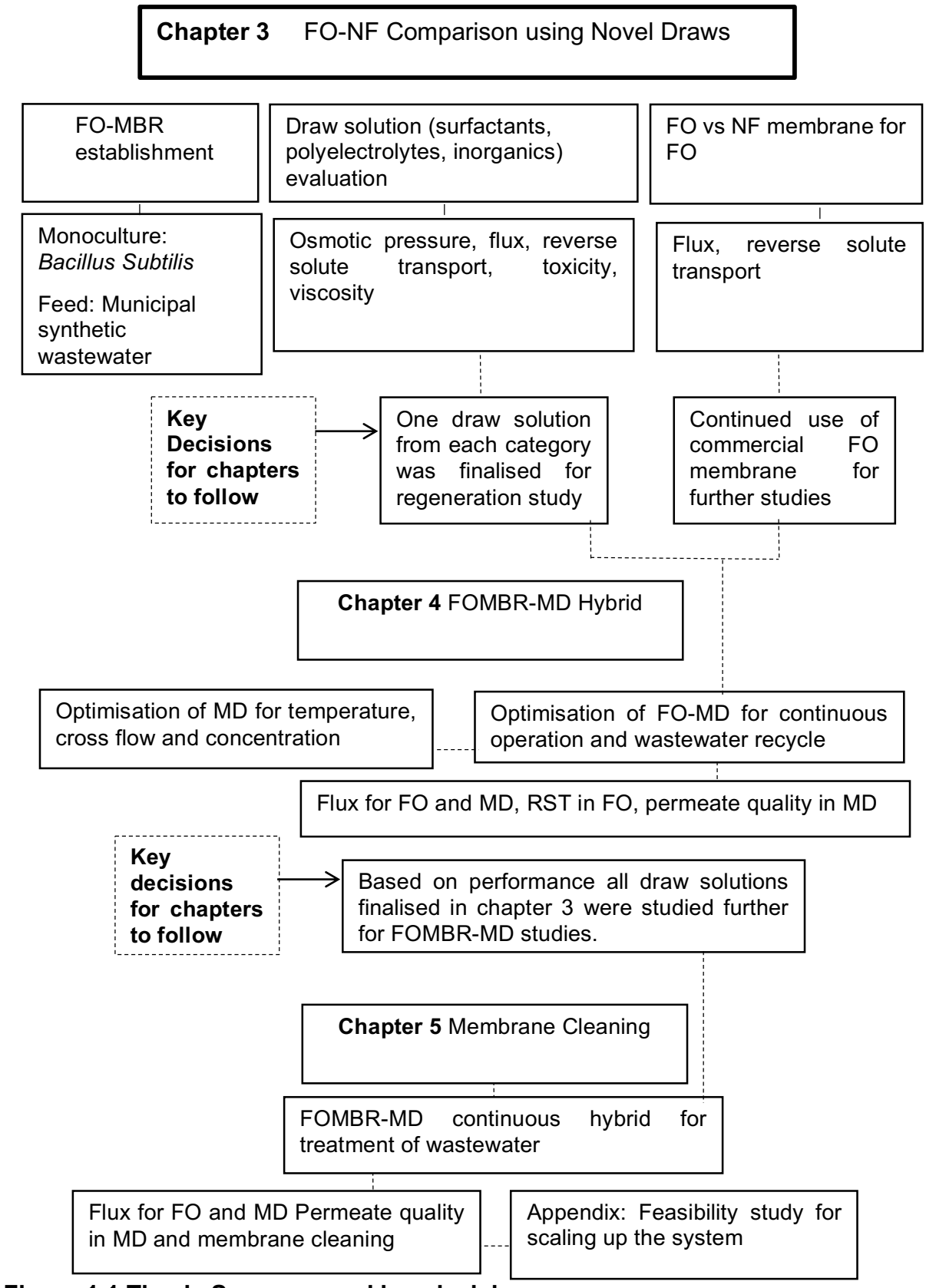


Figure 1.1 Thesis Summary and key decision

1.4 Chapter Summary

In the following, a summary of the scope of the work attempted in each chapter is given,

Chapter 3: Comparative performance of an NF membrane and a traditional FO membrane for use in a Lab Scale FO-MBR

This chapter aims to investigate the application of various novel draw solutions in conjunction with different membrane types for municipal wastewater treatment by FO. A lab-scale FO process was established to conduct the experiments. Nanofiltration (NF) and commercial HTI Forward Osmosis (FO) membranes were tested and compared in a live membrane bioreactor (MBR) for performance comparison. The NF membrane offered the possibility of higher fluxes, but reverse solute transport was also investigated. Synthetic municipal wastewater was selected as a feed, and the *Bacillus subtilis* species was inoculated in the solution and grown overnight for development of a monoculture bioreactor. DI water was used as feed solution for control. Conventional inorganic salts (NaCl, Na_3PO_4) were examined in comparison with the previously untested surfactants (TEAB, SDS) and polyelectrolytes (PDAC, PGBE) as draw solutes. Osmotic pressure, flux, toxicity (due to reverse solute transport) and viscosity were observed for the draw solutions. The high molecular weight draw solutes offered the promise of reducing reverse solute transport while reducing the energy penalty for draw solute regeneration.

Chapter 4: Integration of Forward Osmosis and Membrane Distillation Units for Regeneration of Novel Draw Solutions and Water Reclamation

Using a range of novel draw solutes, a study was carried out to study and optimize the integration of a Membrane Distillation (MD) unit with a Forward Osmosis (FO) unit as a means of recovering clean water from the latter and regenerating the draw solution. In this hybrid system, the diluted draw solution was fed to the MD unit. Indeed, the hybrid setup was used to develop a continuously operating FO-MD system to also study the reverse transport of solute and hence their potential toxicity to the bacterial species in the bioreactor, and the fouling of the membrane over the longer-term operation. Indeed, few if any studies can be found on the longer-term operation of the FO-MD hybrid, especially using a diverse range of draw solutes.

Chapter 5: Optimising the Membrane Cleaning Regime for the FOMBR-MD Lab Scale System

In this chapter, the cleaning of membranes used with different draw solutes was studied using the basic cleaning solution used throughout this study, and a comparison was made with acidic cleaning of the membrane. The membranes were imaged before and after cleaning using SEM imaging and compared. For basic cleaning, 0.5mM EDTA was used with 0.5g/l NaOH. For acidic cleaning, 2% HNO_3 and 2% H_3PO_4 was used for cleaning the membrane. The initial decline in flux was measured in-situ for an integrated FOMBR-MD system prior to cleaning. The capability of the cleaning process to restore original flux and allow sustained operation was investigated later in Chapter 6 and Annexe I.

Chapter 2

Literature Review

2.1 Forward Osmosis Systems- Theory and Principles

Forward Osmosis (FO) is the transport of water across a selectively permeable membrane from a solution of lower osmotic pressure (Feed solution) to a solution of higher osmotic pressure (Draw solution) (Achilli et al., 2009). The osmotic pressure (π) is defined as a function of the number of solute molecules (n), the volume of pure solvent (V) and the temperature, as shown in Van't Hoff's equation (2.1):

$$\pi = \frac{\mathrm{n\ iRT}}{\mathrm{V}} \quad \text{.....2.1}$$

Where R is the ideal gas constant, i is the dimensionless Vant Hoff's factor and T is the temperature. An osmotic coefficient (Φ) is used to correct for deviation of a real solution from the prediction of Van't Hoff's law for an ideal solution and can therefore be presented as

$$\pi = \frac{\Phi \mathrm{n\ iRT}}{\mathrm{V}} \quad \text{.....2.2}$$

Extensive research has been carried out in the field of FO in recent years (Lutchmiah et al., 2014), but its application in wastewater treatment is still in its early stages.

Research on FO claims to have advantages such as; it operates at low or no hydraulic pressure, (Kook et al.,2018), it demonstrates higher rejection for various contaminants, (Amin et al., 2016, Jin et al., 2011), membrane fouling is lower due

to flow resistance being solely responsible for the hydraulic pressure drop in the membrane module. The membrane fouling is reversible and osmotic backwashing is sufficient to recover the membrane efficiency in most cases (Liu and Mi, 2012). There are many disadvantages of FO as well; attaining a steady and large flux is one of the major challenges for large scale implementation of forward osmosis. Although new membranes (thin film) are being developed and new draw solutions, explored to improve the process (Li et al., 2017, Huang et al., 2015, Castrillon et al., 2014, Lay et al., 2011), fouling is still an important problem that occurs in all liquid-phase membrane processes (Lay et al. 2012). In FO, fouling is particularly exacerbated by internal concentration polarization (ICP) in the support layer of the FO membrane. Both external concentration polarization (ECP) on the active layer, and internal concentration polarisation in the support layer, negatively influence the flux of an FO membrane.

It is also important to understand that, in view of practical water recycle and production applications, FO is usually designated as a “pre-treatment” process to directly treat feed wastewaters (Li et al., 2016).

2.1.1. Concentration Polarization

In an osmotically driven membrane process, concentration polarisation is caused by the concentration difference between the feed solution and the draw solution through an asymmetric FO membrane (**Figure 2.1**). As stated previously, both internal and external concentration polarization can occur in FO. Generally, ECP occurs at the surface of the dense active layer while ICP occurs within the porous support layer of the membrane.

Both concentrative ECP and dilutive ECP may occur at the active layer in an osmotically driven membrane process, depending on the membrane orientation. Concentrative ECP occurs on the active layer at the feed side when the membrane support layer is facing the draw solution, while dilutive ECP occurs on the active layer at the draw side when the membrane support layer is facing the feed solution. ECP reduces the net driving force, due to increased osmotic pressure at the membrane active layer interface on the feed side of the membrane, or decreased osmotic pressure at the membrane active layer surface on the draw solution side. However, the adverse effect of ECP on the permeate flux can be mitigated by increasing the flow turbulence or velocity, or optimizing the water flux.

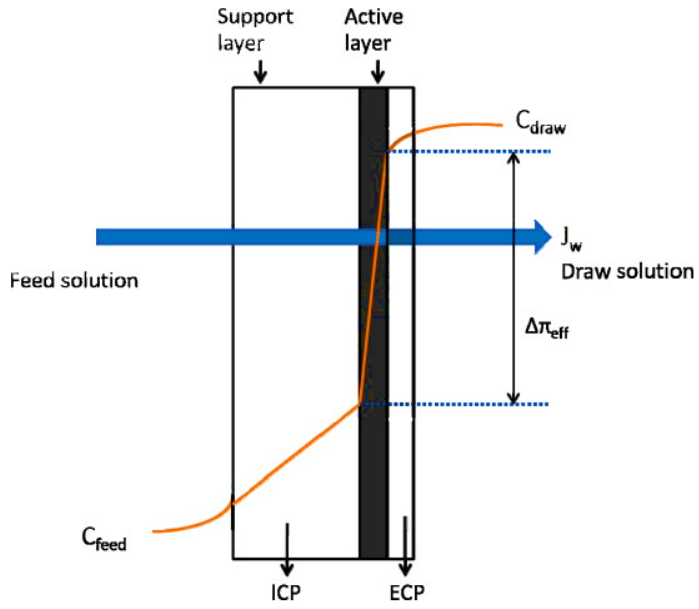


Figure 2.1 Concentration polarization in FO (Zhao et al., 2012). C_{feed}, C_{draw}, $\Delta\pi_{eff}$ and J_w represent the feed solution concentration, draw solution concentration, effective osmotic driving force and water flux, respectively. ICP represents the change in draw concentration across the support layer; ECP is that between the active layer surface and the bulk draw solution.

Significant water flux decline in FO can be caused by ICP. Both dilutive and concentrative ICP can occur in the membrane support layer, depending on membrane orientation (**Figure 2.2**). When (a) the draw solution is placed against the membrane support layer, dilutive ICP will occur within the membrane support layer as water permeates across the membrane from the feed solution to the draw solution. Concentrative ICP occurs (b) as the solute in the feed solution accumulates within the membrane support layer. More critically, because ICP occurs within the support layer, it cannot be mitigated by altering hydrodynamic conditions, such as increasing the flow rate or turbulence.

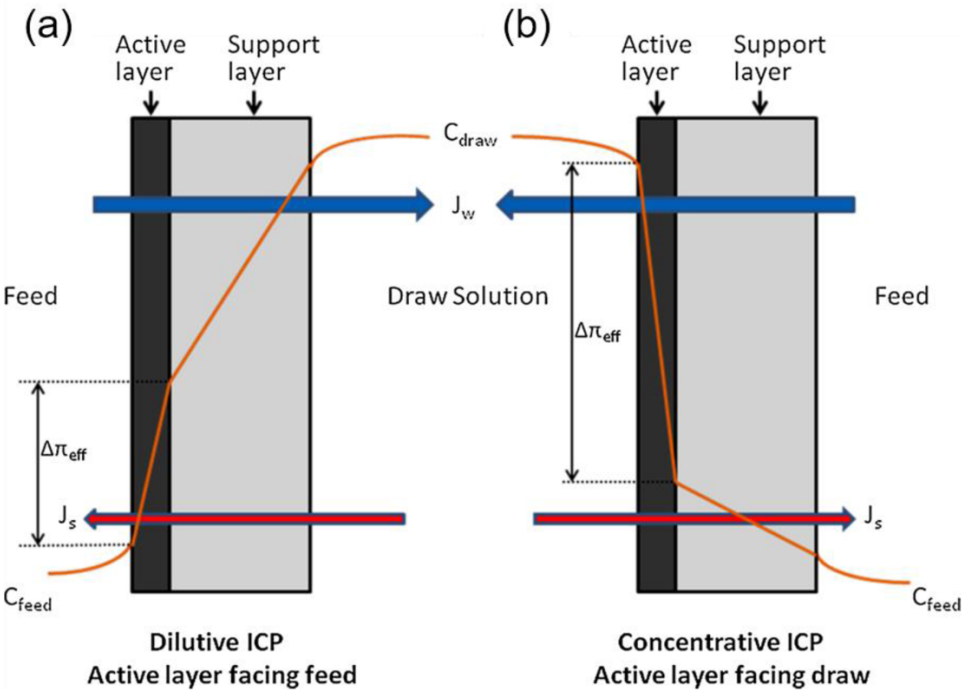


Figure 2.2 Dilutive (a) and concentrative (b) ICP across asymmetric membrane (Zhao et al., 2012). In both cases, ICP is the change in draw concentration across the support layer.

The water permeability coefficient (A), the solute permeability coefficient (B) and the membrane structure (S) describe the inherent properties of an osmotic membrane. An osmotically driven membrane should ideally achieve high flux (high A) and low reverse solute transport (low B), and S must be minimised to reduce internal concentration polarization (ICP). The general equation for flux (J_w) in an osmotically-driven membrane process is often presented in the literature as equation 2.3 (see, for example, Nicolle, 2013):

$$J_w = A\left(\Delta\pi_{eff} - \Delta P\right) \quad \text{.....2.3}$$

where A is the water permeability coefficient of the active layer of the membrane, and $\Delta\pi_{eff}$ and ΔP are the effective osmotic pressure difference and net hydraulic pressure difference across the active layer, respectively. Thus, strictly speaking, this equation is a specific one which applies across the active layer. In a more general equation, the effects of internal and external concentration polarisation should be included (see below).

FO occurs when ΔP is zero and an osmotic gradient is present. Pressure retarded osmosis (PRO) applies a hydraulic pressure lower than the osmotic pressure to the draw solute side. The net flux is in the same direction as FO (towards the draw solution). Reverse Osmosis (RO) uses a hydraulic pressure which exceeds the osmotic pressure ($\Delta P > \Delta\boldsymbol{\pi}$), resulting in flux from a concentrated solution to the permeate. **Figure 2.3** represents the relationship between FO, PRO, and RO.

Internal concentration polarization can occur in FO and PRO due to hindered diffusion of solute in the porous support layer of the asymmetric membrane. The

ICP results in significant decline of flux due to a reduction in osmotic pressure gradient ($\Delta\boldsymbol{\pi}$).

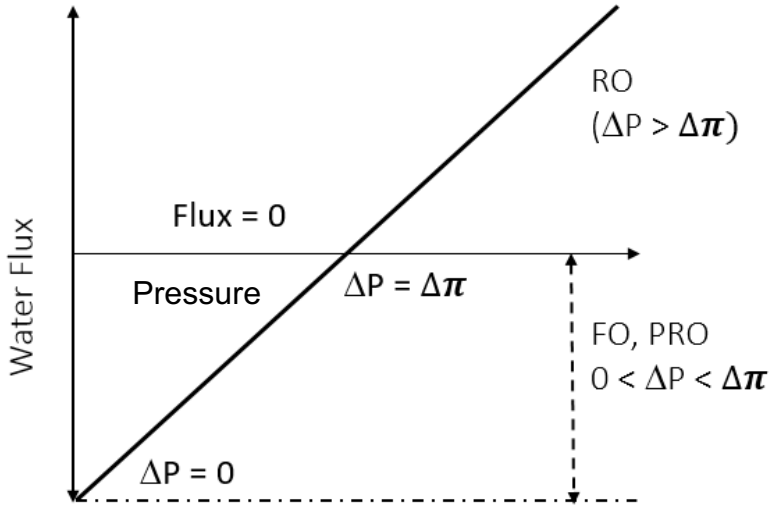


Figure 2.3 Relationship between FO, RO, and PRO (adapted from Lee et al., 1981)

Internal and external concentration polarization (ICP and ECP) can occur in both FO and PRO; the first is due to hindered diffusion of solute in the porous support layer of the asymmetric membrane, and the latter is due to the creation of a mass transfer boundary layer on either surface of the membrane. The ICP and ECP together result in a significant reduction of flux due to a diminution in the osmotic pressure gradient.

The general equation presented in Equation 2.3 can be written as equation 2.4 for a purely FO process (without an applied hydraulic pressure):

$$J_w = A(\pi_{Dm} - \pi_{Fm}) \quad \text{.....2.4}$$

Where π_{Dm} and π_{Fm} are the effective osmotic pressures applying at the draw solution side and feed solution side of the membrane active layer, respectively. However, for this equation to be useful, it would need to be presented in terms of bulk concentrations of the draw and feed solutions. To do this requires a full consideration of the internal and external concentration polarisation effects, as discussed below.

2.1.1.1 Internal Concentration Polarisation

The effect of ICP on FO water flux has been modelled by adopting the classical solution-diffusion theory. In FO mode, with the active layer facing the feed, **dilutive ICP** dominates and the flux (McCutcheon & Elimemlech, 2006) is (if ECP is ignored) given as Equation 2.5.

$$J_w = \frac{1}{K} \ln \frac{A\pi_D + B}{A\pi_F + B + J_w} \quad \text{.....2.5}$$

In PRO mode, with the active later facing the draw, the effect of **concentrative ICP** dominates and flux is given by Equation 2.6 if ECP can be ignored.

$$J_w = \frac{1}{K} \ln \frac{A\pi_D + B + J_w}{A\pi_F + B} \quad \text{.....2.6}$$

Where B is the salt permeability coefficient and K is solute resistivity and is used to measure the solute's ability to diffuse into or out of the membrane support layer; it reflects the degree of ICP in the support layer. Smaller *K* values mean less ICP, resulting in higher water flux (J_w). *K* can be calculated using equation 2.7:

$$K = \frac{t\tau}{\varepsilon D} = \frac{S}{D} \quad \text{.....2.7}$$

where *t*, *τ*, *ε* and *S* are the membrane thickness, tortuosity, porosity and structural parameter, respectively. The structure factor (Alsvik & Hagg, 2013) of the membrane can be calculated using equation 2.8.

$$S = \frac{x.\tau}{\varphi} \quad \text{.....2.8}$$

x is the thickness of the support layer, τ is the tortuosity and φ is the porosity of the membrane. The S value for a commercial, flat sheet FO membrane from CA HTI was reported to be 481 and 575 μm in the literature (Chou et al., 2010; Philip et al., 2010).

An exponential term will be added to the osmotic pressure values based on membrane orientation (see also Figure 2.2). The terms have been presented in the equations to follow. e.g. for **concentrative ICP** equation 2.4 can be presented as Equation 2.9, where the reverse solute flux is neglected and $\pi_{Dm} \approx \pi_{Db}$

$$J_w = A\,[\pi_{Db} - \pi_{Fb}\exp(J_w K)] \quad \text{.....2.9}$$

Here K (defined in equation 2.7) is the solute resistivity. It is the measure of how easily a solute can diffuse in an out of the support layer or the severity of ICP. The exponential term is a correction factor, and can be considered the concentrative ICP modulus, defined as:

$$\frac{\pi_{Fm}}{\pi_{Fb}} = \exp(J_w K) \quad \text{.....2.10}$$

Where π_{Fm} is the osmotic pressure on the inside of the active layer within the porous support. So a positive exponential term indicates that $\pi_{Fm} > \pi_{Fb}$.

Similarly, if reverse solute transport is considered to be negligible and $\pi_{Fm} \approx \pi_{Fb}$ the **dilutive ICP** flux given by Loeb et al. (1997) can be rearranged as equation 2.11:

$$J_w = A\,[\pi_{Db} exp(-J_w K) - \pi_{Fb}] \quad \text{.....2.11}$$

Here π_{Db} is corrected by the dilutive ICP modulus and defined as equation 2.12,

$$\frac{\pi_{Dm}}{\pi_{Db}} = \exp(-J_w K) \quad \text{.....2.12}$$

Where, π_{Dm} is the concentration of the draw solution on the inside of the active layer within the porous support. The negative exponential value indicates that $\pi_{Dm} < \pi_{Db}$.

2.1.1.2 External Concentration Polarisation

Similarly, to ICP modulus, equation 2.13 shows the concentrative ECP modulus while 2.14 shows the dilutive ECP modulus. π_{Fm} and π_{Fb} are the osmotic pressures of the feed solution at the membrane surface and the bulk respectively while π_{Dm} and π_{Db} are the osmotic pressures of the draw solution at the membrane surface and bulk, respectively (McCutcheon & Elimemlech, 2006).

$$\frac{\pi_{Fm}}{\pi_{Fb}} = \exp\left(\frac{J_w}{k}\right) \quad \text{.....2.13}$$

$$\frac{\pi_{Dm}}{\pi_{Db}} = \exp(-\frac{J_w}{k}) \quad \text{.....2.14}$$

k is the mass transfer coefficient (Shirazi et al.,2010) and is given as the ratio of diffusion coefficient (D) and boundary layer thickness (δ).

$$k = \frac{D}{\delta} \quad \text{.....2.15}$$

Mass transfer coefficient can be related to the Sherwood number (McCutcheon & Elimemlech, 2006) as shown in equation 2.16:

$$k = (S_h D)/d_h \quad \text{.....2.16}$$

The Sherwood number can be found using the following for laminar and turbulent flow (Equation 2.17 and 2.18).

$$Sh = 1.85 \left(ReSc \frac{d_h}{l}\right)^{0.33} \text{ Laminar flow .....2.17}$$

$$Sh = 0.04\, Re^{0.75} SC^{0.33} \text{ Turbulent flow.....2.18}$$

Here, Re is the Reynolds number, Sc the Schmidt number, d_h is the hydraulic diameter, and L is the length of the channel. To account for CP in a symmetric membrane (McCutcheon & Elimemlech, 2007) i.e. membrane without a support layer, equation 2.4 can be modified as follows (provided the reverse salt diffusion has negligible influence):

$$J_w = A\left(\pi_{Db} \exp\left(-\frac{J_w}{k_D}\right) - \pi_{Fb} \exp\left(\frac{J_w}{k_F}\right)\right) \quad \text{.....2.19}$$

Dilutive effect is indicated by the negative exponential term modifying the draw solution osmotic pressure. Individual mass transfer coefficients on the feed, k_F, and permeate, k_D, sides of the membrane must also be considered. Although in modelling, they are often considered equal. Where dilutive external concentration polarization occurs on the permeate (draw) side and concentrative ECP occurs on the feed side. In the asymmetric membrane, both ECP and ICP take place because of the porous support layer.

In PRO mode, with hydraulic pressure applied to the active layer draw side, the effect of ICP will be given by equation 2.9. where, the ICP has a positive exponential term, indicating a concentrative effect, and the flux is assumed to be low. For moderate and high flux (and provided the reverse salt diffusion has negligible influence), the ECP on the permeate side must also be accounted for using equation 2.20:

$$J_w = A\left(\pi_{Db}\exp\left(-\frac{J_w}{k_D}\right) - \pi_{Fb}\exp\left(J_w K\right)\right) \quad \text{2.20}$$

The terms in the equation above can be determined through experiments to measure flux (for PRO mode). This can be used to predict the flux for an asymmetric membrane. The model is equation 2.20 assumes that the support layer creates no hydraulic resistance to water transport, and the feed solute can freely enter the support structure such that concentrative ECP does not occur on top of the support layer.

As stated before, Both ICP and ECP occur simultaneously in an FO membrane. For FO mode operation, ICP occurs on the draw side and is dilutive, while ECP occurs on the feed side and is concentrative. Flux can then be calculated using the following equation (2.21):

$$J_w = A\left(\pi_{Db}\exp\left(-J_w K\right) - \pi_{Fb}\exp\left(\frac{J_w}{k}\right)\right) \quad \text{2.21}$$

Equation 2.12 is used to calculate flux in PRO mode. In the model above, it is similarly assumed that ECP does not occur on the permeate side of the membrane because the support layer is completely permeable to the draw solute.

The ECP and ICP moduli influence negatively to the overall osmotic driving force. The negative contribution of each increases with higher flux, which suggests a self-limiting flux behaviour. This explains why increasing the overall osmotic driving force no longer increases the flux, or does so with diminishing effect, above a certain level. Both concentration polarization and reverse solute diffusion are the limiting factors in FO application (Yip & Elimelech, 2011).

Reverse solute transport (J_s) can be calculated using the concentration gradients:

$$J_s = B\Delta C \quad \text{.....2.22}$$

Where, ΔC is the transmembrane concentration difference for the solute across the active layer. J_s is presented in units of g/m^{2}h which has been abbreviated to GMH (analogously to LMH).

An osmotically-driven membrane should be able to achieve high flux (high A) and lower reverse solute transport (low B). Values of “A” and “B” for the HTI flat sheet FO membranes are 0.81 L/m^{2}h bar (2.2 x 10^{-12} m/s Pa) and 0.62 L/m^{2}h (1.7 x 10^{-7} m/s), respectively (Wang et al., 2010). The HTI CTA membrane has been widely studied and variously promoted and criticised for its performance in water treatment (Fam et al., 2013).

Reverse solute transport (RST) can reduce the flux and increase the cost of operation for an FO process. Reverse flux selectivity is used to describe RST and is the ratio of water flux and reverse solute flux, given as J_w/J_s. Although reverse flux selectivity is shown to be independent of the S value (it depends on the selectivity of the AL), a low S value is still important to minimise ICP (Phillip et al., 2010).

Low fluxes can also be attributed to coupling between water and solutes; therefore, the reflection coefficient was introduced (to account for this coupling). It is calculated by taking the ratio of experimental flux and predicted water flux.

$$\sigma = \frac{J_{w.exp}}{J_{w.pred}} \quad \text{.....2.23}$$

The membrane that allows the solvent to pass but not the solute would have a σ of 1.

Alongside ICP and RST, fouling is also an issue in osmotic membrane processes (Alsvick & Hagg, 2013). Research is currently in progress to tackle the issues of performance, RST and fouling, including synthesis of novel draw solutions and membranes. This is described in detail in the sections which follow.

2.2 Forward Osmosis Membranes

It is desirable to have forward osmosis membranes with high flux, low RST and reduced concentration polarization (CP). An improvement in the support layer to reduce ICP is important to develop a high-efficiency FO membrane having high water permeability and low solute permeability, but the latter has not yet been achieved commercially (Uragami, 2017). The most widely used commercial FO membrane is a flat sheet FO membrane made up of cellulose triacetate (CTA) coated on polyester mesh and sourced from Hydration Technology Innovations (HTI). Other commercial suppliers such as Porifera, Aquaporin, Toray and Oasys water now provide commercial FO membranes (Nicoll, 2013) but have not been studied extensively.

As the forward osmosis system relies on the chemical potential difference to drive water molecules across a membrane surface, and due to a lack of hydraulic

pressure gradient, membrane strength is not as important as it is for RO, NF and UF. Therefore, work on the development of single layer FO membranes without a conventional support layer has been ongoing (Gai & Zhang, 2015).

Optimization of an FO membrane that can produce a much higher flux as compared to an RO membrane under typical operating conditions for both is still considered to be a challenge. Indeed, the hydraulic pressure applied in RO is often higher than the osmotic pressure achieved by various existing draw solutions, which calls for higher permeabilities in FO membranes. Therefore, various research groups are trying to produce new FO membranes for further development of this field. A summary of membranes alongside the operating conditions, solute and water permeability and structure parameter are given in Table 2.1.

As stated several times before, the studies on membranes fabrication have often been tested for performance with NaCl and $MgCl_2$ as draws solution and DI water as feed instead of complex feeds such as seawater or wastewater. Indeed, many of the novel draw solutions (discussed later) are not available commercially, and that is one of the main reasons for their lack of application. Lower cost, high osmotic pressure, high diffusivity and higher fluxes make simple inorganic draw solutions easiest viable option, but higher reverse solute transport cannot be neglected and their buildup over time and increase in toxicity for microbes when used in wastewater treatment application cannot be ignored.

Table 2.1 Summary of Operating conditions, performance, structural parameter, water and solute permeability for FO membranes

Draw solution	Feed solution	Membrane	Water flux, LMH	Solute flux, GMH	Membrane orientation	Water permeability (A) LMH bar^{-1}	Solute permeability (B) LMH	Structure parameter (S) μm	Ref.
1.0 M NaCl	DI water	TFC	31.1	8.50	AL-FS	1.69	0.26	205.8	Liu & Ng, 2014
1.0 M NaCl	DI water	TFC	17.1	6.0	AL-FS	0.91	0.25	314	Stillman et al.,2014
1.5 M NaCl	DI water	TFC with lignin additive	27.6	-	AL-FS	1.88	6.26	439	Vilakati et al., 2014
2.0 M NaCl	DI water	TFC	11.8	2.5	AL-FS	1.51	0.44	110	Luo ey al., 2014
1.0 M NaCl	DI water	TFC-nano fiber	15.0	0.5	AL-FS	0.56	0.05	190	Huang & McCutcheon, 2014
0.5 M $MgCl_2$	DI water	SG-PAN	28.6	5.8 g/L	AL-FS	3.79	6.08	250	Lee et al., 2014
0.5 M NaCl	DI water	Nano TFC	27.24	–	AL-FS	1.69	0.24	66	Puguan et al., 2014
0.5 M NaCl	DI water	TiO_2 TFN	18.81	7.35	AL-FS	2.63	0.446	390	Emadzadeh et al., 2014
2.0 M NaCl	0.01 M NaCl	MWCNT-PES	12.0	–	AL-FS	2.31	0.79	2042	Wang et al., 2013
0.5 M NaCl	0.01 M NaCl	TFN	17.1	3.97	AL-FS	1.96	0.384	–	Emazadeh et al., 2013
2.0 M NaCl	DI water	TFI	60.3	11.4	AL-FS	1.15	0.648	38	You et al., 2013

0.5 M NaCl	DI water	PSf N-TFC	21	12.6	AL-FS	3.3		340	Ma et al., 2013
0.5 M $MgCl_2$	DI water	3-bilayer LbL	28	1.97	AL-DS	1.15	3.161	445	Cui et al., 2013
0.5 M NaCl	DI water	TFC-sPPSU	22.51	5.49	AL-FS	1.99	0.0399	163	Zhong et al., 2013
1.5 M NaCl	DI water	Nylon-TFC	6	1	AL-FS	0.917	0.3	1940	Huang & McCutcheon, 2014
0.5 M NaCl	10 mM NaCl	LbL AgNPs	17.9	2.8	AL-FS	3.924	–	–	Liu et al., 2013
2.0 M NaCl	10 mM NaCl	TFN	25	3	AL-FS	3.6	0.103	380	Amini et al., 2013
1.0 M NaCl	DI water	CTA/CA	10.39	4.909	AL-FS	–	–	–	Nguyen et al., 2013
2.0 M NaCl	DI water	TFC-sPPSU	48	7.6	AL-FS	3.23	1.05	65.2	Widjojo et al., 2013
0.5 M $MgCl_2$	DI water	PAI-PES/PEI	20.8	6.448	AL-FS	4.1	0.08	63.3	Setiawan et al., 2013
1.5 M NaCl	DI water	TFC with nano fiber	35.0	8.0	AL-FS	2.04	1.57	109.1	Bui & McCutcheon, 2013
1.5 M NaCl	DI water	PA/ACE-TFC	12.5	1.4	AL-FS	–	–	–	Han et a;., 2013
0.3 M NaCl	DI water	LbL	11	8	AL-DS	–	–	–	Duong et a., 2013
0.1 M $MgCl_2$	DI water	LbL	20.66	0.138 g/L	AL-FS	6.1	–	–	Liu et al., 2013
1.0 M NaCl	DI water	CAB	9.4	3.9	AL-FS	0.51	0.4	–	Ong et al., 2012

0.5 M $MgCl_2$	DI water	PAI/PES	27.5	5.5	AL-FS	15.9	–	–	Setiawan et al., 2012
2.0 M NaCl	DI water	PDA@Psf TFC	24	–	AL-DS	0.6	0.19	151	Han et al., 2012
2.0 M NaCl	DI water	CAP-TFC	31.8	1.6	AL-DS	1.42	0.132	695	Li et al., 2012
2.0 M NaCl	DI water	TFC-PES	32.1	6.15	AL-FS	1.18	0.135	219	Sukipaneerit & Chung, 2012
0.5 M $MgCl_2$	DI water	LbL	42.3	19.516	AL-FS	3.204	0.508	–	Qi et al., 2012
0.5 M $MgCl_2$	DI water	LbL	8	16.8	AL-DS	–	–	–	Su et al., 2012
0.5 M NaCl	DI water	TFC	13	3.6	AL-FS	0.77	0.11	238	Wang et al., 2012
2.0 M NaCl	DI water	TFC	21	2.2	AL-FS	0.73	0.25	324	Widjojo et al., 2011
0.5 M NaCl	DI water	TFC	18.7	1.6	AL-FS	–	–	–	Shi et al., 2011
1.0 M $MgCl_2$	DI water	LbL	28.7	17.136	AL-FS	10.224	3.456	–	Saren et al., 2011
3.0 M NaCl	DI water	PES	30	8.766	AL-FS	–	–	–	Liu &Ng, 2014
2.0 M NaCl	DI water	CA	10	3	AL-FS	0.2	–	–	Zhang et al., 2011
0.5 M NaCl	10 mM NaCl	TFC	12	4.9	AL-FS	1.78	0.338	–	Wei et al., 2011
1.0 M NaCl	DI water	TFC	25	–	AL-FS	1.9	0.33	312	Tiraferri et al., 2011

As mentioned before in chapter 2, the S value for HTI membrane in literature has been reported to be, between 450-600 μm. Most of the values shown in Table 2.1 are very well below the S value for HTI value with the exception of few very high S values. Higher water permeability is related to higher flux and lower solute transport to that of lower solute permeability values. Highest values of fluxes are achieved with a combination of higher A value and lower S value.

Current research on FO membranes is focused on the development of membranes with antifouling capability, such as hydrogel membranes (Li et al., 2017, Huang et al., 2015, Castrillon et al., 2014).

Developing a membrane although very crucial is not the only important aspect. In the studies presented in the Table 2.1, the development of modules to operate at large scale were not discussed, for which hydrodynamic control can be an issue.

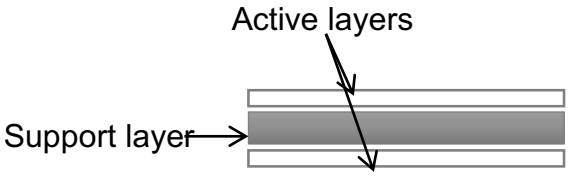


Figure 2.4 Double-skinned forward osmosis membrane to reduce ICP and fouling in FO

The organic polymeric membranes are subject to internal concentration polarization due to their asymmetric membrane structure, but developing a single layer membrane can lead to an increase in reverse salt transport. Therefore, a membrane (**Figure 2.4**) with a highly porous sublayer sandwiched between two selective skin layers was fabricated by phase inversion. The resulting double-skinned cellulose

acetate membrane displayed a water flux of 48.2 LMH and a salt transport of 6.5 GMH, using 5 M $MgCl_2$ as draw solute (Wang et al., 2010). More studies on the membrane are not found. Indeed, this is true for almost all the novel draw solutions and membranes reported from literature. The RST for this membrane is still quite high, despite a low pore sized active layer exposed on both sides of the membrane.

As also observed all the membranes presented in the study have not been tested for FO-MBR operation.

The TFC membranes for FO presented in the table 2.1 were fabricated via interfacial polymerization on a polysulfone substrate containing a disulfonated poly(arylene ether sulfone) hydrophilic-hydrophobic multiblock copolymer to increase the hydrophilicity and reduce fouling. One of the combinations showed an extremely high-water flux of 40 LMH in FO mode and 74.4 LMH in PRO mode, when 2M NaCl solution was used as the draw solute. When feed with 3.5 wt % NaCl was in place, water fluxes of 18.6 and 29.06 LMH were achieved under FO mode and PRO mode, respectively (Zhang et al., 2016). The authors claimed the flux to be one of the highest fluxes achieved however, follow up studies were not found.

Qin et al., (2015) fabricated a nanocomposite FO membrane composed of an oil-repelling and salt-rejecting hydrogel selective layer on top of a polymeric support layer infused with graphene oxide (GO) nanosheets [**Figure 2.5** (left)]. The hydrogel selective layer showed high oleophobicity, resulted in low fouling of the membrane. This membrane was used for shale gas wastewater treatment and showed greater than 99% oil removal and was recommended for saline and oily wastewater treatment.

Reducing ICP and increasing water permeation are important for forward osmosis optimisation. A second generation of forward osmosis membranes have been introduced in the form of graphene sheets and carbon nanotubes, and examples for both are given below.

Graphene is a thin, single, tightly packed layer of pure carbon. It is the world's thinnest and strongest material. Because of the strength, nanoporous graphene can be used as a semipermeable membrane, without the need for a fabric support. Flux was shown to be three times higher than that of typical CTA membranes, with excellent salt rejection, and because of the absence of a support layer, the ICP was reduced to zero (Gai et al., 2014). However, to date, the graphene sheets have only been applied in microscopic-scale systems and full-scale systems have not been realised.

Highly stable and novel supports made of carbon nanotubes were fabricated for both FO and RO. A TFC membrane was fabricated by interfacial polymerization; a dense poly(amide) PA layer was formed on a self-supporting bucky paper made of hydroxyl functionalised entangled carbon nanotubes (CNTs). However, the study conducted was not adequate or complete, and more research is needed to make further conclusions (Dumee et al., 2013).

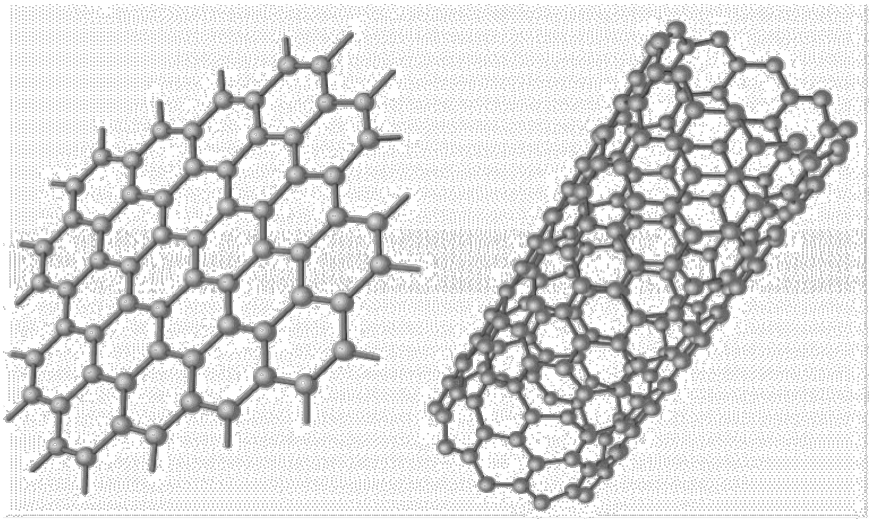


Figure 2.5 Graphene layer (left) on its own and rolled graphene as a nanotube (right)

Overall, a good deal of literature on membranes developed for FO at lab-scale research is available. However, the issues of RST, applications for treatment of diverse feed, CP, fouling and reduction in flux with feed (for lab studies, very often DI water is used as feed instead of industrial or municipal wastewater) haven't been overcome. For large scale application of FO more commercial FO membranes with the ability to tackle all the issues mentioned need to be addressed.

2.3 Forward Osmosis Draw solutions

The draw solution is the driving force and core part of the forward osmosis process. Solute characteristics are mainly expressed in terms of its solubility and osmotic pressure, viscosity of the solution, molecular mass, high diffusivity, reverse solute transport and toxicity. High solubility results in higher possible draw solute concentrations in the solution, leading to a higher osmotic pressure driving force and a higher water flux. However, as discussed above, flux only increases linearly

up to a certain concentration, while higher concentrations often lead to higher concentration polarization and diminishing flux returns. The lower the draw solution viscosity, the better the molecules are transported across a solution, ensuring higher exchange across the membrane and lower concentration polarization. Lower molecular mass generates higher osmotic pressures (per given mass concentration), are highly diffusive with lower tendency towards ICP or ECP, and hence yield fluxes but result in higher reverse solute diffusion as well.

Table 2.2 Novel draw solutions studied by various research groups

Draw solute	**Method of Recovery**	**Drawbacks Noted in Literature**	**References**
Ammonia and carbon dioxide	Heating	Energy intensive	Neff,1964
Organic acids and inorganic salts	Temperature variation or chemical reaction	Complicated procedures, corrosive chemicals involvement	Hough, 1970
Al_2SO_4	Precipitation by doping $Ca(OH)_2$	Toxic by-products	Frank,1972
Glucose- Fructose	None	Not for generating pure water	Kessler & Moody, 1976
$MgCl_2$	None	Not for generating pure water	Loeb et al., 1997
KNO_2 & SO_2	SO_2 recycled through standard means	Energy intensive, toxic	McGinnis, 2002
NH_3 & CO_2 (NH_4HCO3) or NH_4OH-NH_4HCO_3	Moderate heating (60^oC)	High reverse draw solute flux, insufficient removal of ammonia, toxicity to biomass in FO-MBR	McCutcheon et al., 2005; McCutcheon et al., 2006; Nawaz et al., 2013
Salt, ethanol	Pervaporation-based separations	High reverse draw solute flux and low water flux	McCormick et al., 2008

Magnetic nanoparticles	Recycled by external magnetic field	Agglomeration	Ling et al., 2010; Ge et al., 2011
Stimuli- responsive polymer hydrogels	De-swelling of the polymer hydrogels	Energy intensive, poor water flux	Li et al., 2011
Hydrophilic nanoparticles	Ultra filtration (UF)	Poor water flux	Ling and Chung, 2011
Fertilizers	None	Only applicable in agriculture	Phuntsho et al., 2011
Fatty acid – polythethylene glycol	Thermal method	Poor water flux	Iyer and Linda, 2011
Sucrose	Nano filtration (NF)	Relatively low water flux	Su et al., 2012
Polyelectrolytes	UF	Relatively high viscosity	Ge et al., 2012
Thermo- sensitive solutes (Derivatives of Acyl-TAEA	Not studied	Poor water flux	Noh et al., 2012
Urea, ethylene glycol and glucose	Not studied	Low water flux and high draw solute flux	Yong et al., 2012
Organic salts	RO	Low water flux, energy intensive	Bowden et al.,2012
Polyglycol copolymers	NF	High viscosity, severe ICP	Carmignani, 2012
Hexavalent phosphazene salts	Not studied	Not economical and practical	Stone et al., 2013
Volatile solutes (e.g. SO_2	Heating or air stripping	Toxic	McCutcheon et al., 2006
Copper sulphate	Metathesis precipitation reaction	Complex regeneration process	Alnaizy et al., 2013
Dendrimers	Wide range of pH value and UF	Very expensive to regenerate	Adham et al.,2009

Source: Adapted from (Ge et al., 2013)

The major challenge for FO is the present lack of an ideal DS which can simultaneously achieve high water flux, low RST, and allows for an efficient and inexpensive recovery. Indeed, the use of many existing draw solutes in the form of small molecules, salts, and electrolytes cause difficulties in recovery and salt leakage and induce clogging in the supporting layer (they can get trapped in the

support layer due to poor diffusion), the latter leading to severe fouling and internal concentration polarization. All of these which may not be economical nor acceptable in practice. Several strategies for draw regeneration have been proposed, such as heating/distillation, magnetic separation, precipitation, ultra- and nano-filtration, RO, membrane distillation, and physical triggers such as pressure or temperature swings. **Table 2.2** shows a review for draw solutions and their regeneration methods, majorly UF, NF, heating and application of magnetic field etc.

2.3.1 Inorganic Solutes

Several inorganic draw solutes have been tested for forward osmosis including simple salts, inorganic fertilisers, and hydroacid complexes. Some are presented in this section starting with the most recent publication.

Trung et al., (2017) evaluated ammonium iron (II) sulfate, ammonium iron (III) sulfate, and ammonium iron (III) citrate as novel draw solutes. Water flux was in the range of 8.9 LMH to 12 LMH with DI water as feed in AL-DS configuration. More than 90% of iron complexes were recovered by an NF-90 membrane. Ammonium iron (II) sulfate [$(NH_4)_2Fe(SO_4)_2 \cdot 6H_2O$], showed negligible reverse solute flux with a moderate water flux of 8.9 LMH, while Ammonium iron (III) sulfate [$FeNH_4(SO_4)_2$] showed a reverse solute flux of 2.5 GMH and a water flux of 11.66 LMH. Ammonium iron (III) citrate [$(NH_4)_5Fe\ (C_6H_4O_7)_2$] showed a reverse solute flux of 1.3 GMH and a water flux of 8.7LMH, and Ammonium bicarbonate [NH_4HCO_3] showed a reverse solute flux of 1.2 GMH and a water flux of 8LMH. The flux values are comparable to NaCl the RST values are also high and the study has not been extended to testing a more complex feed e.g. water flux of 8LMH and 15LMH could be achieved in FO

and PRO mode respectively but the RST increased to 5GMH compared to 1.5 GMH achieved with FO mode (Ren & McCutcheon, 2014).

Some novel draw solutions aim at reducing the RST in FO. A combination of 0.5 mM Triton X100 with 0.55 M Na_3PO_4 draw solution (AL-FS) was used as draw solute to achieve this end. With the said combination, the RST was only 0.13 GMH and water fluxes of 4.89 LMH and 1.15 LMH were achieved for brackish water (total dissolved solids: 4090 ppm) and seawater (TDS: 36,800 ppm) respectively. Thus, flux values were comparable to other inorganic solutes but the RST was reduced by an order of magnitude. However, the overall fluxes achieved were still lower than desired high fluxes for large scale operation. Furthermore, a UF-NF recovery system was able to achieve 98% recovery of the draw solute (Nguyen et al., 2015). Even though very low RST and very high recovery was achievable the flux us still very lower than what will be required to scale up a plant.

Inorganic fertilizers (Mishra & Shrivastava, 2015) have also been evaluated as draw solutes (AL-FS), to eliminate the need for the removal and later regeneration of draw solutions but instead for direct use of the final product water, in a process known as fertigation. Six inorganic fertilizer draw solutes, including ammonium nitrate (NH_4NO_3), sodium nitrate ($NaNO_3$), potassium chloride (KCl), potassium nitrate (KNO_3), di-ammonium phosphate (DAP), and mono-ammonium phosphate (MAP), were tested as potential draw solutes at 1 and 2 M draw solution concentrations with DI water as a feed. The highest performance ratio (percentage ratio of experimental to calculated flux) was shown by the low molecular weight ammonium nitrate (8.46 LMH) and potassium chloride (9.39 LMH) at 1M concentration, whereas DAP (14.67 LMH) with the highest molecular weight showed the worst performance ratio at 2M draw solution concentration. This is indeed one of the major

limitations for high molecular weight draw solutions i.e. their osmotic pressure is reduced per mass concentration and lower fluxes are achieved.

Ge et al., (2014) assessed cobaltous hydroacid complexes as FO draw solutes and compared them with the ferric hydroacid complex. Solutions of cobaltous hydroacid complexes produced a high osmotic pressure, due to the presence of abundant hydrophilic groups that dissociated to form multi-charged anions and Na cations in aqueous solution. Their expanded molecular structure also led to a lower reverse solute transport. Cellulose triacetate, a TFC membrane on a PES support and a hollow fiber polybenzimidazole/polyethersulfone (PBI/PES) membrane were used to evaluate the draw solutes and relatively high fluxes were achieved. With DI water as feed in PRO (AL-DS) mode, the TFC membrane produced a high water flux of 39-48 LMH at 2.0 M draw solute for Fe-CA. A water flux of 17.4 LMH (Fe-CA) was achieved when 3.5 wt% NaCl was used as a feed and Co-CA gave a flux of 13 LMH. This hydroacid complex was easily regenerated using NF. However, a potential set-back is their higher cost as compared to other inorganic solutes. Another major area of concern is nearly 50% drop in flux as the feed is changed from DI water to seawater. This also needs attention of researchers in the area.

Achilli et al., (2010) extensively tested fourteen inorganic draw solutions in the laboratory for water flux and RST through an FO membrane (Symmetric). The measured water fluxes ranged from 10.9 LMH for KCl to 5.5 LMH for $MgSO_4$ at 2.8 MPa osmotic pressure. Other draw solutions in their order of ranking (based on performance and replenishment cost) included NH_4Cl, KBr, NaCl, $CaCl_2$, $CaSO_4$, $NaHCO_3$, $Ca(NO_3)_2$, $MgCl_2$, $(NH_4)_2SO_4$, $KHCO_3$, Na_2SO_4, NH_4HCO_3. DI water was used a feed. Larger-sized hydrated anions showed the lowest reverse solute diffusion, regardless of their cationic counterpart. $CaCl_2$, $KHCO_3$, $MgCl_2$, $MgSO_4$,

and $NaHCO_3$ ranked high for performance, due to high flux or low RST. $KHCO_3$, $MgSO_4$, NaCl, $NaHCO_3$, and Na_2SO_4 ranked high in terms of lower replenishment cost. $KHCO_3$, $MgSO_4$, $NaHCO_3$, ranked high for both criteria. $CaCl_2$ and $MgCl_2$ ranked high for the three criteria of water flux, RST, and low RO permeate concentration while NaCl and Na_2SO_4 ranked low for these same criteria. The study provided a working protocol to select a draw solution for forward osmosis, and again highlighted that ICP lowers both the flux and the RST by decreasing the effective draw solution concentration. However, the range investigated was limited to inorganic draws and other types were simply excluded in the study.

2.3.2 Organic Draw Solutions

Similarly, to inorganic solutes, many organic solutes have found their application in forward osmosis including sodium salts of acid, polyelectrolytes and polymer hydrogels, micellar draw solutions, magnetic nanoparticles and dextran. While some of these draw solutions have shown promising results in the lab, their application on a large scale is yet to be achieved. Some of such draw solutes, their weaknesses and strengths are discussed here.

Long and Wang., (2016) synthesised a series of carboxyethyl amine sodium salts (**Figure 2.6**) as novel draw solutes, including ethyleneimine pentapropionic acid sodium (EDTP-Na), diethylenediamine pentapropionic acid sodium (DTPP-Na), triethylenetetramine hexapropionic acid sodium (TTHP-Na), and tetraethylenepentamine heptapropionic acid sodium (TPHP-Na). DI water was used as a feed with AL-FS. The application of TTHP-Na as adraw solute for dye wastewater treatment via FO was evaluated. The draw solution was recovered by NF and the performance and energy efficiency was recorded. A very high water flux of 23.07 LMH was achieved with 0.5 g/ml (0.64M) of TTHP-Na, with a reverse solute

transport of 0.75 GMH in PRO mode. Similarly, DTPP and EDTP also showed fluxes over 20LMH and RSTs below 0.5GMH in PRO mode. The fluxes dropped to 15LMH and under for FO mode and RSTs between 0.6-0.8 GMH were observed (Long & Wang, 2016). The authors also synthesized a series of organic phosphonate salts (OPSs) by the one-step Mannich-like reaction. Their osmotic pressure, viscosities and FO performance were evaluated. In general, a high flux of 47-54 LMH with a very low reverse solute transport was observed, using a homemade TFC membrane. Tetraethylenepentamine heptakis(methylphosphonic) sodium salt (TPHMP-Na) exhibited the best performance at 0.5M out of the following: diethylenetriamine pentakis(methylphosphonic) sodium salt (DTPMP-Na), tetraethylenepentamine heptakis(methylphosphonic) sodium salt (TPHMP-Na), polyethylenimine (methylenephosphonic) sodium salt (PEI-600P-Na) and polyethylenimine (methylenephosphonic) sodium salt (PEI-1800P-Na). Recovery with 92% rejection was observed in an NF recovery system. These draw solutes were stated to be novel with potential use in FO (Long et al., 2016) but the cost, regeneration and reuse data were not reported.

The same group also synthesized a series of renewable, non-toxic gluconate salts as FO draw solutes suitable for food processing applications; potassium gluconate salt (Glu-K), sodium gluconate salt (Glu-Na), zinc gluconate salt (Glu-Zn), and iron(II) gluconate salt (Glu-Fe(II)). Apple juice was used as a feed solution. The results showed that 2M Glu-K draw solution generated a comparable water flux (~23.17 LMH) to that of NaCl solution, but with a significantly lower solute leakage (~1.09 gMH) in PRO mode. The salts were recovered by NF and their application in the food industry was proposed (Long & Wang, 2016). However, their reuse

efficiency was not given and no data was presented on their potential for ICP or fouling.

Magnetic nanoparticles (MNPs) have recently been presented as a group of draw agents with improved fluxes and regeneration. Some of such studies are presented in **Table 2.3**.

Alongside aggregation, progressive attrition and breakage during cycles of reuse are the major issue for MNPs application. The reverse solute transports for the studies are often not reported.

Polyelectrolytes and polymer hydrogels are another set of novel draw solutes being significantly evaluated for seawater desalination (Ou et al., 2013).

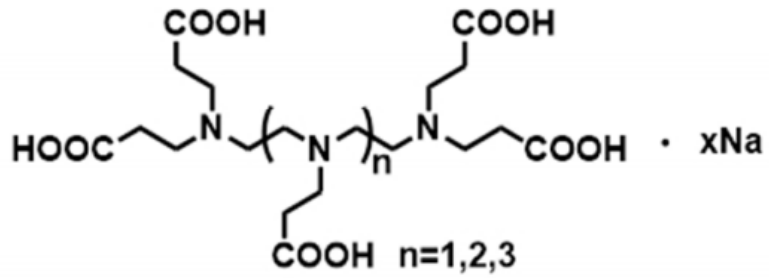


Figure 2.6 Carboxyethyl amine sodium salts; (DDTP-Na) (n=1); (TTHP-Na) (n=2); (TPHP-Na) (n=3).

In more recent studies, a mechanical force has been applied to squeeze poly(sodium acrylate-*co*-2-hydroxyethyl methacrylate) hydrogels that contained water drawn osmotically from a seawater feed, **Figure 2.7**. The addition of sodium acrylate into the hydrogels increased salt rejection. After four cycles of use, the hydrogel was still in a good and useable condition. The flux was not reported in this study, but the

hydrogels were recommended for use in both FO and RO (Yu et al., 2016). Operating with such a hydrogel at full scale, the design of a suitable mechanical press which could operate continuously was not reported but represents a significant challenge.

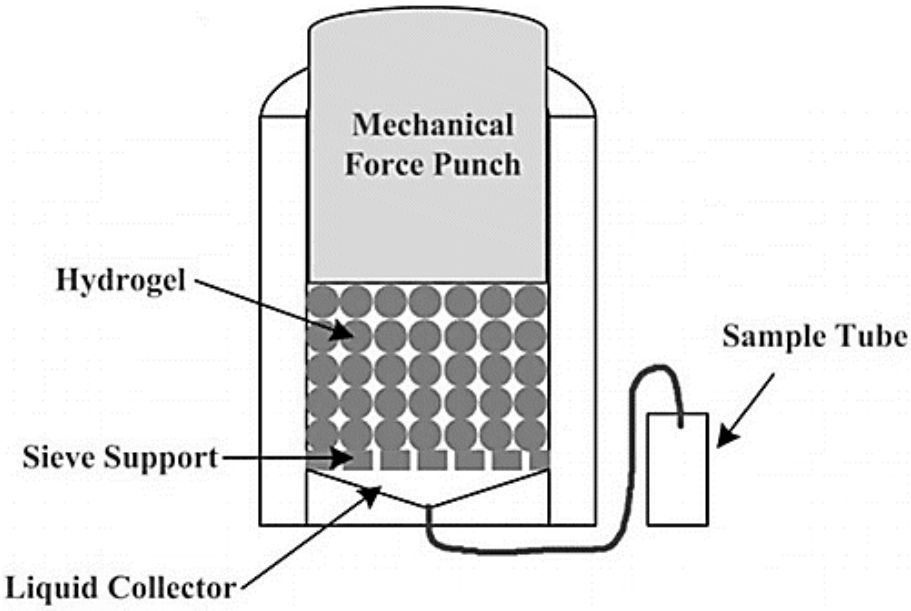


Figure 2.7 Hydrogel mechanical squeezing (Yu et al., 2016)

Na+-functionalized carbon quantum dots (Na-CQDs) that are biocompatible in nature have also been proposed as FO draw solutes. With a 0.4g/ml draw solution concentration and seawater as feed, a reasonable high flux of 10 LMH was observed. Again, the cost of synthesis, especially at large scale, is likely to be an issue. Membrane distillation was used to recover the draw solute (Guo et al., 2014).

Table 2.3 MNPs application for FO

Draw Solution	Performance	Issues	Recovery	Reference
Hyperbranched polyglycerol-coated magnetic nanoparticles (HPG-MNPs)	water flux of 6.7 LMH was produced when DI water was used as a feed and using 300 mg/ml MNP as draw solution concentration (AL-DS)	Despite the complexity and cost of synthesis and regeneration, flux comparable to inorganic draw solution and the RST was not given.	Combined FO-UF process	Yang et al., 2014
Magnetic poly(N-isopropylacrylamide-co-sodium 2-acrylamido-2-methylpropane sulfonate) (NIPAM-co-AMPS)	Flux: 0.65 LMH DS concentration: 0.10 g/ml (AL-DS)	Very low fluxes due to particle aggregation and lower osmotic pressure	Magnetic field	Zhou et al., 2015
Poly sodium acrylate-coated MNPs	water flux: 5.3 LMH DS concentration: 1.3 g/l when Feed: DI water (AL-DS)	Very low fluxes	Magnetic field	Dey & Izake, 2015

citrate coated MNPs	Flux: 17.3 LMH DS: 0.02 g/l (AL-DS)	Rapid decline in flux due to interaction between MNPs and CTA membrane	Magnetic field (Magnetic field control was set in place to draw the MNPs away from CTA membrane) resulted in stable flux of 13 LMH	Na et al., 2014
poly(ethylene glycol)diacid-coated (PEG-$(COOH)_2$-coated) magnetic nanoparticles (MNPs)	10 LMH (HTI, DI water) (AL-DS)	21% decrease in flux due to aggregation	MF (upto 9 cycles)	Ge et al., 2011
Dextran coated Fe_3O_4 MNPs	DS: 2M Flux: 7-9 LMH feed 0.016 M $MgSO_4$ (AL-DS)		MF	Bai et al., 2011

A thermoresponsive copolymer, poly(sodium styrene-4-sulfonate-co-*n*-isopropylacrylamide) (PSSS-PNIPAM), was used as draw solute for seawater desalination. The draw solute was regenerated using MD above the lower critical solution temperature. A water flux of 4LMH was achieved with seawater as feed (Zhao et al., 2014). Co-polymers are not easy to synthesize in bulk and lower fluxes pose a question to their long term application in water and wastewater treatment using FO.

Zeng et al., (2013) used reduced graphene oxide (rGO) composite hydrogels as draw solutes. The composites were prepared by incorporating 0.3 wt% to 3 wt% rGO into poly(sodium acrylate) (PSA) and poly(sodium acrylate)-poly(*N*-isopropylacrylamide) (PSA-NIPAM). The results showed an enhanced flux for composite hydrogels, with a small percentage of rGO. Compared to the pure hydrogels, PSA 1.2 wt% rGO and PSA -NIPAM 1.2 wt% rGO showed a greater than 200% increase in flux when 2000 ppm NaCl was used as a feed. With DI water as feed, PSA 1.2 wt% gave a water flux of 8.2LMH and PSA-NIPAM 1.2 wt% gave 6.8 LMH. The fluxes for feed water containing 2000 ppm of NaCl was lower than than achieved with DI water. The addition of rGO also enhanced the solar dewatering of the composite polymers.i.e. Recovery of freshwater from a swollen hydrogel by placing it under a sunlight stimulator. Results were not presented for the effect of rGO on fouling potential or the cost of manufacture at large scale.

Stone et al., (2013) synthesized two novel, multivalent salts based on phosphazene chemistry (**Figure 2.8**). Hexachlorocyclotriphosphazene was reacted with the sodium salt of 4-ethylhydroxybenzoate to yield hexa(4-ethylcarboxylatophenoxy) phosphazene, followed by neutralization with NaOH or LiOH, yielding water-soluble sodium and lithium phosphazene salts. The lithium salt was found to be more ionized

than the sodium salt. Nearly 7LMH of flux was achieved for the Li salt, followed by 6LMH for the Na salt at 0.067 M draw solution concentration. However, due to the high pH (8) of the salt, hydrolysis of the membrane was observed which could eventually lead to its degeneration.

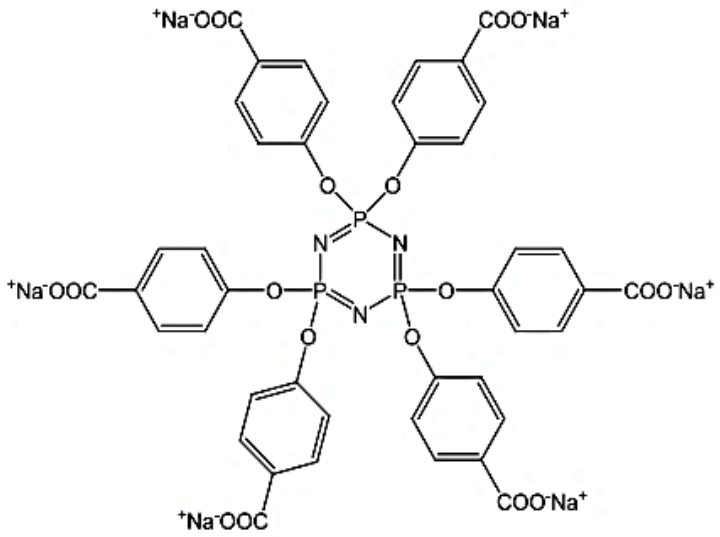


Figure 2.8 Hexa(4-ethylcarboxylatophenoxy)phosphazene salt structure (Stone et al., 2013)

Micellar draw solutions (using cationic and anionic surfactants) have been tested in FO. The fluxes reported were quite high (4-13 LMH) and the reverse solute transport was 3-300 times less than that of NaCl under comparable conditions. The surfactants were easily recovered (up to 99%) using a UF cell, and an attempt was also made to recover them using Krafft temperature solubility swing phenomenon (i.e. by a temperature swing). Fluxes between 4-13 LMH were achieved and the micellar solutions were presented as potential draw solutions for forward osmosis (Gadelha et al., 2011). However, no attempt was made to develop a continuously circulating and regenerating FO system, and scale-up remains uncertain.

2.4 Membrane Distillation

For draw solution recovery in the current study, membrane distillation was applied and is therefore discussed in the current section.

Membrane distillation is a thermally-driven membrane separation process that allows only vapours to pass through a hydrophobic microporous membrane. The major driving force in MD is the vapour pressure difference induced by the temperature difference across the membrane. This process has found its applications in various areas, particularly in seawater desalination, wastewater treatment and food concentration (Alkhudiri et al., 2012).

MD offers several advantages over other membrane technologies, such as;

- A lower operating temperature than other conventional separation technologies,
- The hydrostatic pressure is lower than for pressure-driven membrane processes,
- The average membrane pore size is larger (ranging from 10nm to 2μm) leading to higher flux,
- MD has higher rejection factor and suffers less fouling,
- It has the feasibility to be combined with other membrane technologies, such as UF (Gryta et al., 2001),
- It is cost effective and can utilise other energy sources, such as solar energy.

There are some drawbacks of the technology as well, such as;

- Heat loss by conduction is quite high,
- It is susceptible to temperature and concentration polarization,

- Lastly, trapped air in the pores results in mass transfer resistance (Alkhudiri et al., 2012).

According to the operating method for the cool side of the membrane, MD can be classified as Direct Contact Membrane Distillation (DCMD), Vacuum Membrane Distillation (VMD), Air Gap Membrane Distillation (AGMD) and Sweeping Gas Membrane Distillation (SGMD). DCMD (**Figure 2.9**) is the most studied configuration, because of easy installation (Liu & Wang, 2013).

Electrodialysis (ED), nanofiltration (NF) and reverse osmosis (RO) have drawn more attention for their separation capabilities, but have problems due to the formation of polarization films, fouling, and by-products which may become contaminated with microbes. This can be overcome by using MD for desalination and other water treatment applications. The possibility of operation via the utilisation of waste heat for MD makes its application increasingly attractive for wastewater treatment. Most of the large distillation units in the world derive their source of thermal energy from steam that has been used for other purposes e.g. power generation (Boubakri et al., 2014); however, the use of MD at a full industrial scale is still rare (Kezia et al., 2015).

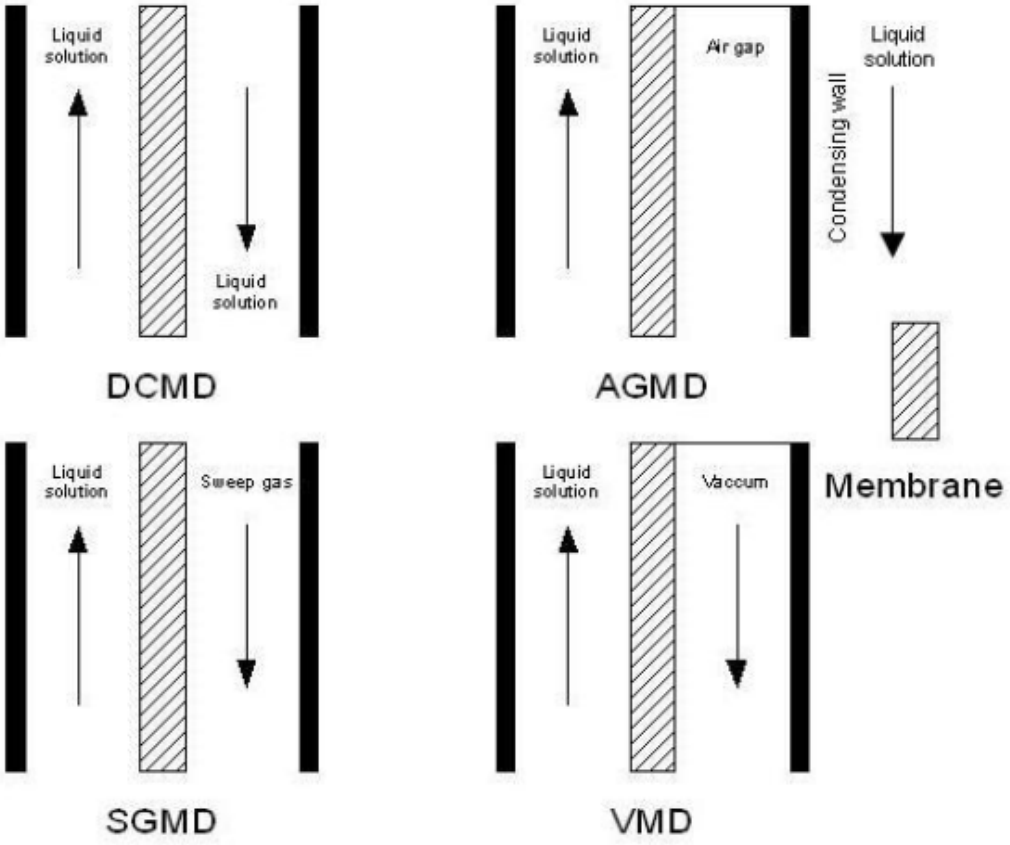


Figure 2.9 Membrane distillation configurations: DCMD; AGMD; VMD; SGMD

2.4.1 MD Membrane Characteristics

The hydrophobic membrane can be prepared using polymers with low surface energy, such as Polypropylene (PP), Polytetrafluoroethylene (PTFE), and Polyvinylidene fluoride (PVDF) (Gryta, 2012). The hydrophobicity of the membrane is quantified through liquid entry pressure (LEP). The liquid should not enter the membrane pores, so the pressure applied should be less that the LEP. LEP can be estimated via the capillary pressure equation:

$$\Delta P = P_f - P_p = \frac{-2B\gamma_i \cos\theta}{r_{max}} \quad \text{.....2.24}$$

Where, P_f and P_p are the hydraulic pressure on the feed and permeate side, *B* is a geometric pore coefficient (it is 1 for cylindrical pores), γ_i is liquid surface tension, θ is the contact angle and r_{max} is the maximum pore size (Franken et al., 1987).

The MD membrane should have low resistance to mass transfer, and low thermal conductivity to prevent heat loss across the membrane. The membrane should have good thermal stability against temperature and harsh chemicals. Membrane thickness, therefore, has an important role in MD. There is an inverse relationship between membrane thickness and permeate flux (Alkhudiri et al., 2012).

The thermal boundary layers are established because vaporization occurs on the hot side of the membrane and condensation takes place on the other, cool side of the membrane. The ratio of the temperature change across the membrane to that between the bulk liquid and vapour is known as the temperature polarization coefficient (Schofield et al., 1987); see equation 2.33 below.

Although the tendency for fouling in MD is significantly lower than that in pressure driven membrane filtration where particles are evident to deposit on membrane surface, but it can still arise in MD. Fouling in MD depends on the membrane properties, module geometry, feed solution concentration and the operating conditions of the setup (Shirazi et al., 2010). Inorganic fouling or scaling, particulate or colloidal fouling, organic fouling and biological fouling may all take place in MD. Scaling of the membrane may lead to partial membrane wetting, which then leads to additional thermal resistance and hydrophobic breakdown, allowing the draw solution to move through the membrane directly (Gryta, 2005).

2.4.2 Applications of Membrane Distillation

MD has found potential applications in (1) clean water production, (2) food concentration, and (3) heavy metal removal and wastewater treatment. A few such studies are presented here.

Gunko et al., (2006) concentrated apple juice using DCMD with a PVDF membrane having a pore size of 0.45 μm. Nearly 50% of solid content was obtained in the retentate when the permeate flux reached 9 LMH. However, when the concentration of the juice reached >60% in solid content, productivity was reduced to < 4 LMH (3-3.8LMH). The study was more focused on studying the membrane properties with time rather than its long term application in reconcentration. Fouling and temperature polarization were not presented in detail.

Shirzai et al., (2012) studied desalination using three hydrophobic membranes available commercially, specifically PP, PVDF, and PTFE in a DCMD configuration. The results showed that the feed temperature is the most important parameter in MD. The PTFE membrane showed better performance for fouling and long-term operation.

Hsu et al., (2012) used NaCl and real seawater as a feed for an MD desalination process. A PTFE membrane with a pore size of 0.2μm and a thickness of 175 μm was used in the study. The accumulation rate of scaling was depressed by reducing polarization when NaCl was used as feed; however, this effect was not very obvious when seawater was used as feed (Hsu et al., 2012).

Schofield et al., (1990) also studied pure water, NaCl, and sugar as feed with a PVDF membrane having a pore size of 0.4μm. Concentrations up to 25 and 30% salt and sucrose solute gave fluxes 60-70% lower than that of pure water feed. The

decline in flux for NaCl was due to vapour pressure reduction, while in the case of sucrose, the decline in flux was attributed to increasing viscosity.

MD has also been recommended for heavy metal removal from wastewater. Solutions containing Nickel were tested and upto 99% rejection was reported (Zolotarev et al, 1994). Oil mill wastewater treatment and concentration have also been investigated with MD. The commercially available membranes polytetrafluoroethylene (TF200) and polyvinylidene fluoride (GVHP) were used in a DCMD configuration to test permeate water quality and polyphenols retention. The membrane TF200 showed a better separation coefficient (99%) after 9 hours of DCMD operation than the membrane GVHP (89%) (El- Abbasi et al., 2013). In general, PTFE membranes have been reported to show better flux and rejection in MD application.

Yu et al., studied the application of DCMD for the treatment of cooling tower blowdown water (CTB) using a bench scale set up with a PP membrane having a pore size of 0.1µm. A flux of 30 LMH with nearly 99.95% salt rejection was achieved at 60ºC. Membrane fouling was found to be the major issue with such complex feed solutions. Thus, scaling was investigated and it was found that in silica free CTB water, insoluble calcium carbonate is the major contributor, while in the presence of silica, calcium carbonate, silica and sulfate precipitated together. This scaling resulted in a decrease in the performance efficiency by reducing the flux and salt rejection. Therefore, membrane cleaning was applied to recover the membrane performance (Yu et al., 2013).

DCMD has also been applied for ammonia removal in wastewater, as the latter is a common wastewater pollutant that results in eutrophication in water bodies. A PVDF

HF membrane with a pore size of 0.22μm was used. Ammonium chloride was added into distilled water and the pH adjusted. The ammonium stripping was observed. The permeate had a receiving solution of 0.01 mol/L sulfuric acid. Ammonia removal of up to 99.5% was achieved within 105 minutes. Feed pH was an important factor in MD performance up until a pH of 12.2. The increase in feed temperature and velocity also increase the removal efficiency of the pollutant (Qu et al., 2013).

Thermal cogeneration plants need purified water at various steps, such as boilers, district heat make-up water systems, and flue gas condensate treatment. A rig was deployed at Idbäcken Cogeneration Facility (Nyköping, Sweden) with a five-module MD unit capable of producing 1–2 m^3/day of purified water. A district heating supply line was employed for heating while municipal water was used for cooling; feedstocks included municipal water and flue gas condensate. The flux of MD was highly dependent on the feedstock temperature, flow rate and temperature difference across the membrane. The performance was stable for up to 370 hours of operation. After 13 days of operation, both scale formation and permeate flow rate deterioration occurred. However, the clogging was partial and performance was recovered again very close to the original performance (Kullab & Martin, 2011).

Despite better performance MD also faces issues like fouling, CP and TP. To understand the fouling better, temperature and concentration polarization is discussed in the following section.

2.4.3 Heat and Mass Transfer in MD

Heat and mass transfer occur simultaneously in MD operation (**Figure 2.10**). Heat is transferred between the bulk feed and the membrane surface via conduction, while across the membrane heat transfer takes place by conduction and convection

from the hot feed to the cold permeate. Therefore, heat transfer with additional terms accounting for latent heat carried by vapours is used to represent the process.

Heat transfer across the membrane can be represented by the following equations:

$$Q_f = h_f(T_f - T_{fm}) \quad \text{2.25}$$

$$Q_p = h_p(T_{pm} - T_p) \quad \text{2.26}$$

$$Q_m = N\lambda + \frac{K_m}{\delta}(T_{fm} - T_{pm}) \quad \text{2.27}$$

Where Q is the heat flux, h is the heat transfer coefficient, K_m is the thermal conductivity across the membrane, T is the temperature, δ is the membrane thickness, N is the transmembrane flux and λ is the latent heat of vaporization (Qtaishat et al., 2008, Schofield et al, 1987).

Thermal conductivity can be represented by:

$$K_m = \varepsilon K_g + (1 - \varepsilon)K_{mp} \quad \text{2.28}$$

Where ε is the porosity of the membrane, K_{mp} is the thermal conductivity of the membrane, K_g is the thermal conductivity of the gas/ vapours. At steady state, the thermal flows should all be the same i.e.

$$Q_f = Q_p = Q_m \quad \text{2.29}$$

MD flux in DCMD is generally presented as

$$N = K(P_{fm} - P_{pm}) \quad \text{2.30}$$

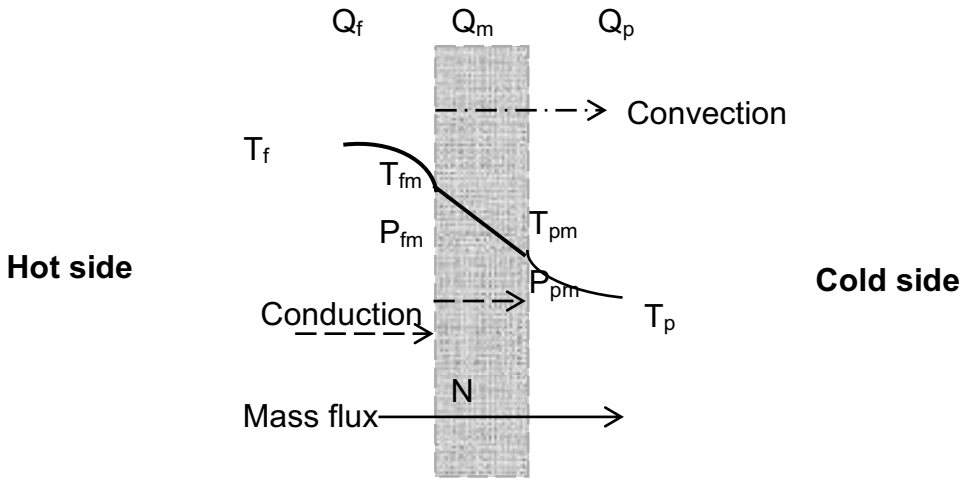


Figure 2.10 Heat and mass transfer across a DCMD membrane (Adapted from Histove et al., 2015)

Where P is the partial pressure of water vapour and K is the membrane coefficient. K depends on the diffusivity of the water vapour and on the membrane properties.

For pure water, the relationship between water vapour pressure and temperature (Khayet & Matsuura, 2001) is given by the Antoine equation:

$$\mathrm{P_w^0} = \exp\left(23.20 - \frac{3816.44}{\mathrm{T}-46.13}\right) \quad \text{.....2.31}$$

Where T is the absolute temperature. For aqueous solution, the vapour partial pressure is given by equation 2.32, where α_w is the activity coefficient of water.

$$\mathrm{P_w} = \alpha_\mathrm{w}\mathrm{P_w^0} \quad \text{.....2.32}$$

2.4.4 Temperature Polarization (TP)

Temperature polarization is the ratio of the temperature change across the membrane and the temperature difference between the bulk liquid feed and the permeate. It develops in non-isothermal processes and reduces the driving force of

the permeate flux (Gryta, 2008), since the difference in the vapour pressure on each side of the membrane is reduced.

Schofield et al (1987), expressed temperature polarization coefficient as

$$\mathrm{TPC} = (\mathrm{T_{fm}} - \mathrm{T_{pm}}) / \left(\mathrm{T_f} - \mathrm{T_p}\right) \quad \text{.....2.33}$$

Thermal efficiency η is also used to assess the amount of useful heat flux in an MD system:

$$\eta = \frac{N\lambda}{Q} \quad \text{.....2.34}$$

Where Q is the overall heat transfer for the feed stream.

2.4.5 Fouling in MD

Lokare et al., (2017) evaluated the performance of several membranes for the DCMD treatment of produced water. Hydraulic fracturing used for natural gas extraction from unconventional onshore resources generates large quantities of produced water that needs to be managed. PP and PTFE membranes showed the highest permeate flux, presumably due to a reduced tendency for fouling. DCMD was able to achieve 73% water recovery at a TDS of 300,000 mg/L. Fouling by iron oxide showed a negligible impact on permeate flux. As mentioned previously, the fouling propensity is generally low in MD; however, fouling can still be the most challenging issue in MD.

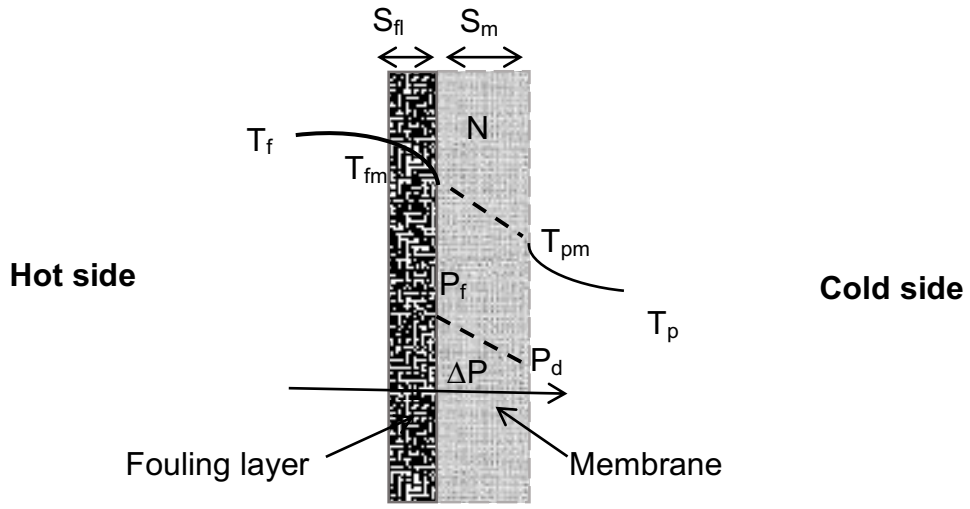


Figure 2.11 Temperature distribution in an MD process with a fouled layer

An MD membrane was analysed for fouling (Nguyen & Lee, 2015). The organic deposits characterized by FTIR (Fourier Transform Infrared Spectroscopy) were polysaccharides, proteins, and humic-like substances, while the inorganic foulants mainly consisted of calcium carbonate, calcium sulfate, and halite. NaOCl was added in the feed to control fouling and wetting, and 3% HCl was used to clean the membrane and was found to be very beneficial.

2.5 Membrane Bioreactors (MBRs)

Membrane bioreactor technology combines the activated sludge treatment with membrane filtration, where removal of suspended, dissolved and pathogenic material is achieved by filtration rather than gravity (Hasar, 2009). MBR technology is emerging as a wastewater treatment technology of choice over the conventional activated sludge process (ASP) (Lorhemen et al., 2016), but its economic feasibility and widespread application is still an issue.

MBR offers several advantages over conventional wastewater treatment plants such as;

- MBR can be operated to ensure simultaneous nitrification and denitrification and phosphorus removal by precipitation (Melin et al., 2006).
- The effluent is of high quality and the use of the membrane eliminates the need for secondary (to remove pathogens, dissolved and organic matter) and tertiary treatment (Bhatti et al., 2009) resulting in a smaller footprint.
- Operational conditions are more controlled, as an independent sludge retention time (SRT) and hydraulic retention time (HRT) can be maintained. At the same time, a high sludge concentration allows better treatment of wastewater.

The disadvantages of the MBR include;

- MBR is expensive to install and operate.
- Frequent monitoring and maintenance of the membrane is required.
- Certain limitations are caused by the need for temperature, pressure and pH values to satisfy membrane tolerances and the sensitivity of membranes to some chemicals.
- Oxygen transfer may be less efficient because of high MLSS concentration, and also if there is surplus sludge its treatability is doubtful (Melin et al., 2006).
- Membrane fouling reduces membrane filtration capacity by reducing filtration flux (Dias et al., 2003). Microbes responsible for treatment of wastewater are also responsible for biofouling of the membrane (Wagner and Loy, 2002).

Major microorganisms present in wastewater are bacteria, protozoa, metazoa, algae and fungi but bacteria make up most (95%) of all the wastewater

microorganisms in activated sludge, and have an important role in wastewater treatment (Gerardi, 2006).

Nutrient removal is done through two major processes:

- Fixed film processes
- Suspended growth processes

The fixed film processes are based on the ability of microorganisms to grow on surfaces because of the availability of food, and their protection from high velocity currents and other environmental conditions. Physical forces such as adhesion and adsorption are responsible for attachment.

As the adsorbed microorganisms grow and reproduce, extracellular polymeric substances (EPS) is produced and a gel matrix layer is formed on the surface; this film is known as biofilm. Removal of wastewater nutrients in fixed film processes is only attained when the wastewater is brought into contact with the biofilm. Simultaneous nitrification and denitrification (SND) occurs within flocs or inner zones of the biofilm that allows heterotrophic denitrifiers to produce nitrogen gas (Yang et al., 2009).

In suspended growth, the bacterial flocs are in continuous contact with wastewater. Bacteria, protozoa and metazoa dominate suspended growth processes (Curtis, 2003). Most of the bacteria are Gram negative heterotrophic and rod shaped in aerobic conditions, including *Pseudomonas, Chromobacter, Achromobacter, Alcaligenes* and *Flavobacterium*. Coliforms are said to enter wastewater from the influent and are not considered indigenous. Nitrifying bacteria as well as filamentous bacteria (*Beggiatoa, Thiothrix and Sphaerotilus*) are also present in wastewater and form biofilms.

Various kinds of bacteria play their role in treating wastewater and the important types are filamentous bacteria, methanogenic bacteria, polyphosphate accumulating bacteria, sulfate-reducing bacteria, nitrifying bacteria, and denitrifying bacteria (Reyes et al. 2015).

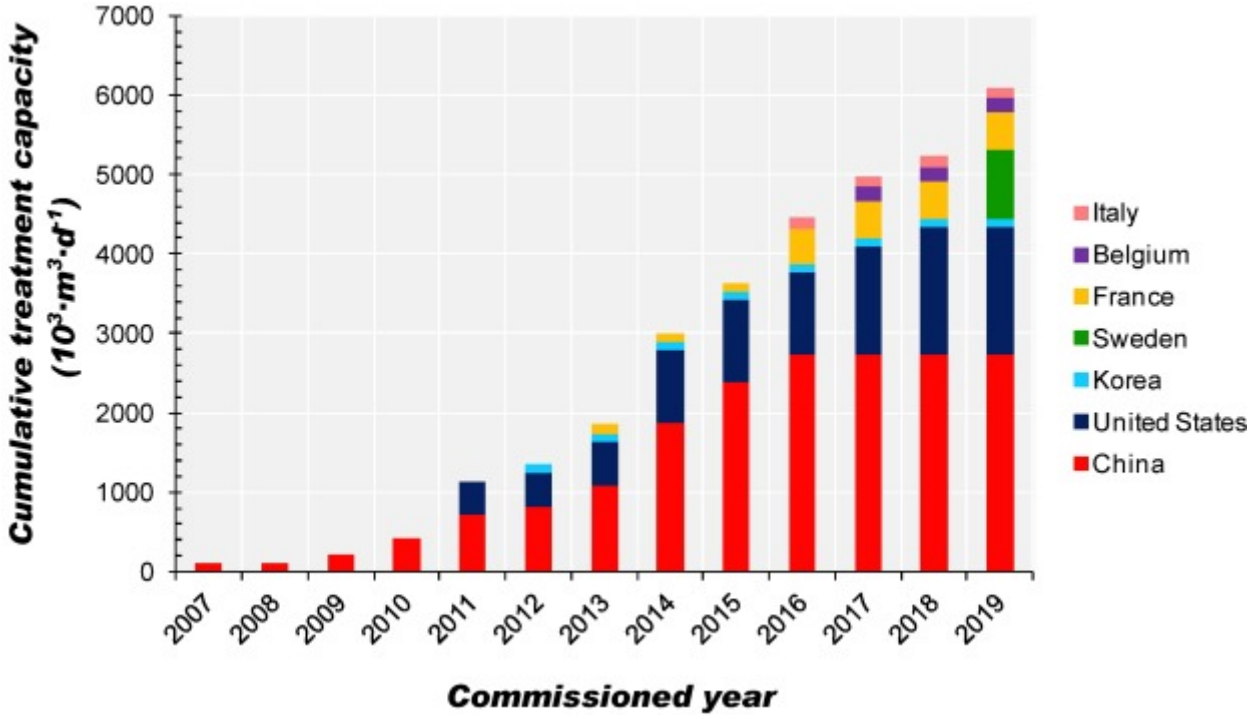


Figure 2.12 Development of the large-scale MBR plants around the world (the capacity of each plant > 100,000 m^3/d) (Meng et al., 2017)

Research on MBRs has been ongoing for several decades, and large-scale MBR plants have majorly been implemented in the gulf countries. However, its application worldwide is increasing, e.g. the commissioning in China has significantly increased in recent years (**Figure 2.12**).

2.5.1 Forward Osmosis Membrane Bioreactor (FO-MBR)

In an FO membrane bioreactor (MBR), a semipermeable membrane is placed in an activated sludge bioreactor that is continuously aerated to supply oxygen for the microbial growth (**Figure 2.13**). Osmosis results in permeation of water from the feed stream via the reactor tank to the draw stream. The diluted draw is then regenerated by processes such as membrane distillation and RO (Achilli et al., 2009).

Both submerged and external (side stream) configuration can be set in place for FO-MBR. The FO process when applied in the osmotic membrane bioreactor (OsMBR), offers several advantages compared to other membrane technologies, such as much higher rejection (an RO type membrane versus a microporous membrane) at a lower applied hydraulic pressure, more reversible fouling as compared to pressure driven systems, and less frequent backwashing. During osmotic backwashing in AL-FS mode, water flows from the support side of the membrane to the active side, thereby reversing the direction of flow through the FO membrane and potentially removing foulants on the active layer surface.

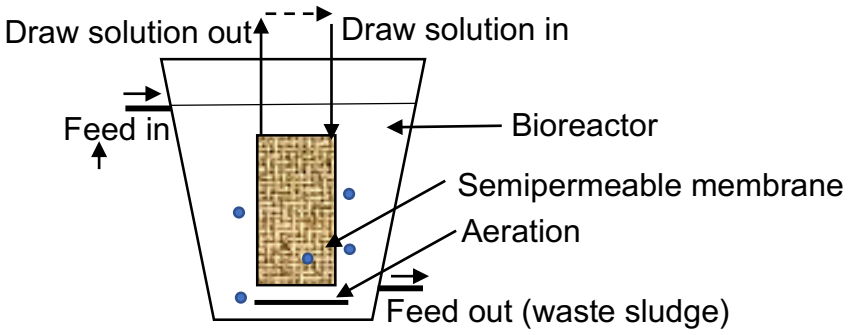


Figure 2.13 A simple graphical demonstration of a submerged FO-MBR (with a continuous draw and feed solution loop)

One major technical limitation of the FO-MBR is the salinity build-up occurring in the submerged OMBR tank; this is due to accumulation behind the membrane of salts from the influent, as well as reverse solute transport. This build-up affects the biodegradation efficiency due to the finite salinity tolerance of the organisms present in the reactor tank Optimising draw solutions, the selection of membranes, and operation at lower sludge retention time were all recommended to improve the performance of the FO-MBR (Wang et al., 2016). Although a continuous regeneration system in place can reduce the salinity build-up in the feed, extended membrane filtration units and independent operation of the FO-MBR can still face operational issues including fouling, power cost etc (Blandin et al., 2018).

A study (Blandin et al., 2018) aimed at retrofitting an existing MBR into an FO-MBR to minimise cost and salinity and to improve water quality was conducted. A flux of over 10 LMH was achieved. The study proved the possibility to (partly or fully) transform existing MBR facilities while improving existing performances obtained by other OMBR designs /configurations /membranes in the literature. Comparison between MBR and FO-MBR revealed that the low fouling propensity and low energy consumption claims are somewhat contradictory for FO-MBR. A high water flux and permeate quality can certainly be of interest in water reuse but technical and economic assessments are still needed to support application of the FO-MBR

Another recent study compared submerged and sidestream FO membrane module configurations (under similar conditions) in the FO-MBR (Morrow et al., 2018). The initial water flux and water flux after fouling versus time was the same for submerged and sidestream configurations. The steady-state water flux of fouled membranes was the same for submerged and sidestream configurations using two specific draw solution concentrations, leading to the concept of a homeostatic flux in FO-MBRs

similar to the critical flux in conventional membrane bioreactors. Thinner cake layers were formed in the sidestream configuration where fouling is mitigated with hydraulic crossflow as compared to the submerged configuration where fouling is mitigated via air scouring. Hydraulic pressure from recirculation pumping on the feed side of the sidestream configuration may have also resulted in a more compact cake layer over time. Note that the submerged configuration uses additional aeration for air scouring while in sidestream configuration additional pumping is needed for recirculation. A higher draw solution concentration increased fouling and scaling. All of these factors need to be taken into consideration for FO-MBR application

An FO-MBR with 1M NaCl as draw solution to treat wastewater showed 96%, 43% and 100% removal of PO_4^{3-}-P, NH_4^+-N, and total organic carbon. As reported in previous studies, an increase in salinity was observed in the feed tank due to reverse solute transport. Water flux was reduced with increasing salinity, with membrane fouling occurring at elevated salinity levels on the feed side. At 7-day intervals, 2.5 L of supernatant was withdrawn from the FOMBR for phosphorus recovery as magnesium phosphate and sodium hydrogen phosphite hydrate. The FOMBR enriched phosphate ions by six times, reducing the costs of chemical use for pH adjustment (Hunang et al., 2015).

A number of studies showing the removal efficiency of FO-MBRs is presented in Table 2.4, while FOMBRs are described in more detail in Table 2.5. It can be observed from Table 2.4 that greater removal efficiencies are achieved with FO-MBRs.

Table 2.4 A summary of the removal efficiencies of FO-MBRs for organics, nitrogen and phosphorus. (Wang et al., 2016)

Type	Wastewater	Removal efficiency					References
		TOC	COD	NH_4^+–N	TN	TP	
Submerged FOMBR	Synthetic sewage	>90%	–	–	–	–	Wang et al., 2014
Submerged FOMBR	Synthetic sewage	99.8%	–	97.7%	–	–	Achilli et al., 2009
Submerged AnFOMBR*	Synthetic sewage	–	96.7%	–	–	100%	Chen et al., 2014
Submerged AnFOMBR	Synthetic sewage	92.9%	–	–	–	–	Tang & Ng, 2014
Submerged AnFOMBR	Synthetic sewage	–	95%	–	–	100%	Gu et al., 2015
Submerged FOMBR	Synthetic sewage	98%	–	80–90%	–	>99%	Qiu & Ting., 2014
Submerged FOMBR	Synthetic sewage	>99%	–	–	–	–	Lay et al., 2011
Submerged FOMBR	Synthetic sewage	98%	–	98%	–	–	Qiu & Ting, 2013
Submerged MFFO-MBR**	Synthetic sewage	>99%	–	>98%	–	–	Wang et al., 2014
Submerged FOMBR	Real sewage	–	>96%	–	>82%	>99%	Holloway et al., 2014
MBR	High strength landfill leachate	-	70%	96%	95%	-	El-Fadel & Hashisho, 2014

* Anaerobic FO-MBR, ** Hybrid Microfiltration FO-MBR, *** Hybrid Ultrafiltration FO-MBR

Table 2.5 Summary of forward osmosis membrane bioreactors (FO-MBRs) in literature (Wang et al., 2016)

Configuration	Membrane	Producer	Type	Orientation	Draw solution	Temperature (°C)	Sludge Concentration (g/L)	SRT (d)	Operating time	Stable salinity	Initial flux (LMH)	Steady flux (LMH)	References
Submerged	CTA-FO	HTI	FS	AL-FS	1 M NaCl	25±0.5	1.02±0.10	10	32 d	50 mS/cm	7.36	2.45	Wang et al., 2014
Submerged	CTA-FO	HTI	FS	AL-FS	1 M NaCl	25±0.5	1.06±0.12	15	39 d	65 mS/cm	8.62	1.82	
Submerged	TFC-FO	Made in NTU	HF	AL-DS	0.5 M NaCl	23	–	10	55 d	6–7 g/L	23	3.9±0.5	Zhang et al., 2012
Side-stream	CTA-FO	HTI	FS	AL-FS	0.5 M NaCl	20±2	10	–	7–8 h	–	5.8	5.1	Cornelissen et al., 2008
Side-stream	CTA-FO	HTI	FS	AL-DS	0.5 M NaCl	20±2	10	–	7–8 h	–	7.1	6.2	
Submerged	CTA-FO	HTI	FS	AL-FS	50 g/L NaCl	23±1	5.5	15	28 d	4 g/L	11	9	Achilli et al., 2009
Submerged anaerobic	CTA-FO	HTI	FS	AL-FS	0.5 M NaCl	25	3.9–4.6	90	155 d	20.5 mS/cm	9.5	3.5	Chen et al., 2014
Submerged anaerobic	CTA-FO	HTI	FS	-	0.712 M NaCl/0.7 M $NaSO_4$	–	0.376/1.17	30	100 d	35/11 mS/cm	4.5/4.7	0.25/0.96	Tang & Ng, 2014
Submerged anaerobic	CTA-FO	HTI	FS	AL-FS	0.5 M NaCl	35	–	90	120 d	20 mS/cm	10	3.0	Gu et al., 2015
Submerged	CTA-FO	HTI	FS	AL-FS	48.4 g/L $MgCl_2$/49 g/L NaCl	23.2±0.5	7	50	63 /40 d	15.1/33 mS/cm	7.8	6.46/5.62	Qiu & Ting, 2014
Submerged	CTA-FO	HTI	FS	AL-FS	0.5 M NaCl	20–22	–	20	73 d	7.2–8.1 g/L	3.2	2.7	Lay et al., 2011

Side-stream	CTA-FO	HTI	FS	AL-FS	0.5 M NaCl	20±2	5	–	14 d	–	5.5	About 8.0	Corneliissen et al., 2011
Side-stream	CTA-FO	HTI	FS	AL-DS	0.5 M NaCl	20±2	5	–	7 d	–	7.5	About 10	
Side-stream	CTA-FO	HTI	FS	AL-FS	0.5 M NaCl	32±2	4.953	–	150 h	–	7.2	7.2	Qin et al., 2010
Submerged	CTA-FO	HTI	FS	AL-FS	48.4 g/L $MgCl_2$	23±0.5	7	50	80 d	14-16 mS/cm	7.8	5.45	Qiu & Ting, 2013
Submerged MFO-MBR	CTA-FO	HTI	FS	AL-FS	1 M NaCl	23±0.5	–	10	45 d	5 mS/cm	10.5	5.5	Wang et al., 2014
Submerged	CTA-FO	HTI	FS	AL-FS	32 g/L NaCl	25	–	70	124 d	20 g/L	4.2	0.5	Holloway et al., 2014
Submerged UFO-MBR	CTA-FO	HTI	FS	AL-FS	36 g/L NaCl	25	1.6–3.6	30/60	125 d	<5 g/L	6	4.8	
Side-stream	CTA-FO	HTI	FS	AL-DS	1.5 M NaCl	22.5±0.1	3.4–3.7	–	7 d	4.13 g/L	12	3	Alturki et al., 2012
Submerged	TFC-FO	Made in NTU	HF	AL-DS	0.5 M NaCl	20–22	–	10	–	Around 15 mS/cm	23	3.8±0.3	Lay et al., 2012

2.6 The FO-MD hybrid

Water and wastewater reclamation using FO involves two steps; dilution of the draw solution during the osmotic flow from feed to draw, followed by water reclamation from the diluted draw solution. The recovery method is principally determined by the nature of the selected draw solute. As described in section 2.2, polymer based hydrogels and NH_4CO_3 have been recovered using moderate low-grade heat, because of their ability to change phase with temperature (Li et al., 2011; McGinnins et al., 2002). Magnetic nanoparticles have been recovered by application of a magnetic field because of their magnetic properties (Ge et al., 2011) and by UF because of their larger physical/molecular sizes (Ling & Chung, 2011). 2-methylmidazole based draw was recovered using an FO-MD hybrid based on thermal stability, and divalent inorganic solutes (Na_2SO_4) have been reported to be recovered by FO-NF because of lower molecular weight (Zhao et al., 2012a).

FO-MD is a membrane-based hybrid technology, consisting of FO and MD units where FO draws clean water from a feed such as wastewater and MD re-concentrates the diluted draw solution (**Figure 2.14**). This integration provides high product water quality (the membrane only allows water vapours to pass through), low fouling tendency (because of the membrane being hydrophobic) and the potential utilization of low-grade, industrial waste heat due to the potential for vapour formation at lower temperatures (Ge et al., 2012). Although the FO-MD hybrid has been studied for the concentration of protein solutions (Wang et al., 2007), olive mill wastewater treatment (El-Abbasi et al., 2013), dye wastewater treatment and sewer mining wastewater (Xie et al., 2013), detailed studies on the use of FO-MD for municipal wastewater treatment using novel draw solutions (as opposed to more

conventional ones, such as inorganic salts) is rather scarce. The FO-MD hybrid can be an option for water reclamation compared to pressure intensive membrane filtration systems, as it has demonstrated higher and more stable flux and resulted in a high-quality product water (El-Abbasi et al., 2013; Xie et al., 2013). A summary is given for all studies performed previously in **Table 2.6.**

Advantage of the hybrid systems is that they provide a double barrier to the feed (in terms of contaminants, microorganisms etc) and therefore ensure high quality product water. Particular recovery systems such as magnetic fields and heat are very specific to suitable draw solutes. However, although MD is less likely to foul, fouling can still be an important issue in MD application. For its longer-term application, coupling it with processes like FO is recommended, as FO pre-treats the feed and allows the MD to operate at lower temperature without organic and inorganic scaling. Such a process allows the DS to be recovered and reused continually, and is an ideal hybrid system for advanced wastewater treatment (Xie et al., 2013). Thus, the low fouling and low energy requirement tendency in FO can be easily combined with high quality permeate production in MD (Wang et al., 2011).

On the other hand, the term ‘low energy consumption’, long associated with FO systems, is only valid when the regeneration systems are not required or applied. The challenge now facing FO is that the use of FO hybrid systems to allow the regeneration increases the capital cost as well as the energy demand of the overall system (Chekli et al., 2016).

Wu et al., studied rejection of Hg, Cd, and Pb and the effect of coexisting metals on Hg removal through Forward Osmosis (FO) and Membrane Distillation (MD (Wu et al., 2017). More than 97% rejection for each metal was achieved through the FO

system. It was observed that Hg^{2+} rejection increased with increase in the concentration of the coexisting metals. Approximately 1–10 ppb Hg from the feed solution transported into the draw solution due to permeation. An FO–MD hybrid system was set in place to allow for complete removal of the heavy metals. Approximately 100% rejection of Hg^{2+} was achieved and a stable water flux was observed.

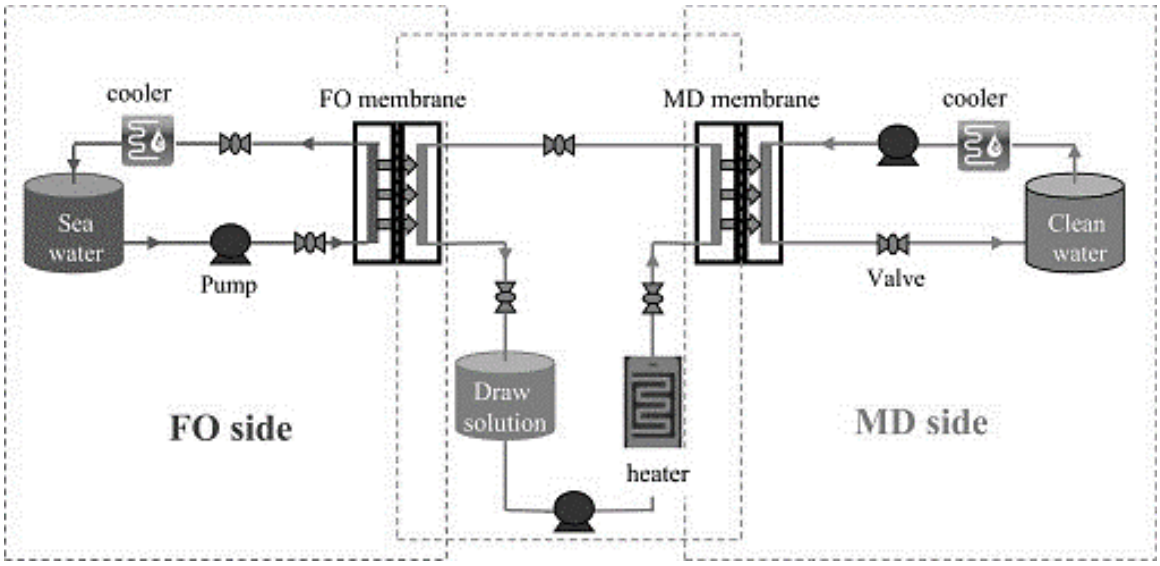


Figure 2.14 Schematic diagram of FO-MD hybrid for desalination (Wang et al., 2015)

More recently, a moving sponge barrier osmotic MBR was integrated using a salt tolerant microbial community. An average water flux of 2 L/m^2 h was achieved during a 92-day operation when 1 M $MgCl_2$ was used as the draw solution with up to 100% efficiency for nutrient rejection. An HTI CTA membrane was used in an osmotic MBR setup while a polytetrafluoroethylene MD membrane (pores = 0.45 μm) was used to regenerate the draw solution. The moving sponge biocarrier- OsMBR/MD hybrid system demonstrated its potential for saline wastewater treatment, with 100% nutrient removal and 99.9% conductivity rejection (Nguyen et al., 2017).

Table 2.6. Summary of hybrid FO–MD processes with different draw solutes (Wang et al., 2015)

Reference	Feed and draw solute	Application	FO/MD flux (LMH)	Remarks
Yen et al., 2010	2-methylimidazole-based compounds	Desalination	11/7 (Feed: DI water) (MD at 70 °C)	(1) Low reverse draw solute leakage.
Wang et al., 2011	NaCl	Protein concentration	7–9/17 (Feed: Protein solution) (MD at 60 °C)	(1) High water flux; (2)High reverse draw solute leakage
Ge et al., 2012	Polyelectrolytes	Treatment of dye-containing wastewater.	15-38/9-23 (Feed: Dye-containing wastewater) (MD at 80 °C)	(1) Excellent dye rejection; (2)Viscosity increases rapidly with concentration; (3) Potential fouling of MD membranes.
Su et al., 2013	$MgCl_2$	Treatment of heavy metal containing wastewater	12.6-19.9/13-16.2 (Feed: Heavy metal containing wastewater) (MD at 80 °C)	(1) High water flux; (2)High reverse draw solute leakage.
Xie et al., 2013	NaCl	Treatment of sewer mining wastewater	4-8/4-8 (Feed: Sewer mining wastewater) (MD at 40 °C)	(1)~80% water recovery; (2)Additional granular activated carbon adsorption or ultraviolet oxidation was required to remove the accumulated trace organic contaminants (TrOC).
Xie et al., 2014	$MgCl_2$	Extraction of orthophosphate and ammonium from anaerobically digested sludge	4-10/5-8 (Feed: Anaerobically digested sludge) (MD at 40 °C)	(1) Excellent rejection (2) Accelerated membrane fouling.

Zhang et al., 2014	NaCl	Treatment of oily wastewater containing petroleum, surfactant, NaCl and acetic acid	40/5.8 (Feed: Oily wastewater) (MD at 60 °C)	(1) >90% water recovery; (2) Reverse draw solute leakage.
Zhao et al., 2012	Thermo-responsive co-polymer	Seawater desalination	4/2.7 (Feed: Seawater) (MD at 60 °C)	(1) High FO flux/Low reverse salt flux; (2) Potential risk for membrane fouling.
Wang et al., 2015	Na_5Fe–CA	Seawater and brackish water desalination	19.2/32 (Feed: DI water) 3.9-6/32 (Feed: Seawater) (MD at 60 °C)	(1) High FO flux/Low reverse salt flux; (2) Low risk for membrane fouling.

2.7 Conclusions

- As mentioned in the introduction and from the discussion on draw solutions it can be observed that FO, FO-MBR and FO-MD hybrid systems mostly use NaCl or $MgCl_2$ as the draw solution and DI water as a feed to achieve higher flux. Although a range of novel draw solutions have been tested (section 2.2) for FO their use has not continued in further studies. There is therefore a need for study that compares such simple draw solutions with novel draw solutions especially in FO-MBR and FO hybrid configurations.
- Similarly, the membranes that have been tested have also focused on NaCl or $MgCl_2$ as a draw solution. There is a need for the research on FO membranes and FO draw solutions to be combined, especially for large-scale application of the systems.
- Some studies on FO-MBR have focused on RST and salinity build-up with time but toxicity studies of the draw solutes over a longer period of time have not been studied.
- Although the FO-MD hybrid has been studied for olive mill wastewater treatment (El-Abbasi et al., 2013), dye wastewater treatment (Ge et al., 2012) and sewer mining wastewater (Xie et al., 2013), detailed studies on the use of FO-MD for municipal wastewater treatment using novel draw solutions is rather scarce and in this thesis, we have tried to evaluate this area of wastewater treatment.

This gap in research in FO aligns with the research objectives of the current study and will be addressed in chapters to follow.

Chapter 3

Comparative performance of a Nano filtration (NF) membrane and a traditional FO membrane for use in a Lab Scale Forward Osmosis Membrane Bioreactor (FO-MBR)

3.1 Introduction

The overall aim of this thesis was to perform an engineering-oriented study to examine the component parts and integrated operation of a continuous and feasible FOMBR-MD system for the treatment and recycle of wastewater. Developing an appropriate combination of membrane and draw solution was a key task, and the research question addressed by this chapter was to ask whether the use of a higher pore- size Nano-filtration (NF) membrane in combination with high molecular weight novel draw solutions for forward osmosis could improve the overall performance of FO-MBR systems; this would be achieved by improving flux without causing excessive reverse solute transport nor toxicity to the feed bacterial consortium.

A single layer nanofiltration membrane was used in this study alongside the HTI FO membrane. Draw solutions were evaluated to test the above hypothesis; relatively higher fluxes will be observed for NF membranes, while potentially higher reverse solute transport might be circumvented by the use of higher molecular weight draw solutions. Inorganic draw solutes (NaCl, Na_3PO_4), Surfactants (TEAB, SDS), and Polyelectrolytes (PDAC, PEGBE) were tested as draw solutes. Fluxes, microbial toxicity and viscosity were observed for the draw solutions.

The basis for this study was to compare the commercially available HTI membrane with a single layer NF membrane for performance (provided by Chuyang Tang, University of Hong Kong), using different molecular size draw solutes and using a biologically active feed. A single layer NF membrane was explored because the conventional RO style FO membranes have very small pore size and a very thick support layer, both of which can contribute to a decline in FO Flux. Thus, the ultimate objective of the current study was to investigate whether the single layer NF membrane can potentially outperform or even replace the commercial double layer FO membranes.

3.2 Methodology

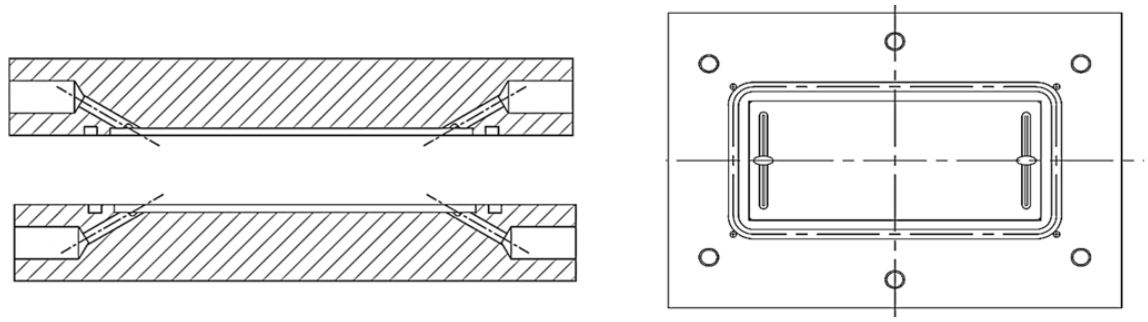
3.2.1 Establishment of FO-MBR

Bench-scale Forward Osmosis Setup

The forward osmosis bench scale setup consisted mainly of a flat sheet membrane module fitted into an acrylic membrane cell (**Figure 3.1**). The cells were fabricated with symmetrical flow channels on both sides of the membrane and sealed with a nitrile rubber gasket. Spacers were placed on each side of the membrane, as it disrupts the concentration boundary layer and increases the permeation rate (Yun et al., 2011). The membrane had an effective surface area of 47.25cm^2. Water flux was calculated using equation 3.1:

$$J=\frac{\Delta \mathbf{m}}{\mathbf{A}\Delta \mathbf{t}} \quad \text{.....3.1}$$

Where J (LMH) is the permeate flux, Δm is the increase in volume of permeate water (L); A is the effective surface area of the membrane (m^2); Δt is the time (h).



(a) (b)

Figure 3.1 Schematic diagram for the external membrane cell: (a) Section of top and bottom plate; (b) Plan view of a single plate.

Similarly, reverse solute transport was calculated using equation 3.2:

$$J_s=\frac{V_t C_t - V_0 C_0}{At} \quad \text{.....3.2}$$

Where J_s (GMH) is the reverse solute transport for the draw solution, C (g) is the concentration and V (l) is the volume; subscript 0 indicates zero time and t indicates t hours.

A schematic diagram for the bench scale setup is presented in **Figure 3.2**

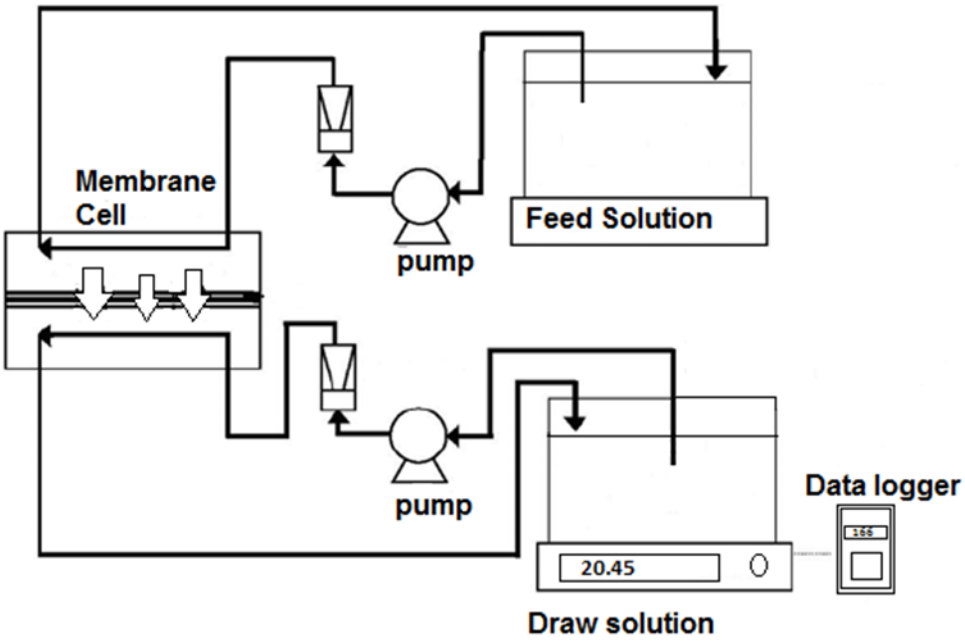


Figure 3.2 Forward osmosis (FO) bench scale setup showing a feed solution and draw solution loop, the tank for the latter being placed on a weighing balance

A forward osmosis membrane bioreactor was established for the treatment of synthetic wastewater. To establish a bioreactor, *Bacillus subtilis* was grown overnight in an incubator at 30°C and inoculated in a 1000ml flask containing municipal synthetic wastewater (**Table 3.1**). *B. subtilis* is known for its ability to aid in digesting waste matter in a sceptic system and was readily available in the lab, and was therefore chosen as monoculture in FO-MBR. Note that a full consortia, as present in activated sludge, was not employed in this work, due to health and safety restrictions in the lab. This flask was placed in a shaking incubator at 120 rpm for 24 hours and used as feed solution for the FO-MBR. A mechanical mixer was placed in the bioreactor to ensure the solution always remained homogenous and to ensure uniform distribution of bacterial species.

Table 3.1 Chemical composition of synthetic wastewater used in FO-MBR studies (Khan et al., 2013)

Chemicals	Formula	Quantity (mg/L)
Glucose	$C_6H_{12}O_6.H_2O$	514
Ammonium Chloride	NH_4Cl	190
Potassium di-Hydrogen Phosphate	KH_2PO_4	55.6
Calcium Chloride	$CaCl_2$	5.7
Magnesium Sulphate	$MgSO_4.7H_2O$	5.7
Ferric Chloride	$FeCl_3$	1.5
Manganese Chloride	$MnCl_2.4H_2O$	1
pH buffer	$NaHCO_3$	142.8

3.2.2 Chemicals and Solutions

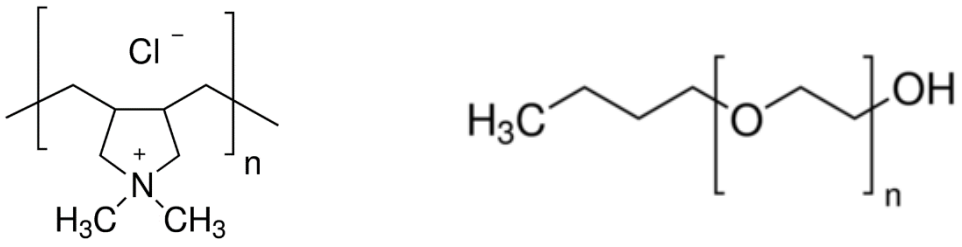
All chemicals were of lab grade and purchased from Sigma Aldrich, majority for the use as draw solutes. Organic and inorganic draw solutes of varying molecular weight were chosen to understand the performance of an FO-MBR for treatment of municipal wastewater, with AL-DS configuration when DI water was used as a feed (to avoid ICP in the support layer), and AL-FS configuration when synthetic wastewater with live bacteria was used as a feed (to avoid fouling by the feed in the support layer).

Table 3.2 Summary of the draw solutions used in the current study; * denotes Mol Wt of each monomeric unit, ** denotes average molecular weight of the polyelectrolyte solution

Draw Solutes (Chemical formula)	Type	CMC (mol/L)	Mol. Wt. (g/mol)	Abbreviation
Sodium dodecyl sulfate: $[C_{12}H_{25}OSO_3Na]$	Anionic-Surfactant	0.008	288.38	SDS
Tetraethyl ammonium bromide: $[(C_2H_5)_4NBr]$ or $[C_8H_{20}NBr]$	Cationic-Surfactant	0.16	210.14	TEAB
Polydiallyldimethylammonium chloride $(C_8H_{16}ClN)_n$	Anionic-Polyelectrolyte	-	161.67* 200,000 - 350,000 **	PDAC
Poly (ethylene glycol) butyl ether $(CH_3(CH_2)_3(OCH_2CH_2)_nOH)$	Cationic-Polyelectrolyte	-	118.17* 400,000 **	PGBE
Sodium chloride (NaCl)	Inorganic	-	58.4	NaCl
Sodium Phosphate (Na_3PO_4)	Inorganic	-	141.96	Na_3PO_4

Sodium chloride (NaCl) was selected as a model draw as it has been well studied (Roach et al., 2014), and sodium phosphate ($Na_3PO_{4)}$ was also considered in the inorganic draw solution category. The surfactants sodium dodecyl sulphate (SDS) and tetraethylammonium bromide (TEAB) were selected because of their ability to form a distribution of aggregates known as micelles at concentrations above their critical micellar concentration (CMC), and the larger molecular size of the micelles causing lower RST as compared to inorganic draw solutions of smaller molecular size (Nawaz et al., 2013).

Recently, polyelectrolytes have been proposed and applied as draw solutions for the following reasons; they are soluble and non-toxic in water, have a larger molecular size and flexibility in structural configuration (Figure 3.3), and possess a lower critical solution temperature to aid solute recovery (Roach et al., 2014). The polyelectrolytes Polydiallyldimethylammonium chloride (PDAC, often used as a coagulant aid in conventional water treatment) and Poly (ethylene glycol) butyl ether (PEGBE) from Sigma Aldrich were used as received in different solution percentages. Draw solutes were tested at 0.1, 0.3 and 0.5M concentrations. Electrical conductivity and total dissolved solids (TDS) were measured to facilitate the analysis of reverse transported draw solute. The osmotic pressure of polyelectrolytes was measured using an osmometer (Micro-osmometer 13/13DR Roebling, Germany). The instrument measured the osmolality, based on the freezing point depression of the solution. Distilled water, which has zero osmotic pressure and phosphate buffer saline, were used for calibration. The osmolality of the solution was then converted to osmotic pressure, using the Van't Hoff equation (Equation 2.1).



(a) (b)

Figure 3.3 Molecular structure for polyelectrolytes used in the current study (a) PDAC $(C_8H_{16}Cl\ N)_n$, (b) PGBE $(CH_3(CH_2)_3(OCH_2CH_2)_nOH)$

3.2.3. Toxicity

Toxicity of the draw solutes is a very important issue, whether with reference to reverse solute transport to the feed side of the bioreactor or to the draw solutes left in the permeate after draw solution recovery. Toxic compounds in the permeate may cause environmental and health issues, and will increase the cost of treatment when using forward osmosis as a follow up treatment will be required to remove the toxic substances from the FO permeate. Toxicity issues may also affect the biological functioning of the FO-MBR.

Table 3.3 Chemical composition of 2X M9 media for bacterial growth in microbroth dilution test with a final pH of 7.0 (Harwood & Cutting, 1990)

Chemical	**Formula**	**Quantity (g)**
Disodium hydrogen phosphate	Na_2HPO_4	25.6
Potassium di-Hydrogen Phosphate	KH_2PO_4	6
Sodium Chloride	NaCl	1
Ammonium Chloride	NH_4Cl	2
Glucose	$C_6H_{12}O_6.H_2O$	0.4

Toxicity of all the draw solutes was evaluated using a microbroth dilution test where a bacterial culture of *Bacillus Subtilis* was allowed to grow in an incubator at 32°C overnight. This culture was then added to individual eppendorfs and centrifuged at 10,000rpm for 15 minutes. The pellet was then filled with 500µl of M9 media and 500µl of individual draw solutions at higher concentration to observe possible sudden shocks

to bacteria in the case of higher levels of reverse solute transport. A range of concentrations that include the RSTs observed were tested. The composition of M9 media (Sigma Aldrich) is given in **Table 3.3**

3.2.4. Viscosity

In addition to osmotic pressure and diffusivity, viscosity plays an important role in draw solution characteristics (Xie et al., 2013a). This characteristic might be more important for polyelectrolytes as compared to other draw solutions, as high viscosity often prevents polyelectrolytes from being used as practical draw solutes at ambient conditions (Nawaz et al., 2016). Viscosity was evaluated for all the draw solutions using an Anton Paar rheometer with a cone plate having a diameter of 24.946mm and at a constant shear rate of 100/s.

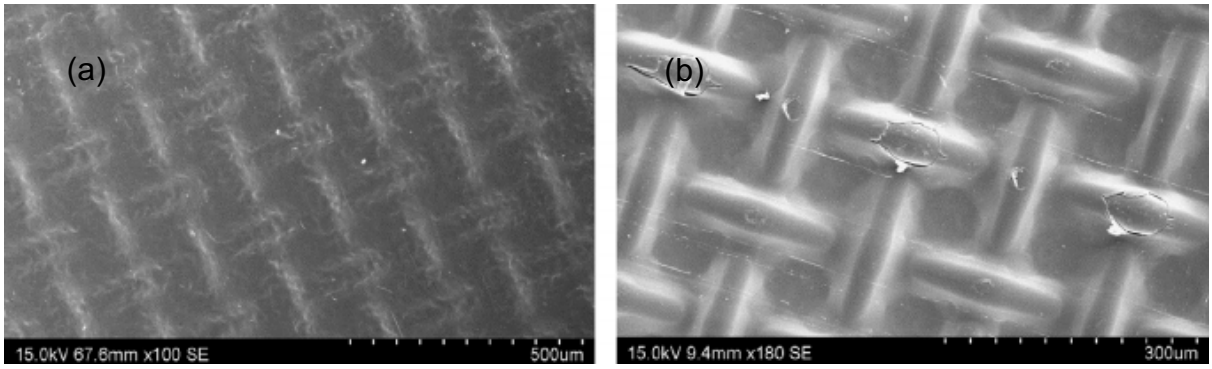


Figure 3.4 SEM images of a flat sheet FO membrane (a) SL (b) AL (Blandin et al., 2014).

3.2.5 Membranes

Scanning electron microscopy (SEM) images for the FO membrane are given in **Figure 3.4** and those for the NF membrane in **Figure 3.5**. The commercial FO membrane is more complex, having an active and support layer in place, while the NF

membrane is a single layer membrane with essentially the same appearance on both sides.

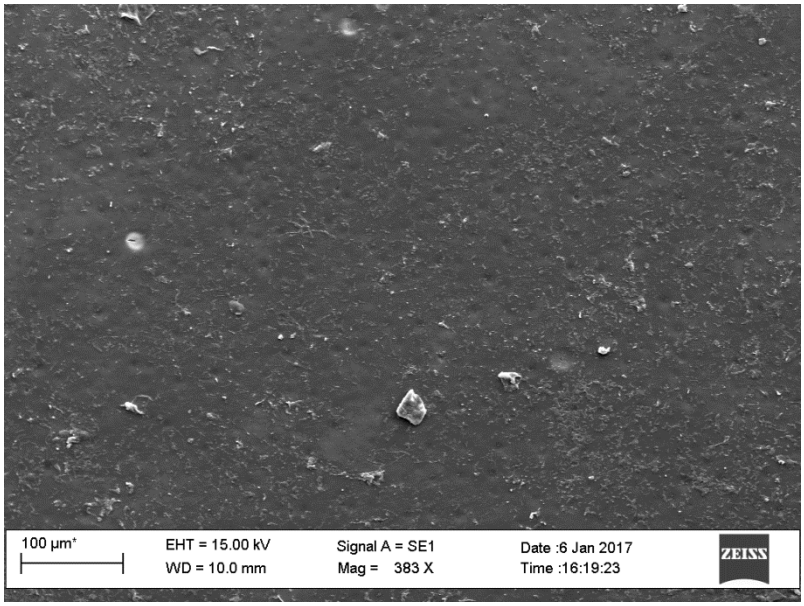


Figure 3.5 Plan view SEM image of NF membrane used in the study

3.3 Results and Discussion

3.3.1 Osmotic Pressure as a Function of Concentration

Osmotic pressure across the FO membrane is the driving force of the process. Results for osmotic pressure calculated using freezing point depression are given in Table 3.4. It is clear from the values reported that inorganic draw solutes give the highest osmotic pressure of all solutes at a given concentration. At the concentration of 0.5M solution Na_3PO_4 and NaCl had similar osmotic pressure but the flux achieved will be lower than that of NaCl (presented in next section) due to lower diffusivity of the higher molecular weight Na_3PO_4. The osmotic pressure for Na_3PO_4 (at 0.1 and 0.3 M) is higher, as 0.5M of NaCl will have 0.5M of Na^+ ions while at the same concentration Na_3PO_4 will have three times greater number of Na^+ ions. It has four particles per

mole compared to that of NaCl that has only two particles per mole. $MgCl_2$ and Na_2SO_4 have been reported to give higher osmotic pressure than NaCl for the same reason (Law & Mohammad, 2017). The osmotic pressure does not increase as much after 0.5M concentration and at 1M the osmotic pressure is lower than NaCl. It can be related to interaction between Na and PO_4 ions in a solution, or with the degree of dissociation of the draw solute at higher concentration, however no such account has been presented in literature. The lower flux for Na_3PO_4 can also be explained with respect to its higher molecular weight compared to that of NaCl. Lower diffusivity in the case of the latter will give a small mass transfer coefficient leading to lower osmotic pressure at the membrane surface for the draw solution [as presented in equation 2.14 for ECP].

TEAB also shows good flux. Although its value at 1M was comparable to that of NaCl as well, but using surfactant at higher concentration is not ideal, as at concentration above the CMC the surfactants tend to become insoluble, due to growth in micellar size. Certainly, sodium chloride solutions are expected to conform most closely to ideal solution behaviour and thus yield the linear trend predicted by the Van't Hoff equation. The osmotic pressure value measured for NaCl at 1M concentration was 4.41 MPa, and this value is close to that reported in the literature i.e. 4.46 MPa at 1M (Johnson et al., 2017), or 4.2 at ~1M (Achilli et al., 2010). In general, osmotic pressures for many draw solutions are not reported in literature. For all draw solutes, the osmotic pressure increases in the following order at 0.5 M draw solution concentration:

PDAC < PGBE < TEAB < Na_3PO_4, NaCl.

Unfortunately, the osmotic pressure value could not be measured for SDS by the freezing point depression method due to spontaneous crystal formation. At lower

temperatures, SDS precipitates and is no longer soluble in water, resulting in lower freezing point depression values than expected. Since all the colligative properties of SDS are then reduced, its apparent osmotic pressure is lower than that expected with complete solubility, and measurement were thus discontinued e.g. Gadelha et al., reported an osmotic pressure of 0.33 MPa for 0.1M SDS concentration. Despite these problems, freezing point depression was deemed a fit method to calculate the osmotic pressure for inorganic draws solutions, the polyelectrolytes and the cationic surfactant, TEAB.

The values observed for polyelectrolytes were comparatively low. This lower osmotic pressure could be the result of a coiled configuration of polyelectrolytes in an

79

aqueous solution, leading to non-ideal solution behavior (see values in Table 3.4). Linear polymers only obey the Van't Hoff equation at lower concentration in a good solvent. At higher concentrations, complex osmotic behaviors are observed due to the high degree of polymerization and hence the interaction between the chains leading to coiling. Their random configuration allows them to occupy larger volumes. An additional virial coefficient that takes the interaction of two chains into account should be incorporated into the Vant't Hoff equation. In short, the non-ideality has a bigger effect for larger molecules than smaller ones.

Ionic surfactants have been reported to produce higher osmotic pressure values compared to anionic surfactants because of the combination of unbound ions and the large repulsive interaction between micelles. But in forward osmosis, using surfactant as a draw solute, actual fluxes have been reported to be lower than the predicted

fluxes and are caused by the combined influences of concentration polarization and viscosity with increasing concentration (Roach et al., 2014).

In the current study various draw solution concentrations (0.1, 0.3, 0.5M) were tested to select the optimum concentration range for FO tests. With an increase in concentration, the osmotic pressure increases and leads to higher flux, this trend is expected from the Van't Hoff equation. The same rising trend has been shown in many different studies for other draw solutes (Mccutheon et al., 2006, Achilli et al., 2009, Choi et al., 2009, Xu et al., 2010). However, it appears that an initially linear relationship shifts to a logarithmic (as observed in the case of Na_3PO_4) one at higher concentration of various inorganic draw solutions. Very high concentration of draw solutions were not tested in the current study, as literature suggests that the ECP and ICP are greater at higher draw solution concentrations or higher fluxes (Tan and Ng, 2010). Concentration of draw solution and increased crossflow also increase the

80

flux. Indeed, the effect of ECP was expected and shown to be minimal when a cross flow setup was in place with a CFV greater than 0.21m/s (Xu et al., 2010).

With no draw regeneration system in place, the FO setup in this work had to be run in batch mode, and a moderate concentration of 0.5M solution was chosen for FO and FO-MBR configurations after initial testing of 0.1, 0.3 and 0.5M concentrations.

In this study, a decline in flux with time was often observed. Since a draw solution regeneration was not in place, the decline may have arisen at least in part as a result of dilution of the draw solution in the absence of a regeneration system, although fouling could also be expected to play a role (see also page 91).

The osmotic pressure values at 0.5M concentration revealed greater values and higher concentration of surfactants were not feasible for use therefore 0.5M draw solution concentration were used for further studies.

Table 3.4 Osmotic pressure for draw solutes determined using measured osmolality values.

Chemical	**Concentration (M)**	**Osmotic pressure (MPa)**
1. Sodium chloride (NaCl)	0.1	0.54± 0.025
	0.3	1.09± 0.025
	0.5	2.13± 0.025
	1	4.41± 0.025
2. Sodium phosphate (Na_3PO_4)	0.1	0.67± 0.025
	0.3	1.18± 0.025
	0.5	2.13± 0.025
	1	2.90± 0.025
3. Sodium dodecyl sulfate [$C_{12}H_{25}OSO_3Na$]	Freezing point depression measurements not practical due to poor solubility and crystallization at low temperature.	
4. Tetraethyl ammonium bromide [$(C_2H_5)_4NBr$] or [$C_8H_{20}NBr$]	0.1	0.42± 0.025
	0.3	0.85± 0.025
	0.5	1.61± 0.025
	1	4.00 ± 0.025
5. Poly Diallyldimethylammonium chloride (PDAC)	0.18	0.05± 0.025
	0.31	0.12± 0.025

	0.61	0.20± 0.025
4. Poly (ethylene glycol) butyl ether (PGBE)	0.2	0.43 ± 0.025
	0.42	0.63 ± 0.025
	0.85	1.30 ± 0.025

Several further observations should be made about the measurements reported in Table 3.4.

1. Each measurement was performed three times; the variance in values suggested a standard deviation of 0.025 MPa, which is the value reported for the estimate in error.

However, a random error analysis suggests an error one order of magnitude smaller, as follows.

The freezing point osmometer measures osmotic pressure indirectly via the depression in freezing point of the solution compared to pure water. This is calculated via the generalized Van't Hoff equation (2.2), for which the concentration, activity coefficient and Van't Hoff coefficient (related to the number of charged species per molecule of species) are lumped into a single term, the 'osmolality'. The measurement nevertheless assumes that osmotic pressure is a colligative property, dependent only on the concentration and not the nature of the solute species, which is unlikely to be true in general.

According to reference (Gonotec, 1996), the depression in freezing point associated with unit osmolality is -1.86°C. The accuracy of temperature measurement is stated as roughly +/- 2 x 10^{-3} °C so the relative error in osmolality measurement is about 1 x 10^{-3}. By taking the log of both sides of equation (2.1) and differentiating, it is seen that

the relative error in osmotic pressure is the sum of the relative errors in osmolality and temperature; this of course ignores the activity terms in the more general form of the equation, (2.2), for which osmotic pressure can in any case no longer be considered colligative (Wallace et al., 2008).

Since the temperature relative error is very much smaller than for the osmolality, and for osmotic pressures on the order of 1 to 5 MPa, the absolute error is thus between 1 and 5 x 10^{-3} MPa. The fact that this is much lower than the standard deviation in the experimental measurements suggests that the accuracy in measurement of the temperature, and equally the accuracy at which it is maintained in the measurement device, is less than the value suggested. Furthermore, the assumption of solution ideality, necessary for accurate measurement, does not hold true (see also point 2). Finally, the concentration of the made up solutions are themselves subject to experimental error, though this is likely to be smaller than one millimolar and thus not contributory to the observed variances.

2. In practice, we can observe from Table 3.4 that equation 2.1 holds better for the simpler solutes (1 and 2) than for the more complex, high molecular weight solutes (4 to 6); the latter demonstrate a marked non-linear relationship between osmotic pressure and concentration. This is indicative of the expected non-ideal interaction between these solutes in solution. It will be seen later that this non-ideality has consequences for both flux response and membrane fouling/cleaning.

3.3.2 Forward Osmosis Membrane versus Nanofiltration Membrane

Figures 3.6, 3.7 and **3.8** show the initial fluxes for CTA and NF membranes for the draw solutions studied, with both DI water (AL-DS mode) as a control feed and live monoculture feed in the FO-MBR (run in AL-FS mode). It can be observed that the

presence of live bacteria greatly influences the flux for all draw solutions for both membranes due to cake formation on the feed side of the membrane. It can also be observed that the fluxes for the HTI CTA membrane are lower than that for the NF. A decline in initial fluxes were observed in bioreactor configuration for both NF and CTA membranes. This can be related to dilutive ICP at the SL and concentrative ECP and biofilm/cake formation at the AL-FS of the FOMBR process (as AL-DS).

Polyelectrolytes

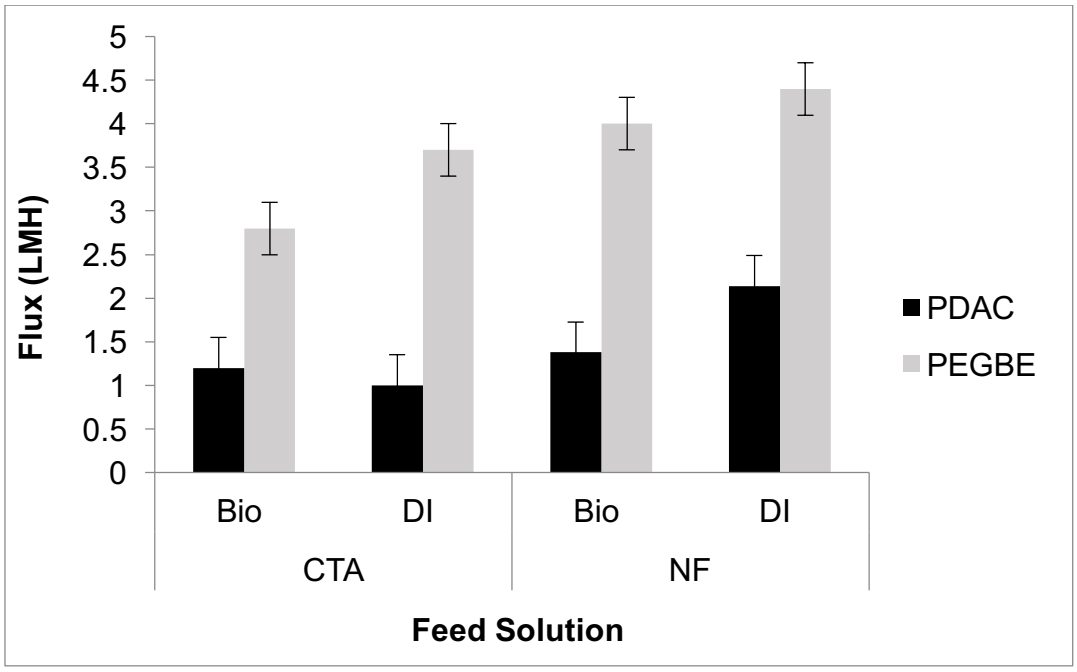


Figure 3.6 Initial fluxes for polyelectrolytes PDAC and PGBE with NF and CTA membranes using both DI water as feed (AL-DS) and a live monoculture FO-MBR feed (denoted 'Bio', AL-FS mode) at 0.5M concentration (CFV: 0.12m/s)

The molecular weight for draw solutes used in this study (e.g. PDAC: M_w 200,000-350,000 and PGBE: 200,000-400,00) were higher and were chosen to get better flux and reduced RST. As shown in **Figure 3.6** the initial fluxes were lower for

polyelectrolytes due to lower diffusivity and higher viscosity (shown in section **3.3.3**). Studies that show high molecular weight is more effective for draw solutes have been published elsewhere. In a study (Zhao et al.,2015) comparing polyacrylamide (PAM) (Mw ~ 300,0000) as draw solute for treating dye wastewater (Reactive Brilliant Red K-2BP (RBR) dye solution), the PAM showed a more stable flux than that for KCl although the latter flux was higher. It was shown that increasing the temperature increased the flux, due to a decrease in kinematic viscosity and an increase in osmotic pressure. The effect of temperature on reverse solute transport was considered to be negligible (0.02-0.07 g/m^2h). The fluxes obtained with PAM were the same in baseline studies both when using DI water as a feed, and when using the dye solution as a feed, with a TFC membrane. The concentration of PAM was chosen to be 20g/L.

Many of the studies conducted using polyelectrolytes are not consistent with each other (Zhao et al., 2015, Jun et al., 2015). High molecular weight PAM gave a reasonable flux (M_w 3,000,000; flux 14-17 LMH) with FO and PRO configurations (Zhao et al., 2015). However, in our study as well as in a few other studies, it was shown that the flux for higher molecular weight polyelectrolytes is lower than that for lower molecular weight polyelectrolytes where PEI performed poorly due to its higher molecular weight (Jun et al., 2015).

Surfactants

A similar pattern of reduced flux was observed for surfactants (**Figure 3.7**) when the two different membranes were used. The flux is higher for the cationic surfactant (TEAB), and lower for the anionic SDS. Note that there was a lot of foam formation in the SDS solution, depending on how freshly the solution was prepared, and this seemed to affect the flux as well as the reverse solute transport. SDS has a higher

molecular weight than TEAB, and yet the reverse solute transport values were higher for SDS in the case of the HTI membrane (see **Table 3.6**).

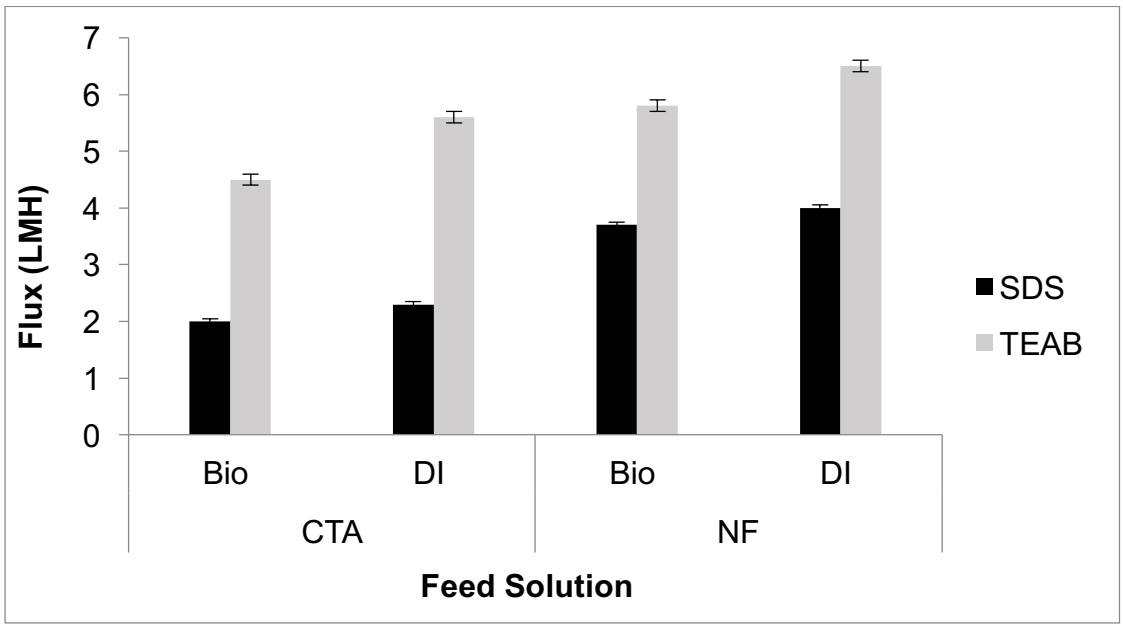


Figure 3.7 Initial fluxes using SDS and TEAB as draw solutes against both DI water (AL-DS) as feed and a live monoculture FO-MBR feed (denoted 'Bio', AL-FS mode) for CTA and NF membranes at 0.05M surfactant concentration (CFV: 0.12m/s).

Surfactants have been previously reported (Hoyer et al., 2016) to produce high osmotic pressure per unit concentration. But the dilution of surfactant in the membrane support layer can lead to a lower osmotic pressure difference across the membrane. This effect of internal concentration polarization (the draw solute cannot diffuse into the support layer rapidly enough) was reported in the same work to be higher for surfactants than for inorganic draw solutes, and was assumed to be because of higher viscosity and lower diffusivity of the surfactant solution.

If the hydrocarbon chain length is long, then a microscopic phase separation can appear i.e. micelles will be formed. Longer chain hydrocarbons have a lower CMC and thus fewer monomers and lower osmotic pressure (as in the case of SDS). The HTI CTA membrane, used in the current study, prevents the passage of micelles, but does allow for the passage of surfactant monomers and thus allows for a higher reverse transport- a clear disadvantage.

In the current study much higher fluxes were observed for TEAB but the decline in flux was also higher. On the contrary lower fluxes were achieved by SDS but the decline in flux for bio feed as well as overtime was lower.

Inorganic Draw solutions

Initial flux for the inorganic draw solutes is shown in **Figure 3.8** for the HTI-CTA membranes. They were not tested against the NF membrane because of the ability of monovalent ions to pass directly through the membrane.

In Table 3.4 it can be observed that both inorganic draw solutions have similar osmotic pressure and therefore same values of flux were expected at 0.5M concentration of draw solution. It can be observed that the flux for Na_3PO_4 has lower flux than that of NaCl in both DI and MBR as feed. This is because draw solution with divalent ions in general yield lower fluxes than monovalent ions even at the same osmotic pressure, which is due to the lower diffusivity coefficients of the divalent ions in comparison with those of the monovalent ions (Holloway et al., 2015). Higher diffusivity is another reason why NaCl is widely used for FO in the literature.

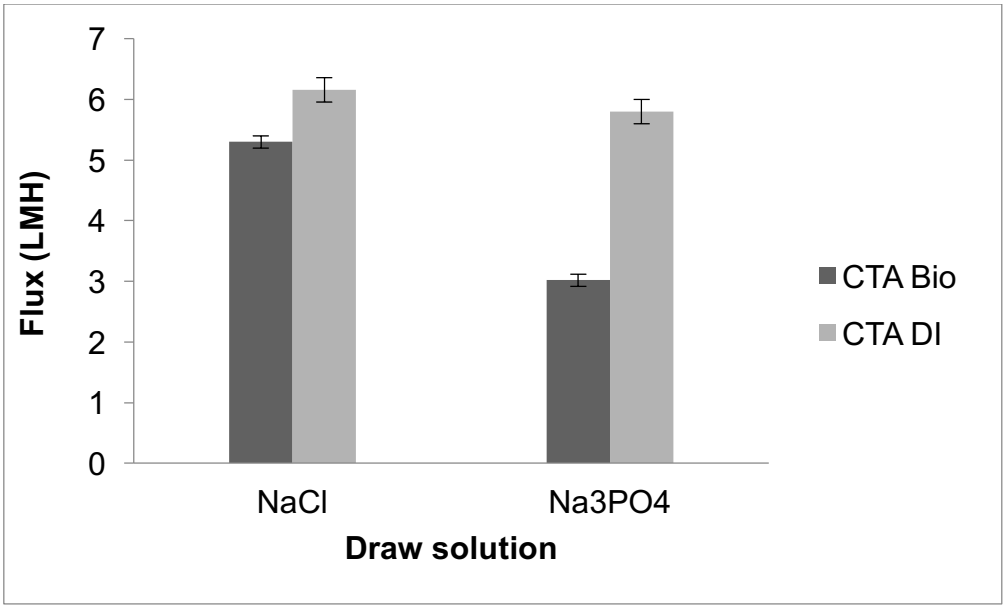


Figure 3.8 initial fluxes for NaCl and Na_3PO_4 as draw solutes using the CTA membrane and both DI water (AL-DS) as feed and a live monoculture FO-MBR feed (denoted 'Bio', AL-FS mode) at 0.5M concentration (CFV: 0.12m/s).

Other reasons for its wide usage is that NaCl costs around 15$/kg and is highly soluble (315g/l at 25°C). A study (Achilli et al., 2010) evaluating various inorganic draw solutes for cost and performance ranked NaCl low for its performance but high for its cost. Divalent ions of inorganic compounds such as Ca^{+2}, Ba^{+2}, Mg^{+2}, SO_4^{-2} and CO_3^{-2} are expected to cause mineral salt scaling. However, $Mg(OH)_2$ only precipitated at a pH greater than 9; therefore, $MgCl_2$ was recommended for use in FO without the risk of scaling.

Increasing flux at higher concentration also results in larger reverse solute transport and 50% or more of the reverse solute transport took place in the first 24 hours of the FO process. This could be because there is a layer of draw solute formed on the membrane surface and it reduces further reverse transport or the membrane pores

got blocked. Draw solutions with smaller ions also have other advantages. As solute radii decrease, the peak density of the ion decreases. Therefore, the strongest osmosis would be expected to occur for the smallest ions, which pull on the water strongly (Cannon et al., 2012). While this will not be ideal for RST but the flux can be increased as observed in the case of NaCl in the current study.

Table 3.5 Flux with HTI CTA membrane at 1h and 8h time intervals with percentage decline in flux using DI water and FO-MBR as feed DI water (AL-DS mode) and FO-MBR as feed (AL-FS mode) at a CFV of 0.12m/s.

Draw Solution	**HTI FO Initial Flux -DI water Feed (LMH)**	**HTI FO flux after 8 Hours -DI water Feed (LMH)**	**HTI FO Initial Flux - Bioreactor Feed (LMH)**	**HTI FO flux after 8 Hours - Bioreactor Feed (LMH)**
0.5M NaCl	6.16	3.8 (38.31% less)	5.3	3 (43% less)
0.5M SDS	2.3	2 (13%)	2.1	1.8 (14.2%)
0.5M TEAB	5.6	4 (28.57 %)	4.5	3 (33.3 %)
0.44M PDAC	1.1	0.8 (27%)	0.9	0.6 (33%)
0.67M PGBE	3.7	3 (18.9 %)	2.8	2.2 (21.4%)
0.5M Na_3PO_4	5.8	3.2 (44.8 %)	3.02	2.1 (30.4%)

Comparison between Fluxes for the FO Membrane and the NF Membrane

The use of NF membranes for FO can be promising, as the fluxes in general can be expected to be higher for an NF membrane compared to a commercial FO membrane (Table 3.5 and 3.6). Fluxes were high for NF and highest for inorganic draw solution followed by surfactants and polyelectrolytes. However, the flux decline over a period of time alongside the decline in initial flux with change in feed cannot be neglected. For the biological feed after 8 hours of operation, the decline was greater for NaCl (43%) at 0.5M solution with the HTI membrane, followed by TEAB (33.3%), PDAC (33%), Na_3PO_4 (30.4%), PGBE (21.4%), and SDS (14.2%) respectively. **Tables 3.5** and **3.6** show the initial fluxes, and the flux after eight hours of operation, for both HTI and NF membranes respectively. The Table also shows the percentage decline in flux. The percentage decline in flux varied with draw solute for the NF membrane. For NF membrane, the initial flux was already very low for PDAC (1.1 LMH) and the percentage decline in the bioreactor was highest (63%) followed by SDS (34%), PGBE (25%), and TEAB (22.5 %), respectively. In the case PDAC, the lower initial flux yields a higher rate of decline and but in general in NF a high initial flux compared to CTA and a decline in flux for both membranes when biological feed was used indicate that cake formation and possibly pore plugging is important.

Table 3.6 Flux with NF membrane at 1h and 8h time interval with percentage decline in flux using DI water (AL-DS mode) and FO-MBR as feed (AL-FS mode) at a CFV of 0.12m/s.

Draw Solution	**NF Initial Flux -DI water feed (LMH**	**NF Flux after 8 hours -DI water feed (LMH**	**NF Initial Flux - Bioreactor Feed (LMH)**	**NF Flux after 8 hours - Bioreactor Feed (LMH)**
0.5M SDS	4	3.5 (12.5%)	3.8	2.5 (34%)
0.5M TEAB	6.5	3.8 (41%)	5.8	4.5 (22.41 %)
0.44M PDAC	1.4	0.6 (57%)	1.1	0.4 (63%)
0.67M PGBE	4.4	3.5 (20.45%)	4	3 (25%)

The literature presents many studies on HTI CTA membranes with many different draw solutes. A high flux of 9.6 LMH was achieved by NaCl at a concentration of 0.6M (Achilli et al., 2010). The same study showed a flux of 8.4 LMH for $MgCl_2$ at 0.36M solution and 7.3LMH for NH_4HCO_3 at a concentration of 0.67M. Similar values of flux were obtained for NaCl (6.16LMH) and Na_3PO_4 (5.8LMH) in our study at a molar concentration of 0.5M draw solution concentration. However, the flux obtained for polyelectrolytes with the HTI CTA membrane are variable Indeed, some polymers show very high flux. Paa-Na (1200) gave a flux of 22LMH at 0.72g/ml with a HF cellulose acetate membrane (Get et al.,2012). Moderate fluxes were obtained with polygycol copolymer, 30-70% solution, which gave a flux of 4LMH with CTA

membrane when 3.5% NaCl was used as feed solution (Carmigani et al., 2012). Such concentration weight percentages reported in the literature for polymers as draw solutes are high and similar concentrations were not used in the current study because of the highly viscous solution obtained.

Literature suggests that the flux decline is severe relative to the initial flux. In a long-term study with municipal wastewater, Wang et. al. (2016), demonstrated the respective contributions of cake enhanced concentration polarization (CECP), ECP and RST to water flux decrease. The flux was calculated and the said parameters were observed at the critical concentration factor (CCF) and concentration factors 1, 3, 5 and 8 times that of the influent sewage. CCF is the ratio of draw solute concentration to that of feed concentration, which is a useful parameter to define the concentration factor where highest flux could be achieved. It was shown that 58.1% of the flux decline is due to RST, followed by 21.9% due to ECP and 20% due to CECP. The contribution of CECP, ECP and reverse solute transport to water flux decline decreased at the points of membrane cleaning. In this case, CECP contributed to 52.8%, RST contributed to 20.7% and ECP contributed to 20.7% of the water flux decline. Overall, CECP was then the highest contributor to the flux decline (Wang et al., 2016). Generally, membrane cleaning is expected to remove cake formation but the decline in flux contributed due to cake formation cannot be neglected.

Overall, for both CTA and NF membrane, a decline in flux was observed over several hours, and initial fluxes were lower for biological feed; the contributory factors were likely to be cake formation on the AL of the membrane, dilution of the draw solution, and ICP in the support layer of the membrane. There is a need for a reconcentration system in place to understand the decline better.

3.3.3 Reverse Solute Transport

Reverse solute transport of ions from the draw solution (DS) to the feed is a potential problem with forward osmosis (FO). RST is reduced when divalent ion salts, such as $MgCl_2$ and $MgSO_4$ with a larger hydrated radius, are used instead of salts with monovalent ions only e.g., NaCl (Holloway et al., 2015). The observed reverse solute transport is reported for all draw solutions with NF and HTI membranes in **Table 3.7.** As mentioned previously, tests were not performed for the inorganic draw solutes versus the NF membrane, but values of RST for monovalents can be expected to be perhaps an order of magnitude greater than for the HTI membrane.

For the HTI membrane, the following order in RST was observed:

NaCl> SDS > Na_3PO_4 > TEAB > PGBE> PDAC

For the NF membrane, the following order was observed:

SDS > TEAB > PDAC > PGBE

It can first be observed that the reverse solute transport is related to the charge of draw solute. For example, for NF the anionic polymer and surfactant show slightly higher RST values than the cationic surfactant and polymer, respectively, while RST for sodium chloride was higher than sodium phosphate for the HTI membrane. It can immediately be seen from the values reported that solute molecular size is an important factor to determine the reverse solute transport of a draw solution. The RST values are lowest for highest molecular weight draw solutes (polyelectrolytes).

In general, values for reverse solute transport are slightly higher for NF than that for HTI but are still of comparable magnitude, and the issue of RST does not prevent the use of NF as an FO membrane when paired to the draw solutes tested, particularly those of larger molecular weight

Table 3.7 Reverse solute transport (GMH) for draw solutes used in the study after 24 hours of FO operation when run in the absence of a draw re-concentration system (AL-DS mode, CFV: 0.12m/s).

Draw Solution	**Formula weight (g/mol)**	**Reverse solute Transport**	
		HTI Membrane (GMH)	**NF Membrane (GMH)**
		DI water feed	DI water feed
TEAB	210.14	6.3	7.07
SDS	288.372	7.66	8.07
NaCl	58.44	9.33	-
Na_3PO_4	163.94	7.2	-
PDAC	161.673	1.14	1.86
PGBE	118.17	1.2	1.56

SDS showed higher RST for both membranes. Micelles may enhance the hydrophilicity of the membrane, and allow monomers to pass through. The hydrophilicity could also result in cake formation on the membrane layer due to adsorption (Zhao et al.,2015).

Few studies can be found on the reverse solute transport of the different draw solutes studied in this work. Surfactants have been reported to be novel and easy to regenerate due to micelle formation and krafft temperature (Nawaz et al., 2013). Although there can be some interaction between the surfactant and the polymer, the main parameter influencing the diffusion was the polymer-free volume fraction of the membrane. A study on a polymeric membrane showed that the water diffusion

coefficients are mainly dependent on the polymer density, and no significant effect of the polymeric surface was found (Valentene et al.,2005).

Unlike RO, solutes in FO can diffuse in both directions i.e. both forward and reverse. The reverse diffusion takes place partly because of concentration polarization and mostly because of the concentration gradient. In a separate study (Hanckok & Cath, 2009). Drawn water flux and reverse salt diffusion increased with increasing concentration for both NaCl and $MgCl_2$. DI was used as a feed and the experiments were run in AL-FS configuration. When both draw solutes were used at similar osmotic pressures, the flux was lower for $MgCl_2$ (by 25-30%) compared to NaCl; the lower diffusion coefficient of the former would lead to an increased severity of ICP The higher viscosity of the $MgCl_2$ also contributed to an increased ECP. The RST was also lower for $MgCl_2$ (by 59-67%). The reverse solute flux for $MgCl_2$ may be subject to Donnan equilibrium, whereby large Mg^2 ions diffuse slower and limit the diffusion of counter ions. Draw solute ions (Na and Cl) were shown to reverse diffuse at nearly equal molar proportions in the case of $MgSO_4$, $CaSO_4$, K_2SO_4, H_3PO_4, and NH_4HCO_3 as feed solutions, but in the case of $Ba(NO_3)_2$ the chloride ion diffused at a faster rate than sodium.

Size exclusion and electrostatic effects clearly have an important role to play in forward and reverse solute transport (Alsvik & Hagg, 2013). At lower and equal flow velocities, the draw solute is concentrated at the membrane surface on the feed side and the concentration boundary layer on the DS side of the membrane is not well mixed and remains diluted. This results in diminishing chemical potential gradient between the DS and feed solution and retardation in the net diffusion of salts into the feed solution and high CFV has an important role to play in diminishing this (Hanckok & Cath, 2009).

Based on the values received use of SDS was not recommended for future studies. Use of NaCl was continued as baseline for comparison in literature. Viscosity and toxicity values were looked at for final selection of draw solution in the chapters to follow.

3.3.4 Viscosity

The viscosity of the polyelectrolyte solution is an important factor for its use as a draw solute in FO, and viscosity results for draw solutes are now reported in **Table 3.8**. As can be seen, the viscosities follow the order:

PDAC > SDS > PGBE > Na_3PO_4 >TEAB > NaCl

As expected, viscosities were highest for the polyelectrolyte solutions. It is interesting to note that the viscosity of SDS is comparable with that of the polyelectrolytes.

The viscosity of a draw solution is inversely proportional to its flux, at constant driving pressure. This can be explained by basic fluid mechanics, where we note Poiseuille's law for the flow of viscous liquids in pipes and the inverse relationship between velocity (leading to high flux) and viscosity at constant driving force.

One of the negative impacts of the higher viscosity associated with larger molecules could be a reduction in water transport from feed to draw solution (Jun et al., 2015). This can, at least in part, explain the lower fluxes obtained for PDAC and SDS with viscosity ≥ 2, compared to other draw solutes.

Table 3.8 Viscosities of draw solution at operational concentrations

Draw solution	Concentration (M)	Viscosity (cP)	Osmotic pressure (MPa)	Flux with DI water (LMH)
NaCl	0.5	1.2	2.13	6.16
Na_3PO_4	0.5	1.5	2.13	5.8
SDS	0.5	2	-	2.3
TEAB	0.5	1.2	1.61	5.6
PDAC	0.44	2.5	0.2	1.1
PGBE	0.67	1.7	0.43	3.7

Increasing molar concentrations to increase flux can be an option and is mostly observed in studies in literature. However, increasing the solute weight fraction increases the solution viscosity and leads to limited function in the process of dialysis (Daniels et al., 1988).

3.3.5 Toxicity

A bacterial monoculture was able to grow in the presence of all draw solutions tested, as shown in **Figure 3.9**. All the bacteria were able to grow in the presence of draw solutions at a concentration ranging from 0.005 to 0.05 M. The growth curve presented here is that at a very high concentration of 0.5M to show that *B.subtilis* was able to thrive in the presence of all draw solution. Na_3PO_4 showed higher growth close to that of the control while SDS proved to hamper bacterial growth at such high concentration. This was because of the availability of phosphate in the solution, which is a source of

phosphorus for bacteria and a constituent of nucleic acids, nucleotides, phospholipids, LPS, teichoic acids etc. SDS too is known to be toxic but the gram negative bacteria still did well at the higher concentration presented.

Few previous studies have been performed on draw solute toxicity for bacteria. For *E. coli* toxicity, eight inorganics were tested in one study (Nawaz et al.,2013); sodium chloride [NaCl], calcium chloride [$CaCl_2$], potassium chloride [KCl], magnesium chloride [$MgCl_2$], potassium sulfate [K_2SO_4], magnesium sulfate [$MgSO_4$], sodium sulfate [Na_2SO_4], ammonium sulfate [$(NH_4)_2SO_4$]. Four surfactants were also tested; TMOAB, DTAB, MTAB, and SDS. SDS was strongly recommended, based on its ability to generate high fluxes and allow E. coli to grow at all concentrations tested. Among inorganic draw solutions, $MgCl_2$, $CaCl_2$ and ammonium sulfate were highly recommended because of high fluxes and non-toxicity, while sodium sulfate was not recommended because of reduced bacterial growth

As a follow up to the study by Nawaz et al cited above, a more detailed study was conducted using *P.aeruginosa* monoculture and an activated sludge mixed consortium to see the effect of draw solution concentration on feed. Four surfactants TEAB, TMOAB, SDS, and 1-OSA were tested for toxicity. Reverse solute transport for surfactants as draw solutions was observed to be much lower as compared to that for inorganic draw solutes. Significant bacterial growth was observed in the presence of TEAB and SDS, and therefore these two draw solutions were recommended for future studies (Nawaz et al., 2016).

This has now been carried on to prove that these draw solutes were not toxic to bacteria even at higher concentration. Inorganic draw solutions were least toxic, followed by polyelectrolytes and surfactants. Because of better bacterial growth PDAC

and TEAB were continued as draw solution and NaCl was selected as baseline for future studies.

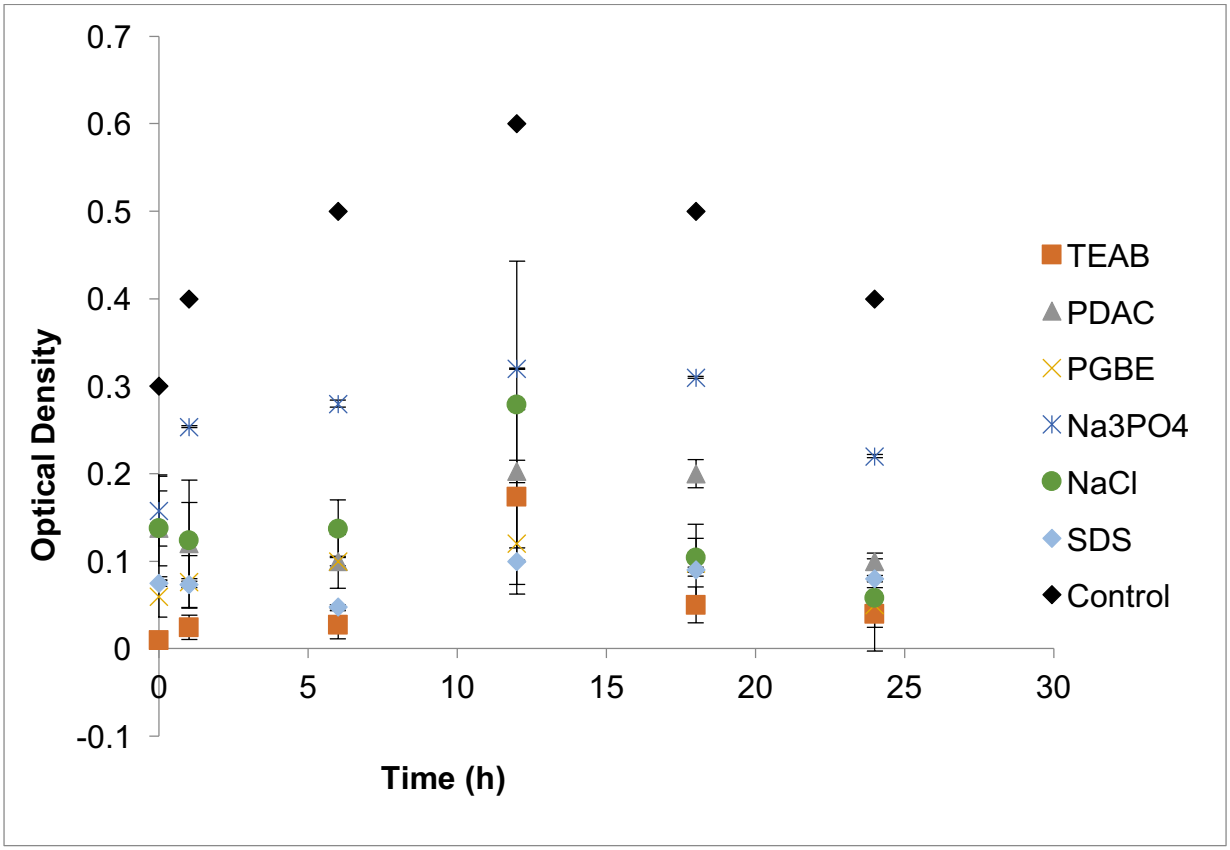


Figure 3.9 Optical density of bacterial solution using microbroth dilution test in minimal media with draw solutes

3.4. Conclusions

- The experimental results were in agreement with the hypothesis that an NF membrane for FO yields better fluxes as compared to the commercial HTI CTA membrane. However, for both FO and NF, the initial fluxes were lower than that achieved with DI water when the feed was changed to monoculture MBR. The decrease in Flux for CTA membrane was:

TEAB (28.5 %), Na_3PO_4 (44.8 %), PGBE (18.9%), NaCl (38%), PDAC (27%), SDS (13%)

While the decrease in flux for NF with the change in feed was as follows:

PDAC (57%), TEAB (41 %), PGBE (20.4%), SDS (12.5%).

- Flux decline over a period of time was also relatively high; however, since a re-concentration system was not in place, it was difficult to conclude whether that was because of increasing concentration polarization in the feed, draw dilution, RST of draw into the feed or fouling of the membrane. For CTA membrane with DI water the decline in flux was 8 hours was as under:

  NaCl (38.3%), SDS (13%), TEAB (28.57%), PDAC (27%), PGBE (18.9%), Na_3PO_4 (19.2%)

  The flux decline overtime for FO-MBR configuration with CTA membrane is given here:

  NaCl (43%), SDS (14.2%), TEAB (33.3%), PDAC (33.3%), PGBE (21.4%), Na_3PO_4 (30.4%)

  All the draw solute have an additional decline in flux in FO-MBR configuration and role of biofouling or cake formation can be noticed.

- Typical levels of reverse solute Transport (RST) were not toxic to bacterial monoculture FOMBRs. At the highest concentration of draw solute tested (0.5M), a significant percentage growth (relative to the absence of the draw solute) was still achieved by all draw solutes. SDS showed the lowest percentage growth of 16% and Na_3PO_4 showed the highest percentage growth of 53%, followed by NaCl (46.5%), PDAC (33.8%), TEAB (28.83%), and PGBE (18.34%) respectively. Yet typical concentration values of draw solute

undergoing RST in this study are below 0.5M and therefore use of these draw solutes with a biological feed is supported by this study.

- Draw solutes that exhibited higher viscosity e.g. PDAC and SDS had viscosities ≥ 2cP, also exhibited lower fluxes. Viscosity of a draw solution is therefore important in draw solution selection.
- Flat sheet/hollow fibre NF membranes in combination with high molecular weight draw solutes provide potentially attractive working systems for the FOMBR because:
    - The fluxes were higher when an NF membrane was in place for the FO-MBR (as shown in **Table 3.5**); however, the percentage decline in flux with time was also higher for the NF membrane.
    - The reverse solute transport values, although slightly higher, were still comparable to the HTI membrane (as shown in **Table 3.6**).

So far, the regeneration of draw solutions has not been considered. Nevertheless, it is important to study the characterization of the membranes and draw solutions being used in the presence of a continuous regeneration system, in order to optimize the process when running under continuous and long-term operation. With this in mind, an FO-MD hybrid was set up in the next phase of the project.

Chapter 4

Integration of Forward Osmosis and Membrane Distillation Units for Regeneration of Novel Draw Solutions and Water Reclamation

4.1 Introduction

The overall aim of this work was to perform an engineering-oriented study of the component parts and integrated operation of a continuous and feasible FOMBR-MD system. In Chapter 3, novel draw solutions were tested for a batch FO system without a re-concentration process. Nevertheless, It is recommended that a continuous recovery system should be put in place to better study such issues as long-term performance and permeate quality. The FO-MD hybrid system was chosen because it was relatively straight forward to establish in combination with the FOMBR in our lab, and is promising as a low (perhaps using waste-grade) energy technique for draw solute regeneration. MD had similar set-up requirements (**Figure 4.1**) to that of the FO setup already established in the lab (**Figure 3.2**). The modest temperature difference at which water recovery could be achieved using MD made it easy to run a continuous hybrid system. Both the FO and MD setups had a similar cell design. The main additions to the setup to run the MD were the water heating (using a water bath) and cooling (chiller) mechanism. The effects of feed and permeate temperature, and the cross-flow velocity, were included in the study.

In this Chapter, an MD setup was established at bench scale and optimized for reconcentrating the draw solution continuously to produce clean water alongside FO. This hybrid setup was used to develop a continuous and self-regenerating FO-MD system to study the reverse transport of solute, toxicity, and fouling of the membrane

for the longer term. There are few published studies on the long-term use of the FO-MD setup (i.e. more than a few hours), much less those which attempt to use a diverse range of novel draw solutes. In the current study, the continuous system was studied over a week for flux, and permeate quality monitored using conductivity. These are the chief contributions made by the study in this chapter.

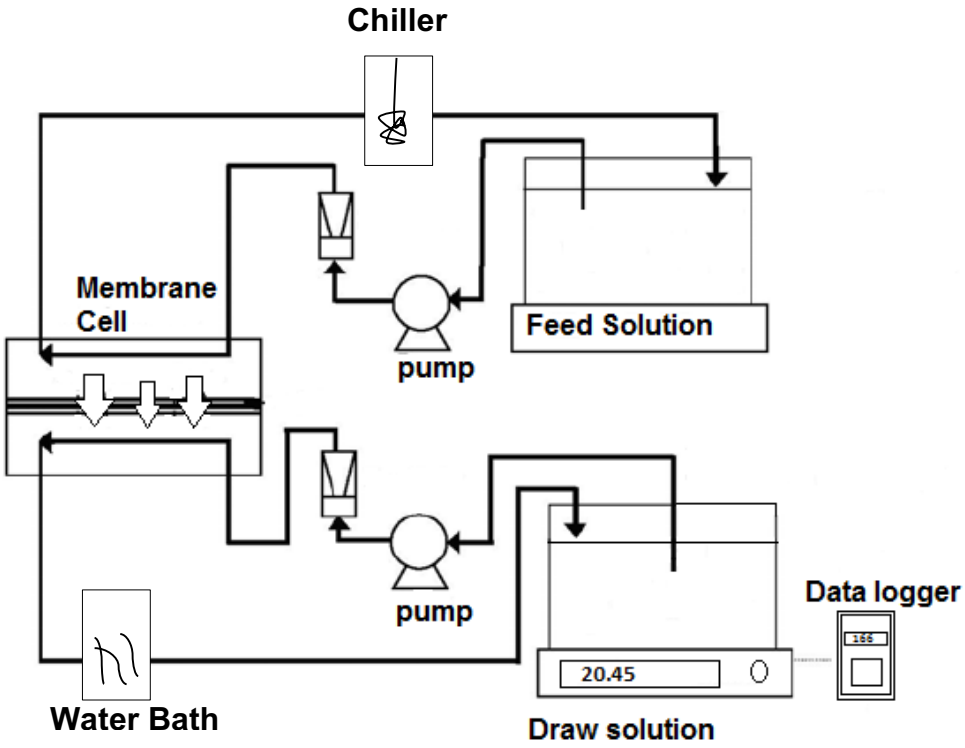


Figure 4.1 Membrane distillation setup established in the lab

4.2 Methodology

4.2.1 Chemicals and Membranes

The draw solutes used have previously been described in chapter 3 (NaCl, PDAC, TEAB). The membrane module for MD was purchased from Membrane Solutions

(Shanghai, China). The hydrophobic membrane was made of PTFE with a PP woven support layer and had a pore size of 0.22μm and nearly 100% rejection to water. The CTA HTI membrane already presented in chapter 3 was used in these FO-MD hybrid studies.

4.2.2 Benchscale Setup

Both setups (FO and MD) principally consisted of a flat sheet membrane module fitted into an acrylic membrane cell (**Figure 3.1**). The effective surface area of the membrane was 36 cm^2 for MD (Membrane solutions, China) and 47.25 cm^2 for FO. For MD, the feed side was facing the AL of the membrane (AL-FS mode). Water flux was calculated for both setups.

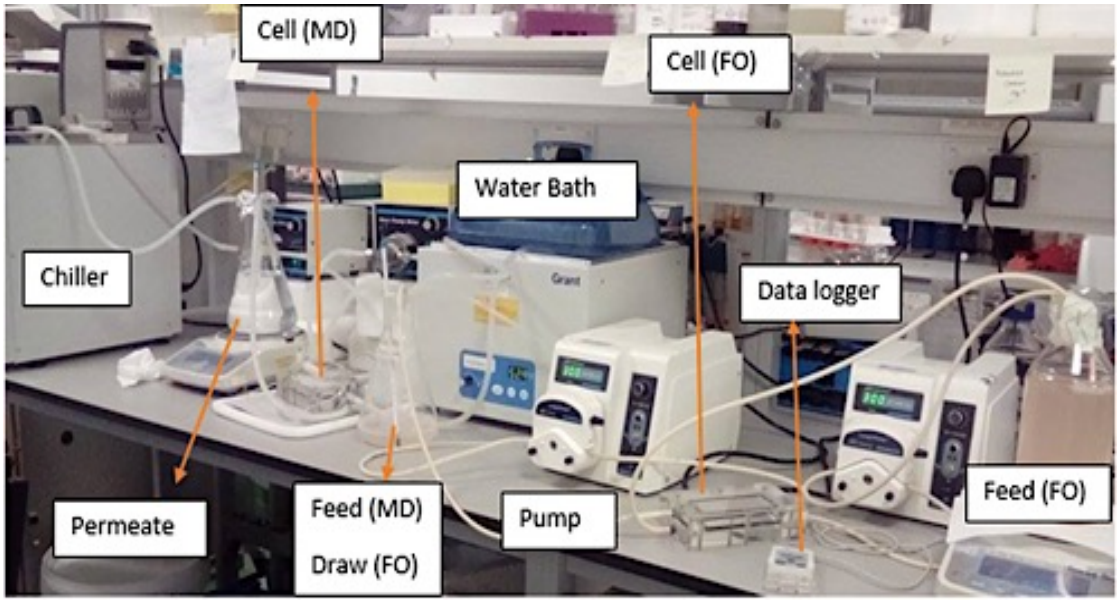


Figure 4.2 Bench scale FO-MD hybrid established in the lab

The draw solution for FO was the feed for the MD. The membrane cell in FO had a DI water feed loop and the draw solution faced the AL for the second loop. For MD, this

same draw solution was in the MD feed loop, which was immersed in a water bath; the permeate, which was immersed in the chiller, was facing the support layer in the MD permeate loop.

A photograph of the FO-MD setup is presented in **Figure 4.2**

Each loop was provided with a circulation pump (Longer pump, China). For the MD unit, the temperature of the feed and distillate temperatures were maintained using a water bath and chiller (Grant, UK) respectively; the latter were connected to pumps (Longer Pump, China) that circulated both streams co-currently within the membrane cell. Conductivity for the permeate and feed was measured using a conductivity meter (YSI, USA) and this was converted into solute concentration by plotting a standard calibration curve for conductivity of a solute against concentration.

4.2.3 FO-MD Hybrid Experiments

For MD, a preliminary experiment was performed using DI water as both a distilland (feed- at warm temperature) and a distillate (permeate- at cold temperature). Direct contact membrane distillation (DCMD) experiments were conducted in batch mode, which resulted in the reconcentration of the feed (that is to say diluted FO draw) solution and produced clean water (for which conductivity was measured) in the permeate stream. Temperature differences of 15 degrees (feed temperature at 35°C and permeate temperature at 20°C), 25 degrees (feed temperature at 45°C and permeate temperature at 20°C) and 35 degrees (feed temperature at 55°C and permeate temperature at 20°C) were chosen for optimisation of the MD process. Three different flow-rates (0.12, 0.17, and 0.21 m/s) were tested for cross flow velocity optimisation. The various feed solutions which had been studied in detail previously in this thesis as draw solutions for the forward osmosis setup were now tested for the

performance of the DCMD setup. The draw solutes included TEAB (surfactant), PDAC (polyelectrolyte), and NaCl (inorganic/baseline). These draw solutes were dissolved in DI water to formulate the initial draw solutions, all at a concentration of0.5M). The experiments were run over several days (3-7) to understand the effects of draw solute dilution and concentration polarization on the flux of the FO and MD membranes. For MD, the membrane orientation was AL-FS and for FO the membrane orientation was AL-DS; this latter was because DI water was used as feed for these optimisation experiments.

4.3 Results and Discussion

4.3.1 Effect of Temperature on MD Flux

The feed temperature is an important parameter in the membrane distillation process as it controls the vapour formation. Since the permeate production rate is proportional to the vapour pressure difference between feed and permeate (Equation 4.1), increasing the feed temperature will increase the permeate production rate.

When the feed temperature and thus the temperature difference across the membrane is low, permeate flux has a direct linear relationship with the partial pressure difference across the membrane (Khayat & Matsuura, 2011), as presented in equation 4.1; it can thus be controlled.

$$\mathbf{P_{mf} - P_{mp}} = \left(\frac{\mathbf{dP}}{\mathbf{dT}}\right)_{\mathbf{Tm}} \left(\mathbf{T_{mf} - T_{mp}}\right) \quad \text{.....4.1}$$

Where $P_{mf} - P_{mp}$ is the transmembrane vapour pressure difference, and $T_{mf} - T_{mp}$ is the transmembrane temperature difference, and dP/dT represents the vapour pressure gradient at T_m. The flux for MD can be represented by equation 4.2:

$$\mathbf{J_w} = \mathbf{C_w}\Delta \mathrm{P_m} \text{ .....} \quad 4.2$$

Where J_w is the permeate flux, C_w is the mass transfer coefficient and $\Delta \mathrm{P_m}$ is the transmembrane vapour pressure difference. Combining both equations, we get equation 4.3:

$$\mathbf{J_w} = \mathbf{C_w}\left(\frac{\mathbf{dP}}{\mathbf{dT}}\right)_{\mathbf{\Delta Tm}}\left(\mathbf{T_{mf}} - \mathbf{T_{mp}}\right) \text{ .....} \quad 4.3$$

Antione's equation describes the relationship between vapour pressure and temperature for water (between 0°C and 373.946°C). Note that for temperatures above the critical temperature (373.946°C), where water is a supercritical fluid, the vapour pressure gradient is practically constant the an inverse slope (i.e. dT/dP) ≈ 235 kPa/°C.

A temperature difference of 15°C (feed temperature: 35°C, permeate temperature: 20°C) was preferred for final operation out of the three combinations available, based on the principle that low-grade waste heat at low temperatures is available on-site in many industrial sites or in homes, and is thus convenient to use for membrane distillation. Note that the concept of using solar-driven MD is also promising for green and environmentally-friendly water treatment and desalination using solar powered membrane distillation (Qtaishat & Banat, 2012; Chang et al., 2010). The draw solutions NaCl (0.5M), PDAC (0.15M) and TEAB (0.5M) were tested against the above temperature differences at a cross flow velocity of 0.12m/s, and the results are shown in **Figure 4.3**.

MD involves simultaneous heat and mass transfer processes, and therefore heat and mass transfer profiles are involved simultaneously, as shown in **Figure 4.4**

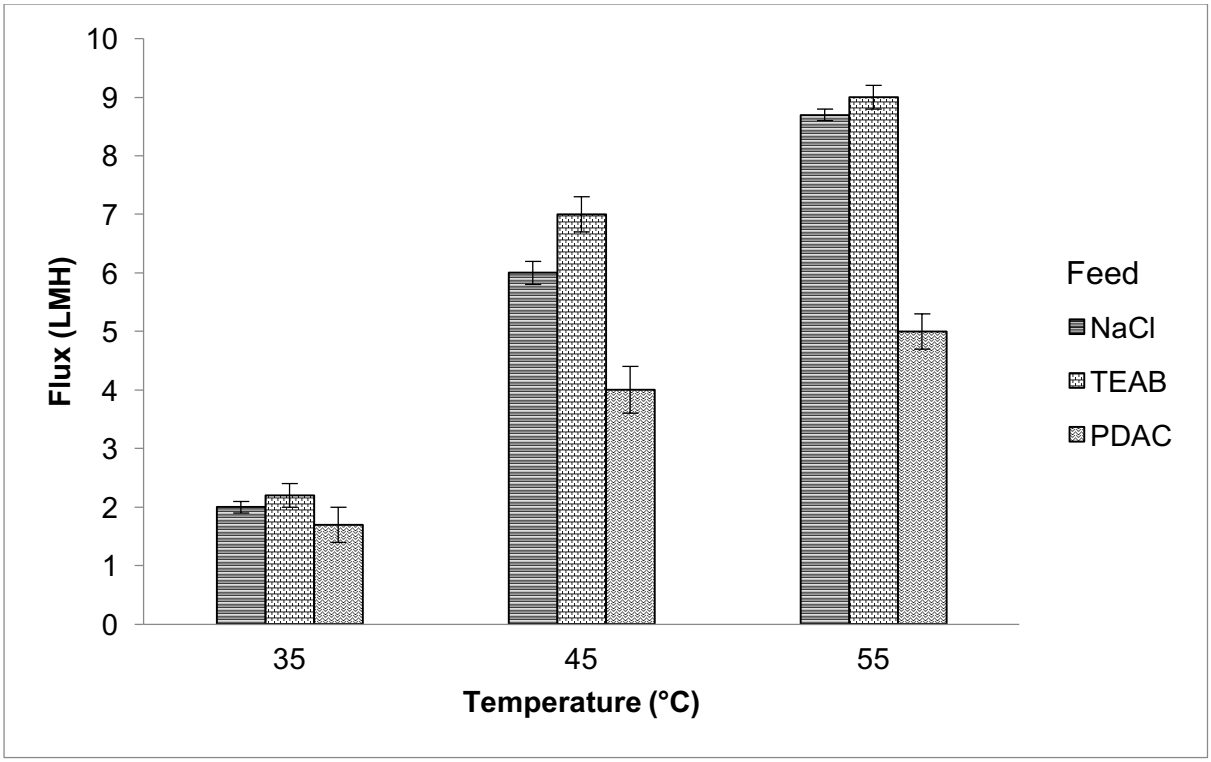


Figure 4.3 MD water flux at different temperatures with CFV of 0.12 m/s at feed temperatures of 35, 45 and 55ºC and draw temperature of 20ºC respectively (AL-FS mode).

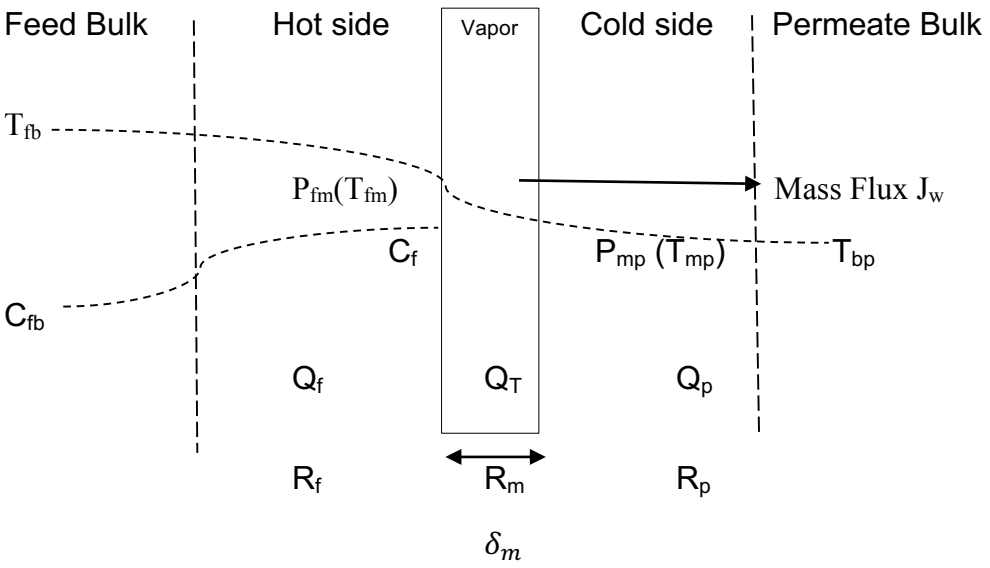


Figure 4.4 Heat and mass transfer profiles during membrane distillation

It was noted that, as the feed temperature increased, the MD flux increased significantly, although the changes were approximately linear with the temperature difference increases (from 15 to 25 to 35°C). Over the modest temperature range, one may expect the vapour pressure gradient to remain failry constant. Note that a small fluctuation in the heating temperature was observed; it was caused by an inefficient internal temperature controlling system. Nevertheless, the small oscillation did not influence the overall results, as the mean values were almost constant. The increase in the feed temperature raises the vapour pressure (Equation 4.1) which results in an increase in permeate flux (Equation 4.3; Martinez-Diez & Vaquez-Gonzalez, 1999), but it is also worth noting that the extra heating demand increases the power consumption in the heating bath.

Nearly all studies on MD similarly confirm (Rashid & Rahman, 2016) the positive relationship between an increase in flux and an increase in temperature. Vapour pressure variation across the membrane is a function of temperature variation across the membrane. For the latter study, at a permeate temperature of 20°C and the varying feed temperatures of 40, 50, 60 and 70°C, the flux increased to 6.5, 8, 10 and 15 kg/m^2hr respectively when the cross-flow rate was kept at 0.6L/min. In the same study, it was shown that when the temperature difference was decreased by increasing the permeate temperature, the overall flux then decreased. Thus, the feed temperature should be increased to a level that is easy to handle and can be maintained so that adequate mass transfer can take place across the membrane.

Ideally, the only heat to be transferred across the membrane pores should be that of the latent heat needed to evaporate the water vapour across the membrane. In reality, there will be an additional amount of unwanted heat transfer caused by conduction

through the membrane. This conductive flux consists of the sum in series of the conductive heat flux through the nonporous part of the polymeric membrane and the conductive heat flux through the water vapour in the pore space of the membrane. The loss due to this conductive flux results directly in a decrease in temperature of the hot feed solution and an increase in temperature of the cold distillate water flowing in the module (normally one or both of these temperatures is constrained at the surface, but the effective difference across the membrane is smaller, and thus the required heating rate is larger than that expected for a certain flux). This leads to temperature polarization across the membrane. In short, a higher temperature difference is needed for MD to achieve a given flux. In addition, the surface tension and viscosity of the water vapour (gas) affects the pore wetting and may result in contamination of the permeate by the feed (Chemical Rubber Co, 1970); leakage is a greater potential problem at higher temperatures.

Temperature polarization is measured with coefficient τ, as shown in equation 4.4:

$$\boldsymbol{\tau = (T_{mf} - T_{mb})/\ T_{bf} - T_{bb})} \quad \text{.....4.4}$$

Where T_{mf} and T_{mb} are the temperatures at the hot and cold membrane surfaces, respectively, while T_{bf} and T_{bb} are the temperatures in the feed and permeate bulk solutions, respectively (Martinez-Diez & Vaquez-Gonzalez, 1999).

As mentioned above, the increase in temperature may also increase the forward transport of the solutes in the feed solution by increasing the fluid-phase movement of these molecules, due to wetting of the membrane (because of increase in diffusion with temperature). In these studies, conductivity in the permeate (20ºC) increased as the feed temperature was increased, indicating a solute leakage across the

membrane, which is another reason for preferring a lower temperature difference for the FO-MD hybrid.

In terms of the safety and permissibility of the draw solutes, PDAC is used in drinking water as a coagulant and is not considered a hazard either by contact or ingestion. It is also important to note that as a part of the manufacturing process, NaCl is a constituent of the PDAC product solution. A maximum dose of 10mg/L PDAC is permitted by the drinking water inspectorate of the UK in their September 2015 report. Similarly, NaCl is commonly found in drinking water but WHO recommends an overall consumption of less than 2g/L of NaCl daily as being more beneficial than >2g/L of salt consumption a day. The limits for TEAB in drinking water are not defined, probably because it is not expected to be present in the drinking water. Note however, that food-grade (i.e. consumable in small quantity) surfactants are available as an alternative.

4.3.2 Effect of Feed Flow on MD Flux

As seen in the section above, optimization of the MD process with respect to temperature is not straight-forward because temperature polarization is a non-linear process and difficult to predict. In addition, because of concentration polarization, cross flow velocity and the concentration of the feed must also be considered during optimisation. Various feed cross flow velocities (0.12, 0.17, and 0.21m/s) were tested to optimize the feed cross-flow velocity for the bench scale lab setup. The results of this experiment are shown in **Figure 4.5.**

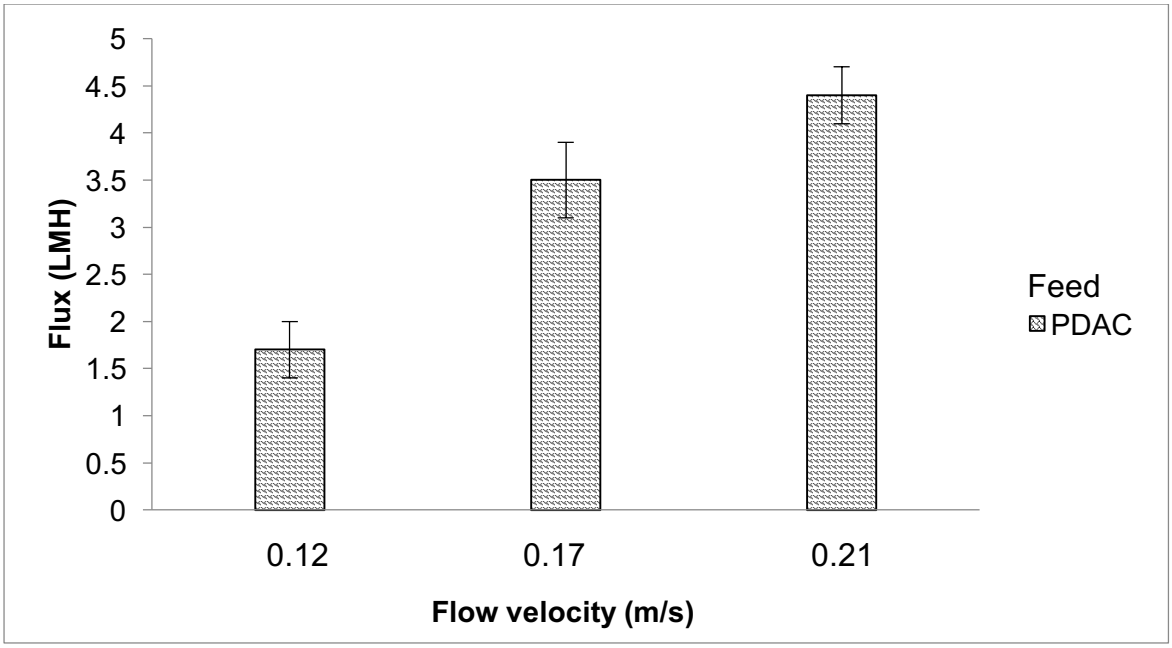


Figure 4.5 Effect of Feed cross flow velocity on flux performance with the feed temperature at 35°C using PDAC as MD feed (AL-FS mode)

A large feed flow-rate and hence cross flow-velocity will increase the turbulence in the flow channel, decrease the thickness of the temperature and concentration boundary layers, and enhance the heat and mass transfer. Normally, a higher feed flow rate will lead to a higher flux rate. In the current study, a 60% increase in permeate flux was observed as feed flow velocity was increased from 0.12 to 0.17m/s; however, there was a minimal difference between fluxes at feed flow rates of 0.17 and 0.21m/s (30%), so the effect of cross-flow approaches an asymptote. It is apparent that the feed temperature has a steady influence on the permeate flux, while the feed flow velocity has a declining effect. Nevertheless, the effect of the velocity should not be ignored, particularly at low values (Martinez-Diez & Vaquez-Gonzalez, 1999).

Dimensionless correlations for heat and mass transfer generally involve power-law relationships with Reynold's number of fractional index. Increasing the feed velocity

results in an increase in the Reynolds number, which decreases the mass and heat transfer boundary layer thickness and increases the mass and heat transfer coefficients (Boubakri et al., 2014b) but at a slower rate of increase.

4.3.3. Effect of Feed Type on MD Flux

Like temperature polarization, concentration polarization also leads to a reduced effective driving force for transport. Concentration polarization is primarily governed by the flux level. Concentration polarization at a membrane surface is quantified using the parameter ς and is presented in equation 4.5 for a feed to the membrane

$$\boldsymbol{\varsigma} = \frac{\mathbf{C_{mf}}}{\mathbf{C_{bf}}} \quad \text{.....4.5}$$

Where, C_{mf} and C_{bf} are the feed concentration at the membrane surface and the bulk, respectively (Martinez-Diez & Vaquez-Gonzalez, 1999).

Since the feed for the MD unit is the diluted draw solution exiting from the FO unit in the FO-MD hybrid, the effect of feed concentration for MD was also studied in the current study. The FO flux was high for simple feeds such as NaCl (2.1LMH), followed by slightly lower values for TEAB (1.9LMH) and then PDAC (1.8LMH) under similar feed with AL-DS mode at 0.12m/s.

An increase in concentration of the solute in the feed can slightly decrease the heat transfer coefficient i.e. at higher solute concentrations; the solution becomes more viscous; the thermal conductivity also becomes lower and reduces the convective heat transfer. Slower rates of heat transfer from bulk flow to the membrane surface increase the temperature polarization.

In a previous study (Boubakri et al., 2014), NaCl solution was used as a feed and it was shown that the fluxes reduced significantly compared to when only distilled water was used as a feed. This is because of the fact that NaCl addition leads to a reduction in the vapour pressure of the water.

In another study (Hwang et al., 2011) at a feed temperature of 60°C, a permeate temperature of 20°C and a cross flow velocity of 0.5m/s, the permeation flux decreased by 10.9% when the feed NaCl concentration increased from 1 to 6 wt%. The associated decrease in bulk vapour pressure was approximately 5.2%. The reason for the bigger than expected drop was attributed to membrane surface temperature polarization that was initially ignored in the study. The temperature polarization layer formed on the PTFE reduces water permeation and the reduction is high when the concentration (of NaCl) and thus flux increases. The effect of salt concentration on flux thus appears to be stronger than the consequent vapour pressure difference alone. This might have arisen as a result of a concentration polarization layer forming on the membrane surface, which would tend to reduce the convection heat transfer due to the latter coupling with the mass transfer.

The highest flux was observed for NaCl, possibly because of the greater ability of fully dissociative salts to reduce the vapour pressure of a solution. This can affect the flux as vapour pressure driving force is reduced.

The vapour pressure of a non-volatile solution is governed by Raoult's law, given in equation 4.6:

$$P_{solution} = (X_{solvent})\,(P°_{solvent}) \quad \text{.....4.6}$$

Where P is the vapour pressure, $X_{solvent}$ is the mole fraction and P° is the vapour pressure of the pure solvent. In this study, water was used as a solvent and has a vapour pressure of 3.16 KPa at room temperature while 0.5 M NaCl solution has a vapour pressure of 2.6 KPa.

For a single feed solute, increasing the concentration can decrease the MD flux. Feed fluxes between 4.5 and 10 wt% NaCl solutions have been studied (Naidu et al., 2017) and the study demonstrated that permeate flux decreased with increasing concentration. This was attributed to a reduction in the driving force to transport the vapour through the membrane pores. This study also showed that addition of $CaSO_4$ or bovine serum albumin (BSA) into NaCl solution did not cause severe fouling. However, an addition of $MgCl_2$ and $MgSO_4$ did have a fouling tendency on the PTFE membrane. This same PTFE membrane, also used in the current study, has been reported for its durability and higher solute rejection compared to that of PVDF which is the second most widely used MD membrane (Cheng et al., 2010).

Surfactant adsorption on hydrophobic surfaces is co-cooperative; surfactant monomers in general do not form micellar-type structures on the surfaces, and instead they form hemi-micelles (monolayers) or admicelles (bilayers) (Naidu et al.,2017). There is strong evidence of surfactants causing a wetting of the membrane. Indeed, surfactant concentration and hydrophobicity have an influence on both membrane fouling and wetting behaviour. Hydrophobic interactions (nonpolar tails) and electrostatic interactions (polar heads) typically play crucial roles in the adsorption of ionic surfactants like SDS. Surfactants can carry both negative and positive charges on their hydrophilic head groups and will be attracted to opposite charges on the membrane surface. However, they can still adsorb on electro-neutral surfaces via hydrophobic (tail-surface) interactions. In general, the higher the concentration, the

higher the adsorption that could be observed. When more SDS monomers were adsorbed onto the membrane surface, they rendered the membrane more hydrophilic, implying the formation of tails-down heads-up monolayers or heads-down heads-up bilayers. The hydrophilic heads may be able to draw more liquid water from the feed into the permeate by reducing the contact angle within pores and will thus increase the wetting of the membrane (Ling et al., 2011), allowing for liquid migration and possible hydrodynamic solute transport into the permeate.

4.3.4 Performance of FO-MD Hybrids with Various Draw Solutions

FO-MD hybrid results with DI water as a feed solution are presented in **Figures 4.6, 4.7 and 4.8.** Relatively simple draw solutes such as NaCl, which are more soluble at a higher temperature and give rise to a higher osmotic flux, also lead to greater lowering of vapour pressure; as a consequence, the rate at which they draw water from the FO feed keeps up with and seems balanced with the rate at which water is being drawn from the draw solution as MD Permeate. However, the fluxes were certainly not as balanced with the higher molecular weight draw solutes TEAB and PDAC; in these cases the MD flux was always higher

The decline in flux for FO with NaCl as draw solute in **Figure 4.6** indicates that the fouling in the FO membrane is significant and takes place in a similar fashion to the experiments without a regeneration system in place (Table 3.5). It was assumed in the latter case that the dilution might result in a decline in flux. However, in the present case with draw regeneration, since FO and MD fluxes are fairly balanced then the dilution is not at all significant. The MD flux on the other hand seems somewhat more stable, and the percentage decline in flux is lower for MD as compared to FO. However, the decline in flux for the FO is low as compared to an FO system running

on its own without regeneration. As presented in chapter 3, Table 3.5, 38% decline in flux was observed after 8 hours, while with the MD system in place, a 27% decline in flux was observed only after 24 hours. Even at the end of day three, a less than 50% decline in flux was observed, although this is still not an ideal result. As stated above, in the current study the MD flux was roughly equal to the FO flux (or exceeded it), suggesting that the draw solution is of steady or increasing concentration; thus the FO flux should remain constant or even increase with time. This supports the hypothesis that membrane fouling is likely to at least be partly the cause, though the effect of reverse solute transport into the feed of the batch-type FO loop cannot be ignored (see below). In a reported study of an FO-MD hybrid (Ge et al., 2012a), the conditions were optimized such that the water transfer rate was the same for FO and MD units. The study doesn't show a decline in flux over a longer time but suggests that the flux performance of an FO-MD hybrid was better than the performance of FO on its own

Compared to the flux for FO, the flux for MD was somewhat steadier and this may be because the temperature of the latter was carefully controlled. However, over the days of the experiment, controlling the temperature at a steady value using the water bath and chiller was not straightforward due to changes in ambient temperature and the water level decrease in the water bath (due to evaporation). Because of this, some variation in fluxes can be expected. The MD flux shows that an increase in temperature during the operation of a continuously running setup may affect the flux but not as severely as for FO. The fluxes throughout a single day were very stable, and a less than 25% decline in flux was observed even after the end of three days of operation. It would certainly be recommended that the membranes be cleaned at the end of daily operation or at least after two days of operation, to keep them clean and to avoid membrane fouling which apparently leads to a steady decline.

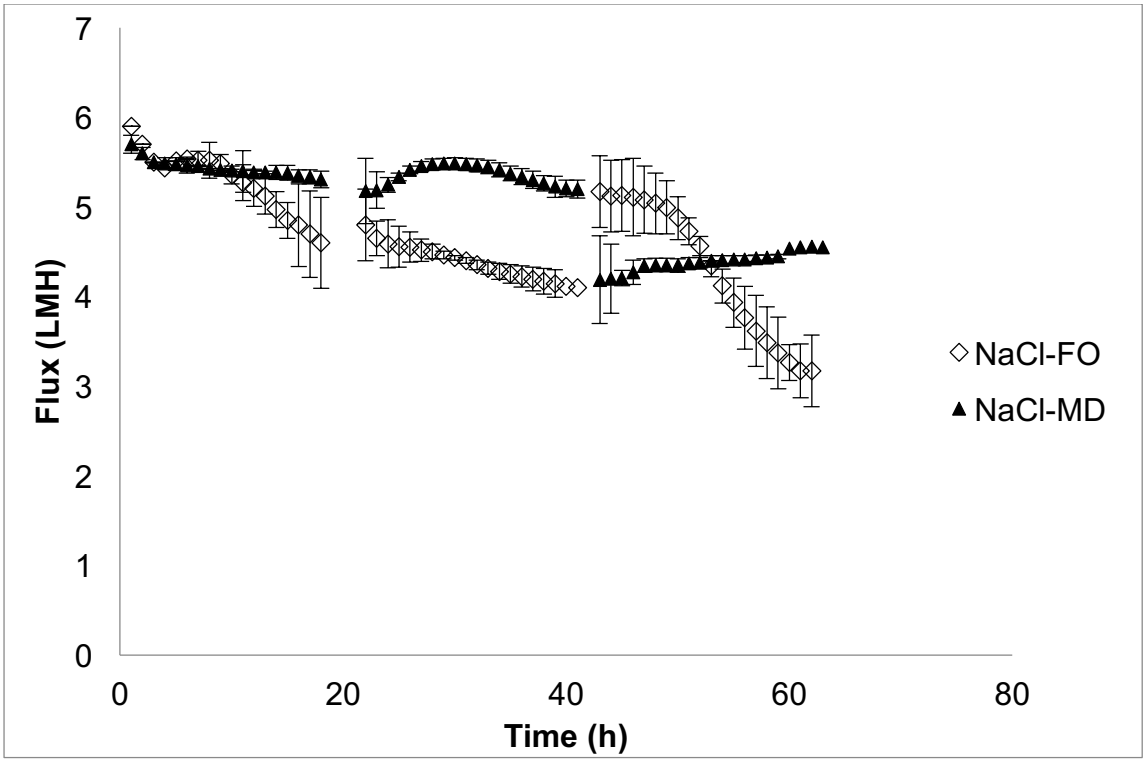


Figure 4.6 MD and FO flux over three days with NaCl as a draw solution and DI water as a feed at a CFV of 0.12m/s (FO: AL-DS, MD: AL-FS)

An increase in temperature increases the solubility of the draw solution; however, due to the increase in diffusion and Brownian motion, the solute molecules and ions are more likely to diffuse across the membrane as compared to the case with no heating system in place for the draw solution (the same heated draw solution enters both FO and MD loops). The FO feed conductivity indicated an increase in RST from 0.2 GMH at the end of day 1 to 1 GMH on day three. As discussed above, this higher RST for NaCl can be linked to a decline in flux in hybrid processes; the feed becomes more concentrated, causing a decline in the driving force. Unlike with FO, the MD solute concentration in the permeate remained very low. Up until the end of the Day three operations, only 0.1GMH was lost. There results show that neither FO nor MD are able to demonstrate 100% rejection for the NaCl ions, but with the FO unit failing far

worse. For this reason, it is advantageous therefore for higher molecular weight draw solutes to be considered and evaluated.

The Na ion has a covalent radius of 0.157nm and an ionic radius of 0.095nm while the Cl ion has a covalent radius of 0.099nm and an ionic radius of 0.181nm. As these ions are very small in size, their permeation into some, if not all, membrane pores is highly likely. Since the MD membranes have a porosity which is on the microscale (0.1-0.22μm), this means that if wetting of the membrane is caused for any reason then the draw solutes could readily leak into the permeate. Therefore, the setup should always be monitored for any wetting changes by continuous permeate conductivity monitoring. Looking at the hydrated size of the two ions, it seems likely that they might also pass through an FO membrane with an effective pore size in the nanometer range.

TEAB has been evaluated previously as a draw solution in Chapter 3 of this thesis. The TEA cation has a hydrated radius of 0.45nm and an ionic radius of 0.385 nm and is most likely to be retained by the FO membrane; however, the Br anion has an ionic radius of 0.196nm. This means that, depending on the membrane size, the smaller ions might be able to pass through. If we look at the flux in **Figure 4.7**, it can be seen that in this case the flux is steadier for FO than for MD. This suggests that as the draw solute increases in molecular weight and becomes more complex in molecular structure, the decline in flux for MD is more obvious as compared to the case of the simple solutes such as NaCl (see below). Nevertheless, at the outset, the system was less balanced with respect to FO (lower) and MD (higher) fluxes than was the case with simple inorganic draw solutes, though The overall decline in flux for TEAB is lower in FO. The lower fluxes for the higher molecular weight draw solutes at similar

concentrations (See also Table 3.5) probably reflects both their lower diffusivity (and greater tendency towards CP) and their lower activity.

The results show that the membrane should be cleaned, depending on the kind of feed used. Because the MD flux exceeds the FO flux, the draw solution is being concentrated at a higher rate than it is being diluted and the flux for FO would be expected to increase. In fact, it remains relatively constant up until day two and then reduces slightly on day three, which is indicative of fouling. This also suggests that very high concentrations of surfactants should be avoided as a draw solution, due to an increased fouling tendency.

The decline in MD flux can be related to the gradual increase in the draw solution concentration and the consequent decrease in vapour pressure driving force. The imbalance in fluxes suggests that the MD flux needs to be more carefully controlled for the higher molecular weight draw solutes, such as via reduction of feed temperature; at the outset of the experiment, the MD flux was too high.

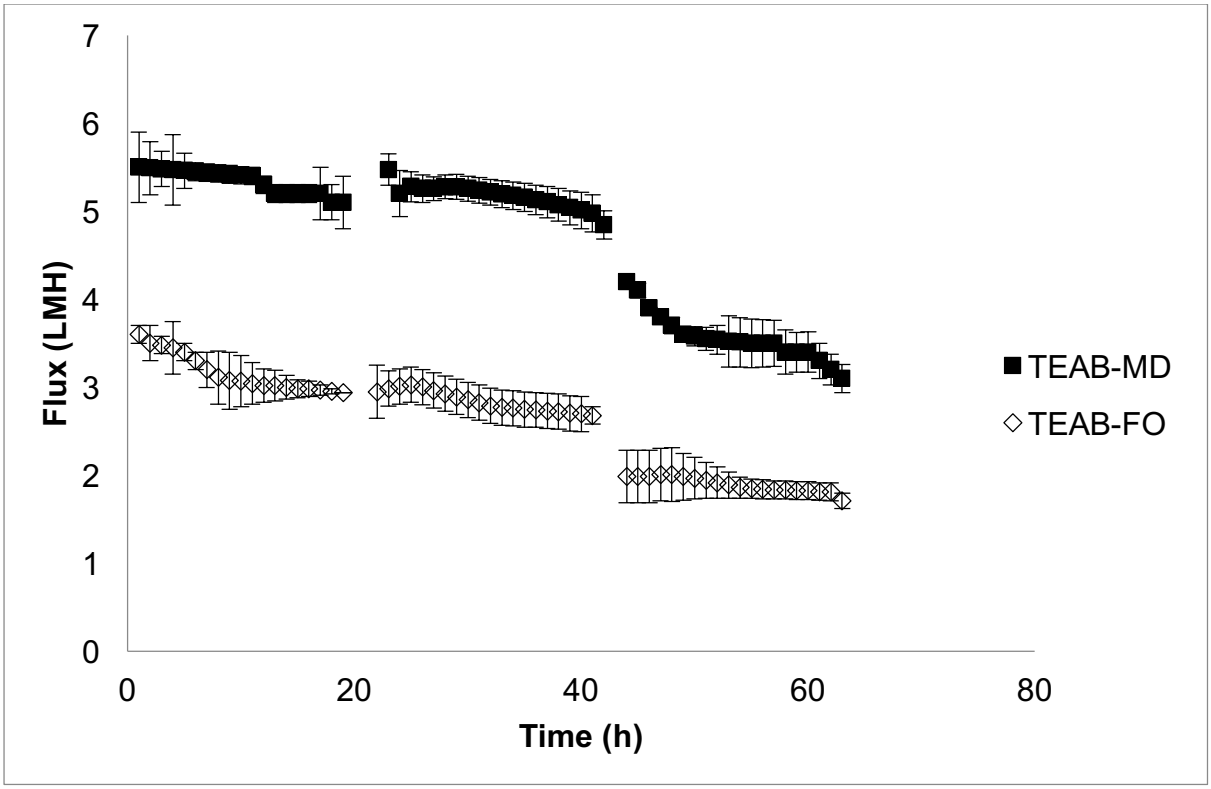


Figure 4.7 MD and FO flux over three days with TEAB as a draw solution and DI water as a feed at a CFV of 0.12m/s (FO: AL-DS, MD: AL-FS)

The RST value for TEAB increased from 0.2 GMH on day 1 to 0.45 GMH at the end of day 3, suggesting that much of the RST takes place in the first 24 hours of FO-MD operation. The concentration of solute in the MD permeate was very low. To evaluate the concentration of TEAB, liquid chromatography analysis was performed to separate out the other ionic species (bromide) present. A calibration curve was prepared, but the presence of TEAB could not be detected in samples as the detection signal remained below the baseline.

To better understand the previous observations and effects, even higher molecular weight draw solutes can be evaluated. Following the previous studies in chapter 3, the polyelectrolyte PDAC was looked at as a draw solution in the FO-MD hybrid system.

It can clearly be observed in **Figure 4.8** that both the FO and MD fluxes are lower for higher (in this case, polymeric) molecular weight compounds. If we look closely, the flux is more stable over a period of days. A stable flux alongside a reduced reverse solute transport in FO and less or no forward transport in MD can render higher molecular weight draw solutes preferable for the FO-MD hybrid.

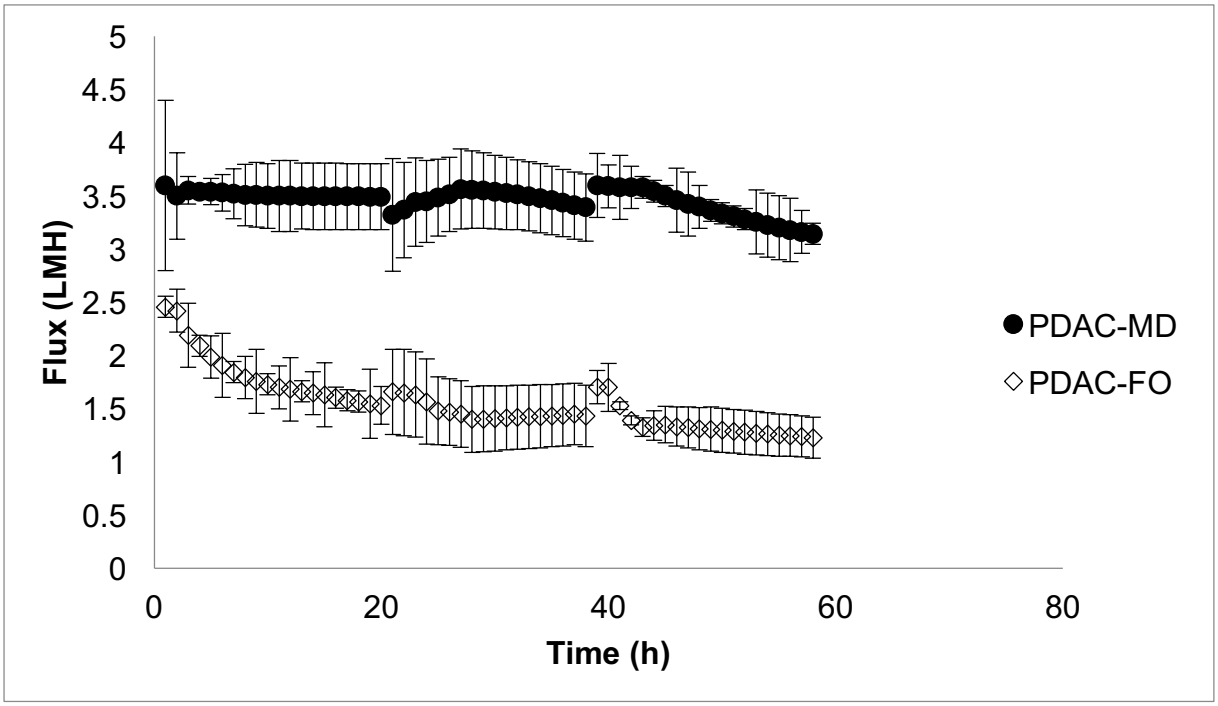


Figure 4.8 MD and FO flux over three days with PDAC as a draw solution and DI water as a feed at a CFV of 0.12m/s (FO: AL-DS, MD: AL-FS).

PDAC has a hydrodynamic diameter of 38.5nm. The polyelectrolyte diameter is very high compared to that of the other draw solutes, NaCl and TEAB. This larger size of PDAC renders it less likely to diffuse and pass through the membrane. The chances of chloride ion escaping from the draw solution side of the membrane seems less likely as well because of the requirement of charge neutrality. However, it may still escape

through an adjustment of the hydrogen ion-hydroxyl ion equilibrium and lead to a change in pH. Although a slight decrease in pH was observed, the same was true for all other draw solutes as well and this seems unlikely.

As was observed with TEAB, a misbalance is observed between FO and MD fluxes; the initial MD flux exceeds the FO flux, unlike the case with the simple inorganic draw solutes, and as before this may be due to a weaker dissociation of the polyion and hence a reduced depression of the vapour pressure. Again, feed temperature control is called for to avoid gradual concentration of the draw solution. The decline in both FO and MD flux is reduced; since the fluxes themselves are lower than seen in figures 4.6 and 4.7, the dynamic magnitude of the draw concentration is reduced, and at the same time a lower fouling tendency is observed for the polyelectrolyte. The much larger molecule may be less able to fully occupy the adsorption sites of the membrane.

The RST values in the feed of the FO and in the permeate of the MD is given in **Figure 4.9**, exhibiting higher values for lower molecular weight draw solutes and lower values for higher molecular weight draw solutes, in broad agreement with the earlier hypothesis. The values of NaCl are higher, but the overall values are negligible in comparison with the RST values obtained in Chapter 3 for FO without a reconcentration system in place. It can be observed that the values of RST for PDAC are low but as observed previously the flux values are $\leq$2 LMH and more membrane space area will be required to achieve higher overall flow (area times flux). TEAB on the other had has an RST comparable to PDAC and a flux closer to NaCl.

While the NaCl RST is highest, it is also the cheapest and gives the highest flux. Therefore, depending on the priority of a large-scale application, e.g., no salinity/draw solute build-up permitted in the bioreactor then TEAB can be preferred, but if high flux

is needed and RST can be tolerated (e.g. where the toxicity is low) then simple inorganic draw solutions like NaCl should be preferred. In all cases, the solute transport into the MD permeate is low and the latter can be expected to be clean.

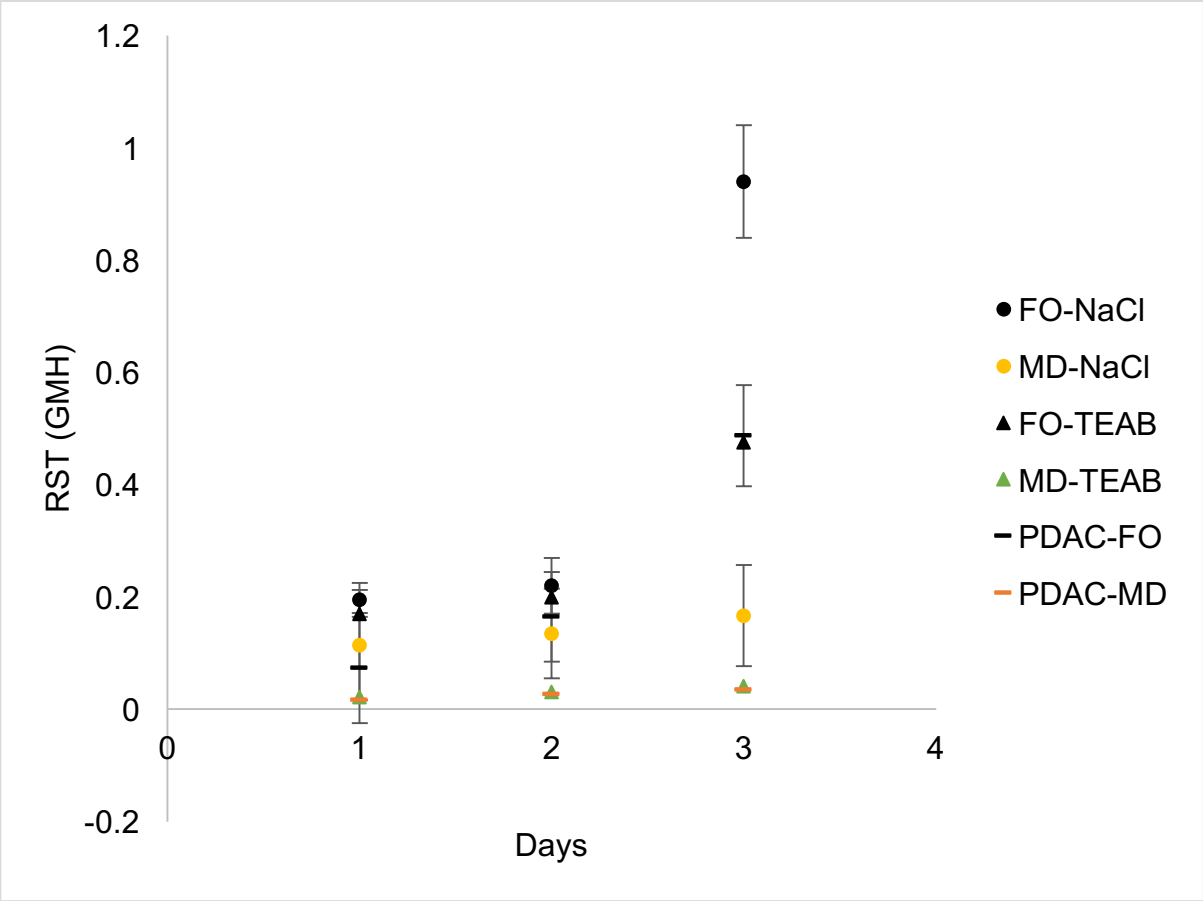


Figure 4.9 RST in FO feed (DI water) and MD permeate (DI water) in a continuous setup at a CFV of 0.12m/s (FO: AL-DS, MD: AL-FS)

4.4 Conclusions

The following conclusions can be drawn from this study:

- In the current laboratory manifestation, DCMD was very similar to FO in its configuration and the two treatment technologies could be used in combination to create a continuous treatment system. When the FO-MD hybrid was running in a continuous mode, the flux was more stable and steady as compared to FO when run on its own.
- When using NaCl as the draw solute, the individual fluxes for FO and MD were both more balanced and higher overall. On the other hand, there was a tendency for the flux to decline which resulted from both fouling and a high RST back to the FO feed loop.
- In the case of TEAB and PDAC draw solutes, however, the fluxes for FO were always lower than that of MD, leading to a rising concentration of draw solution feed to the MD and a subsequent decline in MD flux as a result of feed side vapour pressure reduction. The concentration of the draw solution had much less impact on the FO flux, though in the case of the TEAB fouling eventually caused a decline. For the PDAC, the fluxes were both lower and this diminished the dynamic effect of the draw concentration.
- The greater imbalance in fluxes for the higher molecular weight draw solutes at equal concentrations (as compared to the lower molecular weight draw solutes) partly reflects their lower diffusivities and hence greater tendency towards CP, and partly reflects their lower activity. This can be compensated, for example, by a decreased MD feed temperature, but it highlights the fact that the higher molecular weight draws might require more careful process control in practice.
- When the cross flow was kept constant, the MD flux increased significantly with increasing temperature. A temperature difference as low as 15°C (Feed: 20°C; Permeate: 35°C) can be used for the DCMD process with these draw solutes, and

this means that low grade waste heat from industry can potentially be utilised for the FO-MD process. At relatively low temperature differences, the permeate flux had a linear relationship with the partial pressure difference across the membrane. The increase in flux was higher for NaCl and TEAB (60-80%) when compared to PDAC (20-50%), most likely as a result of less severe concentration polarisation effects arising from the higher diffusion coefficients. The decline in flux was nevertheless severe for NaCl, as well confirming the CP effect.

- A greater feed flow velocity increased the turbulence in the flow channel, decreased the thickness of the boundary layer and increased the flux. Up to a 60% increase in flux was observed when the feed velocity was increased from 0.12 to 0.17m/s, while the increase in flux was not as high when the flow was increased from 0.17 to 0.21m/s. The decrease in flux at lower CFV might be because of conductive heat loss across the membrane and therefore 0.17m/s was chosen as the cross-flow velocity for MD. Higher feed concentrations tend to reduce vapour pressures and hence decrease water vapour transport. Higher concentrations of feed also lead to higher viscosity and will decrease the heat transfer coefficient.
- The FO-MD hybrid enables pure water production and a non-volatile component rejection of nearly 99% with an RST of <0.1 GMH for the draw solutions back to the FO feed and much lower from the MD feed to the permeate.
- The accumulation of solute in the MD permeate is lower than in the FO feed; the latter is higher for lower molecular weight solutes.
- Overall, the FO-MD hybrid can be used in combination for the draw solutes studied to ensure long-term operation and clean water production. NaCl and other low molecular weight solutes are recommended for high fluxes and system stability when high RST leading to salinity or solute toxicity in the MBR tank is not an issue.

Higher molecular weight solutes, such as TEAB or PDAC, are recommended when high flux is less critical and the microbial consortium is expected to be more sensitive to RST and solute toxicity; however, process control becomes more critical for long term operation.

It is important for the FO-MD system to be tested for wastewater treatment, i.e as an FOMBR-MD, because the nature of the FO feed will be different. This system will be presented alongside membrane cleaning in the chapter to follow.

Chapter 5

Optimising the Membrane Cleaning Regime for the FOMBR-MD Lab Scale System

5.1 Introduction

The overall aim of this work was to perform an engineering-oriented study of the component parts and integrated operation of a continuous and feasible FOMBR-MD system. Previous chapters, and chapter 4 in particular, have suggested that membrane fouling is a pertinent issue in the FOMBR-MD process and may lead to a detrimental decline in flux. With this in mind, a study of membrane cleaning regimes to mitigate the effects of fouling and attempt to restore original flux is called for. Prior to this, flux declines were first measured for integrated and continuously operating FOMBR-MD hybrid systems; these studies formed a necessary prior extension of the previous chapter which studied flux changes in the FO-MD system (with DI water as the FO feed).

Membrane fouling in FO has been reported by some workers to be less detrimental and more reversible as compared to RO. Nevertheless, the issue remains somewhat contentious in the research community, and there can be little doubt that membrane fouling remains one of the major drawback for practical implementation of the FO process (Li et al., 2017a). The research to date on FO fouling has mainly focused on organic fouling of the membrane. The organic fouling is caused by organic macromolecules, such as humic acid, or biopolymers, such as proteins (Kwan et al., 2015; Motsa et al., 2014). Alongside foulant, the fouling is also highly dependent upon

the membrane surface properties and the hydrodynamic conditions under which the membrane is being used (Kwan et al., 2015).

Like FO, Fouling is also one of the major obstacles in the application of MD (Srisurichan et al., 2005). Fouling often causes a progressively increasing wettability of a membrane (El-bourawi et al., 2006). It is therefore desirable for the feed water to be pre-treated for fouling control in MD applications. The degree of pre-treatment depends on the nature of the feed solution, the membrane in place, the quality of the product water, and the frequency of the subsequent membrane cleaning (Motsa et al., 2014; Gryta, 2005; Karakulski & Gryta, 2005; Karakulski et al., 2002).

In this chapter, membranes which were used with different draw solutes were cleaned using the same basic cleaning solution, with a chelating agent, which has been applied throughout this study. This cleaning procedure was also compared with acidic cleaning of the membrane. The basic membrane cleaning solution previously optimised in the lab (Nawaz et al., 2016) was found not to be very effective for membranes that have been used for long durations in an MBR setup.

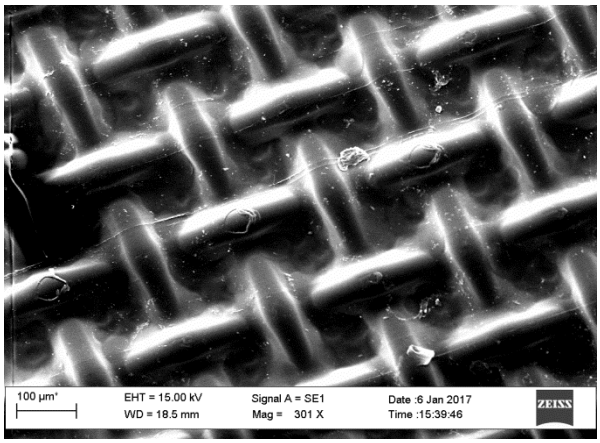
In previous cleaning studies by the group, flux recovery was used as a bench-mark indicator for cleaning efficacy, whereas in the current study the flux performance as well as the separate effect on both the AL and SL was looked at. Literature on FO fouling lacks in depth studies on the need to treat both sides of the membrane separately. After the cleaning procedure, the membranes were then imaged microscopically using SEM and compared for cleaning performance.

5.2 Methodology

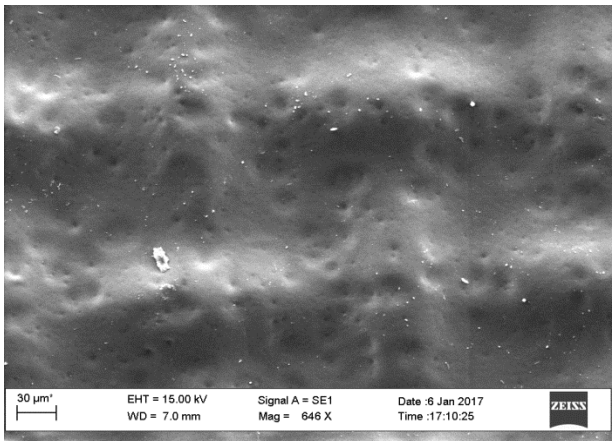
The FO-MBR hybrid was run for NaCl, PDAC and TEAB as draw solutes using the optimised conditions presented previously in chapter 4. The same membranes were first used for the FO-MD process; the feed was then DI water, and was now followed by biological feed in the FOMBR-MD hybrid. The membranes were then cleaned using the different cleaning agents, and observed under the microscope to make further conclusions; since the already used membranes were cut into pieces to perform the microscopic observation, the flux was not observed afterwards.

Biological feed with synthetic wastewater and a *B.subtilis* inoculum was set in place for the MBR. The feed was topped up with synthetic wastewater and autoclaved DI water daily during long-term operation. Bacterial count of the feed was taken daily to check the health of bacteria after fresh food addition and under the effect of possible reverse solute transport.

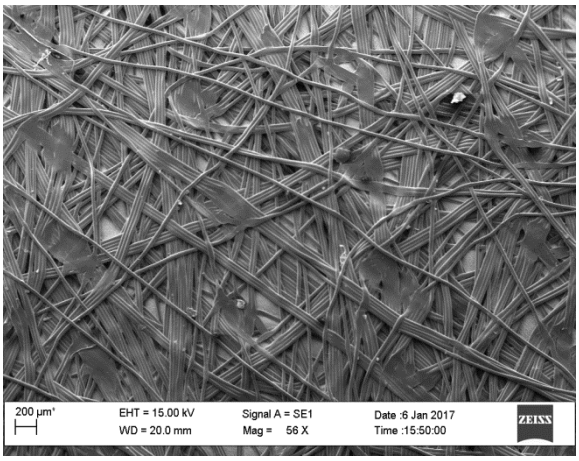
For SEM imaging, membrane samples were dried. Appropriate size samples were cut so they could be fixed onto a specimen holder (stub) to be placed in the SEM chamber. The surface to be analysed was mounted upwards on the aluminium, SEM stub. A Scanning Electron Microscope- Carl Zeiss Evo LS15 VP, with SE (secondary electrons) detector, was used for imaging at varying working distances.



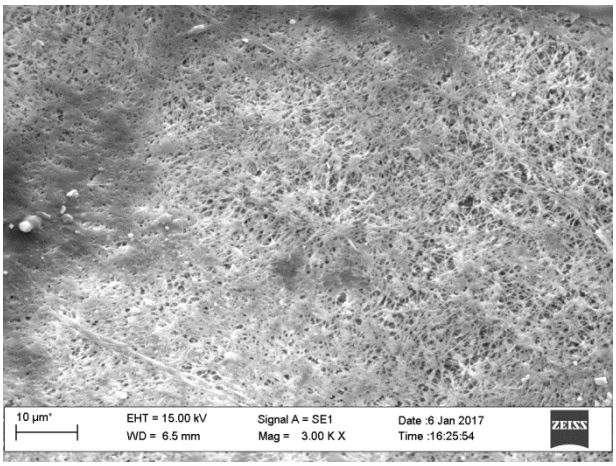
(a)



(b)



(c)



(d)

Figure 5.1 SEM images for a nascent forward osmosis cellulose triacetate membrane (a) Active layer (b) Support layer, and a PTFE MD membrane (c) Support layer (d) Active layer

The samples were gold coated beforehand for better quality imaging. A SC7620 Mini Sputter Coater was used to gold coat the samples. It had an Au/Pd insert and a plasma current of 18mA; with a coating time of 120s, it gave a thickness of 10nm.Images for nascent membranes are given in **Figure 5.1**

5.2.1 Basic Cleaning of the Membranes

The basic cleaning solution comprised of NaOH in combination with EDTA in solution. EDTA in its dry state is a crystalline acid, with a great tendency to form chelates with ions when added to a solution. It is used as a sequestering agent in various lab scale and industrial scale operations. Normally, low pH (acidic) solution is used to remove mineral scale while high pH (basic) solution is used for the removal of organic material. But quite often detergents or chelating agents like EDTA are added to the cleaning solution to aid the removal of colloidal, biological and organic matter.

A high pH enhances the solubility of EDTA and allows it to perform better. The final pH of the cleaning solution thus lay between 11-12. Note that the carboxyl groups of EDTA are not dissociated at low pH, and undissociated carboxyls (COOH) have no charge because the hydrogen is covalently bound; thus, EDTA in the acid form is almost insoluble in water (Zauner & Zha, 2011) while dissociated EDTA is ionic and can therefore dissolve in water.

The membranes were cleaned by immersion and then rinsing with DI water for ten minutes followed by immersion in the cleaning solution for 30 minutes. They were then rinsed with DI water and stored in DI water prior to analysis.

5.2.2 Acidic Cleaning of the Membranes

Many inorganic compounds are soluble in acidic solutions. A cleaning solution with low pH was therefore used for the removal of inorganic membrane fouling (Wallberg et al., 2001). The foulant doesn't completely dissolve in an acidic solution; however, even partial dissolution allows the foulants to be flushed away from the membrane surface. On the other hand, the pH cannot be too low, as many polymeric membranes will degrade under highly acidic conditions. HCl, H_2SO_4, H_3PO_4 and HF have all been

used for cleaning various membranes. In the current study, 2% HNO_3 and 2% H_3PO_4 was used for cleaning the membrane. Various concentrations of the solution were tested and the pH was kept at 2 or above, according to the instructions of the membrane manufacturers i.e. HTI and Membrane Solutions.

As before, the membranes were first cleaned with DI water for ten minutes, followed by the cleaning solution for 30 minutes. They were then cleaned with DI water again before being stored in DI water prior to SEM imaging.

5.3 Results and Discussion

5.3.1 FO-MBR Hybrid

The FO-MBR hybrid flux for 0.5 M NaCl, TEAB and PDAC as draw solutes is shown in **Figure 5.2.** After this set of experiments, the membranes were taken out of the cell and cut into samples for cleaning analysis.

It was expected from chapter 4 that the MD flux would be more stable because it has a simpler inorganic, low molecular weight feed i.e. NaCl solution, while the FO feed loop is itself being fed by the MBR (synthetic wastewater with a *Bacillus subtilis* inoculum in it). Because of a continuous reconcentration system in place, it was also desired (and anticipated from the results in chapter 4) that the draw solution would ideally remain at a concentration of 0.5M at all times.

At the beginning, the flux graph shows that the NaCl draw solute with its high osmotic potential is able to draw water molecules from the wastewater tank During this time, the MD setup is acclimatizing to the experimental conditions and temperature, and is stabilising as time passes. The increasing concentration polarization (due to a gradual increase in feed concentration; we are after all operating a batch reactor) and gradual

dilution of the draw solution causes a rapid decline in flux for the forward osmosis until day two. On the other hand, the MD flux gradually increases before decreasing and then finally becomes steady by day two up to day four. It is believed that in the case of NaCl, after two days the critical flux for the MD was reached. Critical flux (Field & Pearce, 2011) is defined as "a flux below which a decline of flux with time does not occur; above it, fouling is observed". When compared with the FO-MBR hybrid for TEAB and PDAC as a draw solute, it can be observed that with a small molecular weight draw solute like NaCl (**Figure 5.2**) FO membrane fouling occurs in the first two days and then the FO-MBR becomes a self-sustainable system. Flux for both FO and MD remain the same after a certain amount of time and fouling. For larger molecular weight compounds, on the other hand, a different pattern was observed (see below).

In a particular study (Aimar et al., 1989), in the first two days as the membrane fouled, permeate flux declined, partly because the hydrodynamic conditions at the membrane surface changed with time. The decline in flux was accounted for by overall ICP, ECP and membrane fouling on the membrane surface. The results also suggested that critical flux for osmotic and vapour pressure-driven membrane systems is reached later than for pressure driven membrane systems.

Because of the higher flux evident for regeneration than for FO in the case of TEAB, the draw solute for the FO process in this case might become more concentrated than its initial concentration, and this higher concentration might have led to the greater chemical fouling of the membrane.

When PDAC was used as a draw solution in the FO-MBR hybrid setup, the fluxes for both the FO and MD processes were steadier in the first three days and started to decline more rapidly on the fourth day. In this hybrid setup, it could be observed that

once the draw solute was more concentrated, the flux for forward osmosis started to increase, as was observed on day 4. However, in relative terms, the fluxes observed remained rather too low to consider using these draw solutes on a larger scale (values between 10-20 LMH or above are preferred).

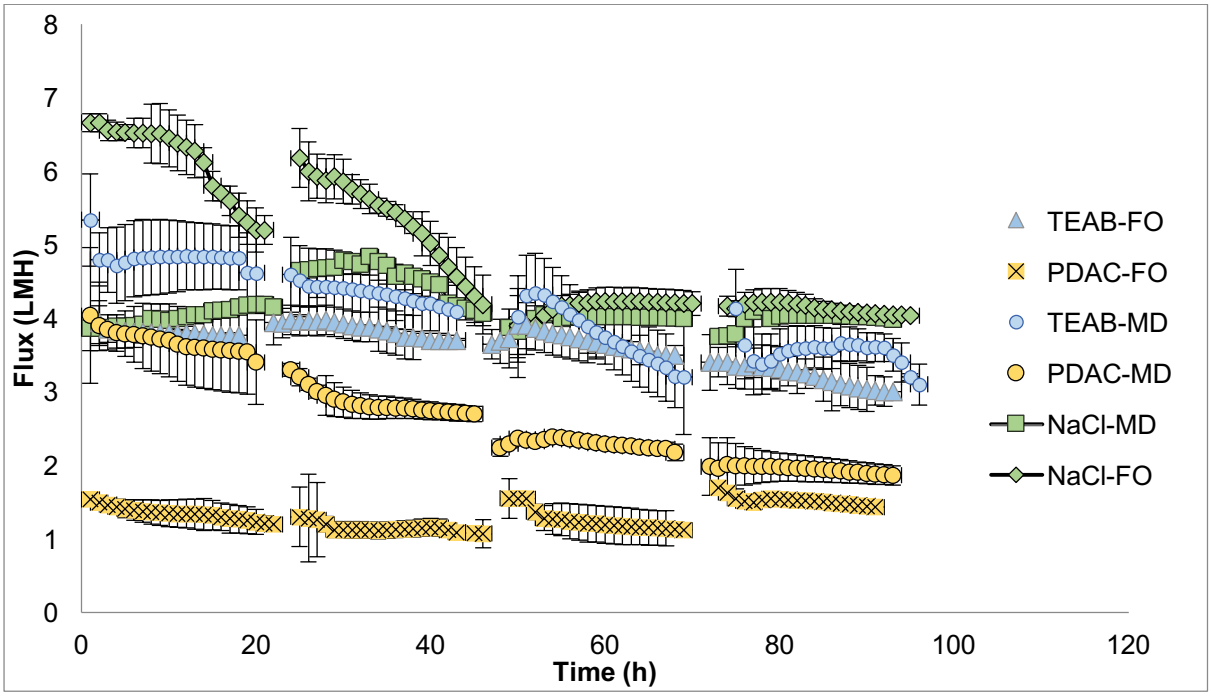


Figure 5.2 MD and FO flux over three days with NaCl, TEAB and PDAC as the FO draw solution and synthetic wastewater with bacterial inoculum as the FO feed in an FOMBR-MD hybrid at a CFV of 0.12m/s (FO: AL-FS, MD: AL-FS)

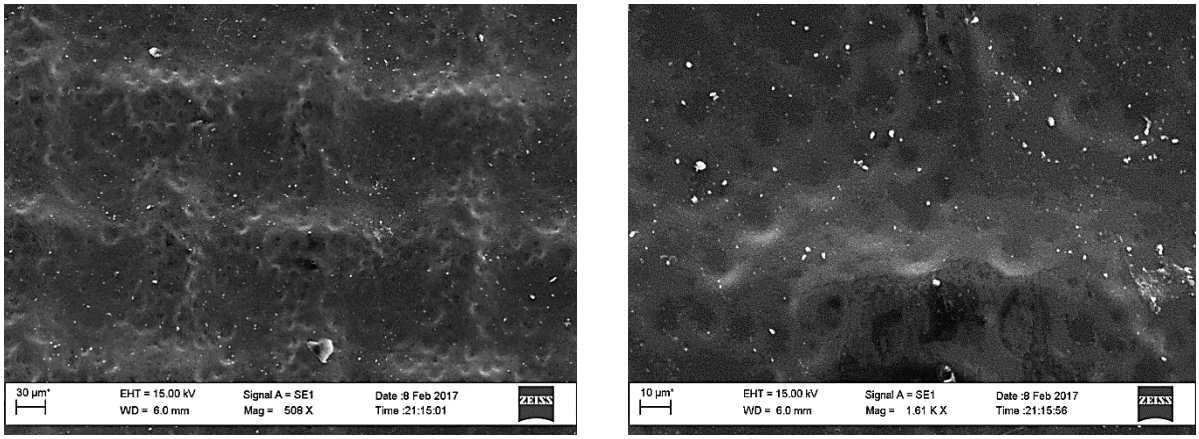
It is worth noting that, for all the draw solutes in Figure 5.2, the FO and MD fluxes tend towards equalisation despite initial differences, so that a stable operating point is always reached regardless of the type of draw solute. But for the reasons already suggested in chapter 4, this flux tends to be lower for higher molecular weight and more complex draw solutes.

Because of the complexity of the feed, the reverse solute transport could not be calculated in the FOMBR unit. However, the bacterial count of the MBR was checked daily to observe any decline in the bacterial count. It was noted that the overall health of the MBR remained very good, suggesting that the reverse solute transport (even though not measured) did not have a deleterious effect on the microbial consortium Only the forward solute transport to the MD permeate was looked at using electrical conductivity, to analyse the quality of the product water. The forward solute transport was less than 0.1 GMH at the end of day 7 of the FOMBR-MD hybrid.

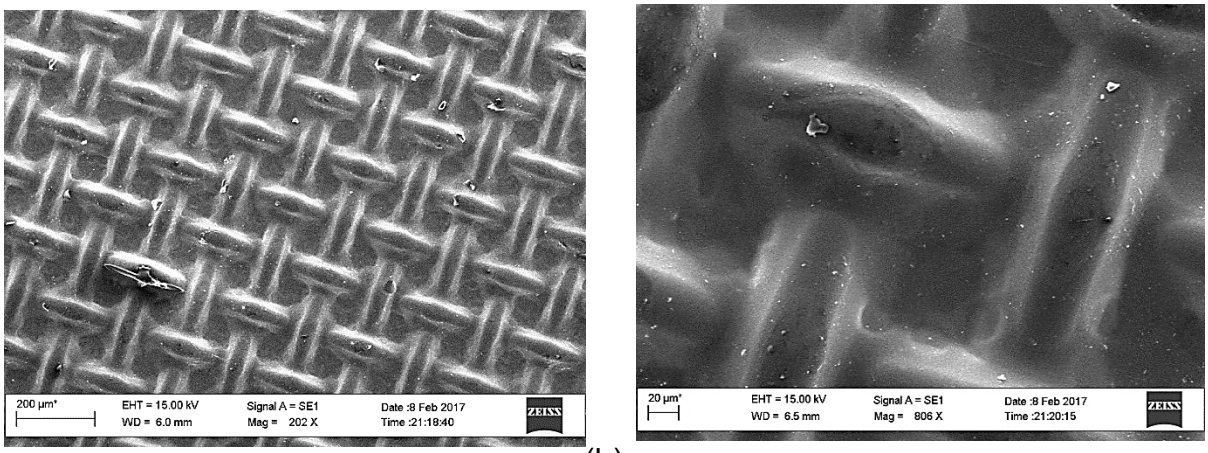
5.3.2. Membrane cleaning-NaCl Draw Solution

Basic cleaning- NaCl Draw Solution

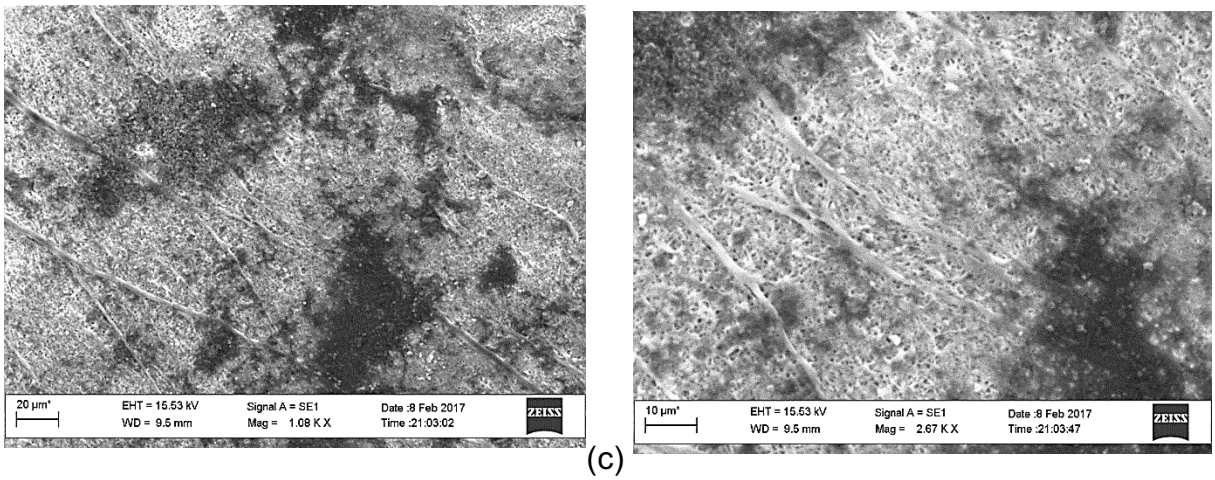
The SEM image for membranes cleaned with basic solution with chelating agent (NaOH and EDTA) is shown in **Figure 5.3.** Each image indicates the membrane surface and the solution it faced. The figures in (a) show that there is draw solution deposition on the FO support layer, while those in (b) show that the microbial growth/ biofilm production on the active layer is minimal and the membrane condition remains very close to that of the virgin membrane so that the fouling is reversible or at least removable. Similar to FO, the MD membrane in (c) also seemed to remain very close to its nascent state (compare also with Figure **5.1 (d)** and the basicity of the solution does not seem to have damaged the membranes.



(a)



(b)



(c)

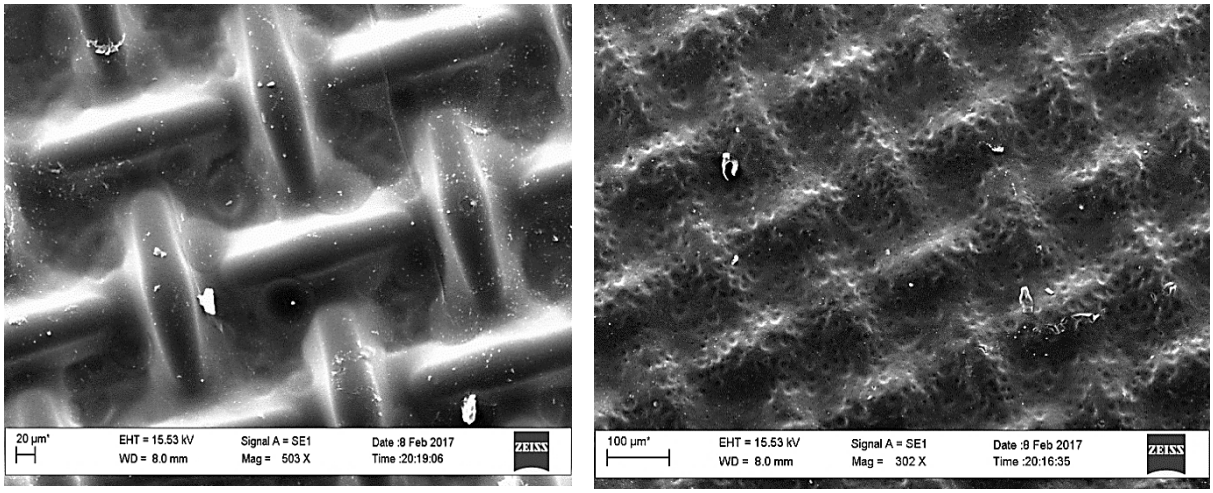
Figure 5.3 SEM image when NaCl was used as a draw solute after basic cleaning at two different magnifications (a) SL-DS, FO (b) AL-FS, FO (c) AL-FS, MD

Acidic cleaning- NaCl Draw Solution

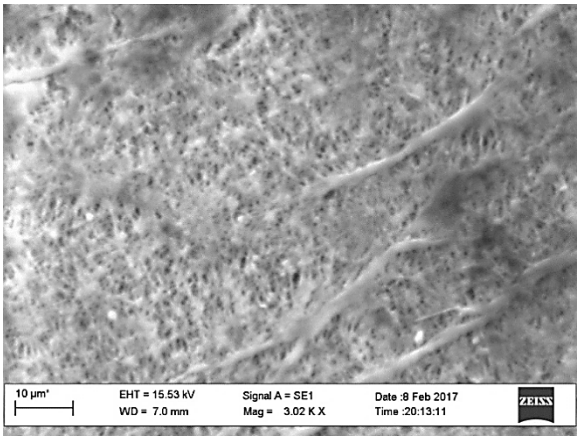
Similar to the case of basic cleaning, in the acidic cleaning process the final draw solute (Figure 5.4 (a)) and feed component deposition (Figure 5.4 (b)) on the membrane surface was minimal and quite a large area of the membrane was observed to be clean. Indeed, for acid cleaning, the draw solute deposition on the support layer was lower and cleaning was more effective than for basic cleaning. Irrespective of having a larger pore size of 0.2 microns, the MD membrane appeared to be very clean as well (Figure 5.4 (c)).

In pressure-driven membrane processes, membranes with a larger pore size tend to foul more severely. The pore size of the membranes in relation to the sizes of the particles in the wastewater feed stream in membrane filtration systems can thus have an effect on membrane fouling. The pore blocking mechanism tends to increase in importance with increasing membrane pore size (Guglielmi & Andreottola, 2010). However, in our current work we found that the MD membrane had a relatively stable flux and seemed to foul less than the FO membrane irrespective of a larger pore size ($0.2\mu m$).

Due to the hydrophobic interactions occurring between the membrane surface material, the microbial cells and the solutes, membrane fouling is more severe for hydrophobic membranes compared to hydrophilic membranes, particularly for MBR systems (Le-Clech et al.,2006). Hydrophobic compounds such as fatty acids will cause hydrophobic membranes to foul more readily than hydrophilic membranes (Al-Amoudi,2010).



(a) (b)



(c)

Figure 5.4 Membrane after acidic cleaning when NaCl was used as a draw solute in FO-MD (a) SL-DS FO (b) AL-FS FO (c) AL-FS MD

5.3.3. Membrane cleaning-TEAB Draw Solution

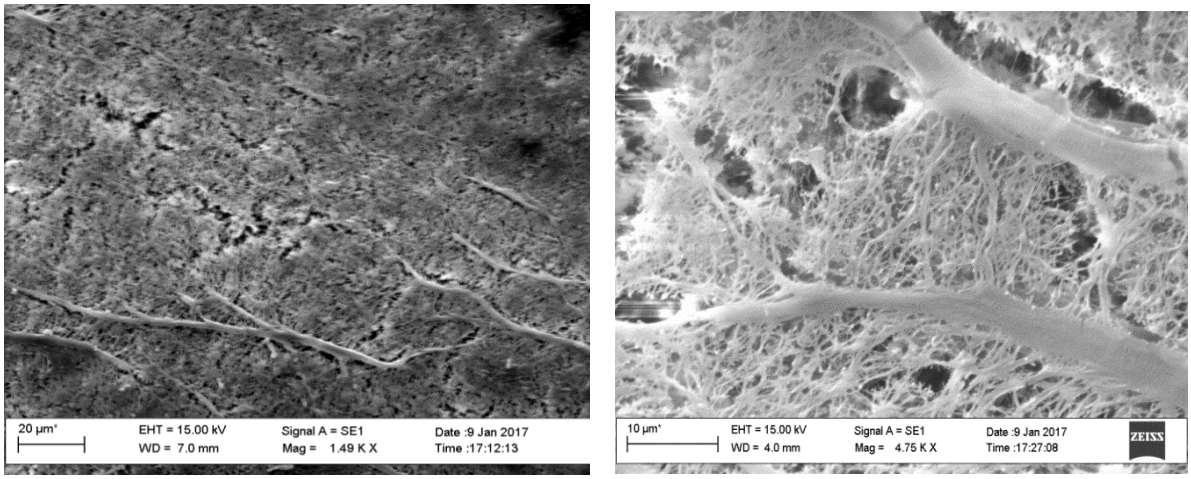
Acid Cleaning- TEAB

After cleaning, the bacterial growth is more visible on the active layer when TEAB is used as a draw solute compared to when NaCl is used (Figure 5.5 (b)). As with the active layer, the support layer shows more draw solution deposition after cleaning

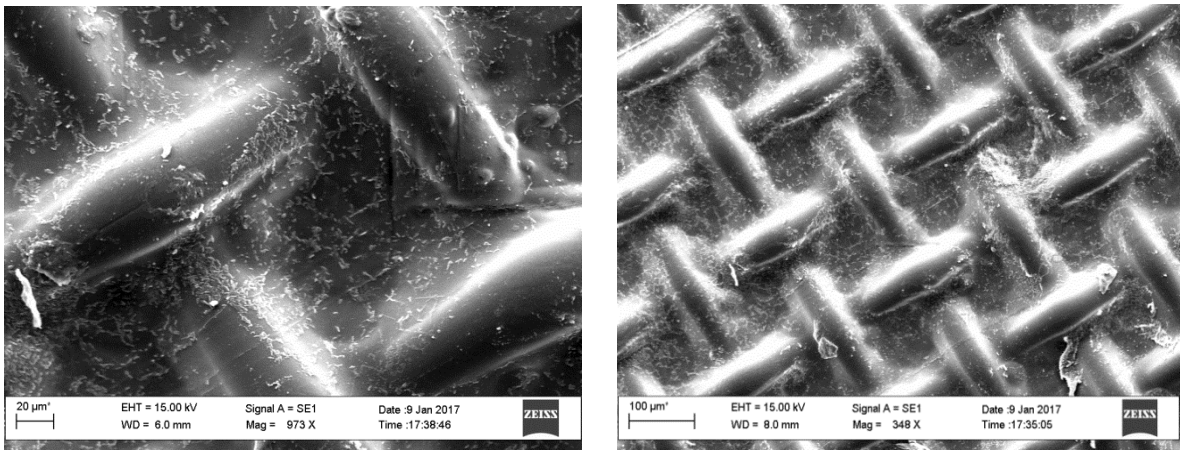
(Figure 5.5 (c)). This suggests that larger molecular weight draw solutes that are able to osmotically draw water through a membrane because of their chemical potential also contribute to higher levels of chemical fouling to the membrane. This fouling tendency can also be related to the hydrophobic and associative characteristic of surfactants, and their ability to adsorb and cause wetting is clearly an issue with respect to MD membranes (Figure 5.5 (a)).

Basic Cleaning-TEAB Draw Solution

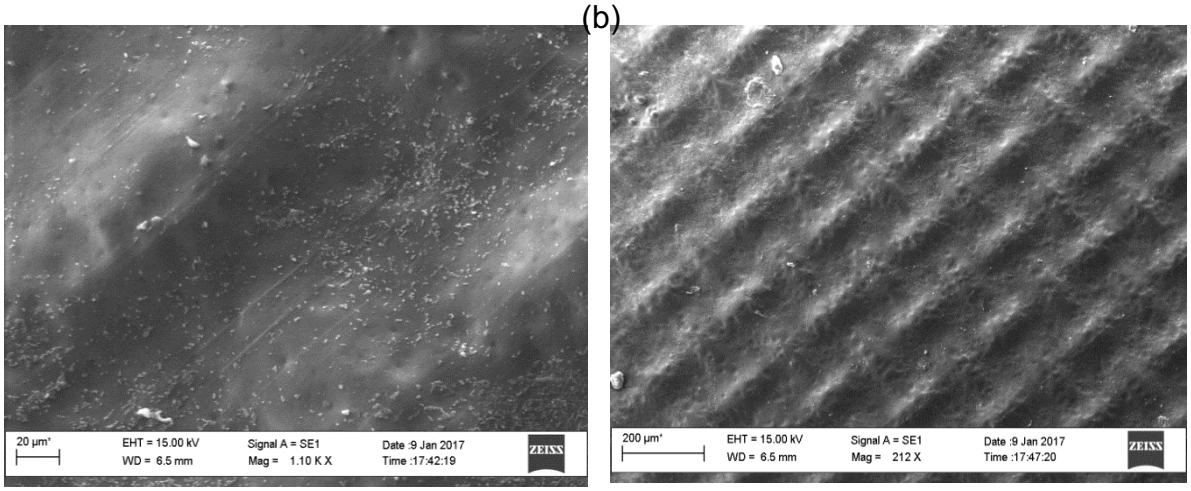
The cleaning potential should be compared with respect to the cleaning agents. When basic cleaning is compared with acidic cleaning (note that basic cleaning was used throughout the project), the SEM images below suggest that it is not as effective as acidic cleaning of the membrane. The MD membrane seemed to have fared well for all cleaning techniques (Figures 5.3 (c), 5.4 (c), 5.6 (a)). However, unlike the MD membrane, both the AL and SL sides show major foulant deposition on the FO membrane surface after basic cleaning for the TEAB draw solution (Figure 5. 6 (b) and (c)).



(a)

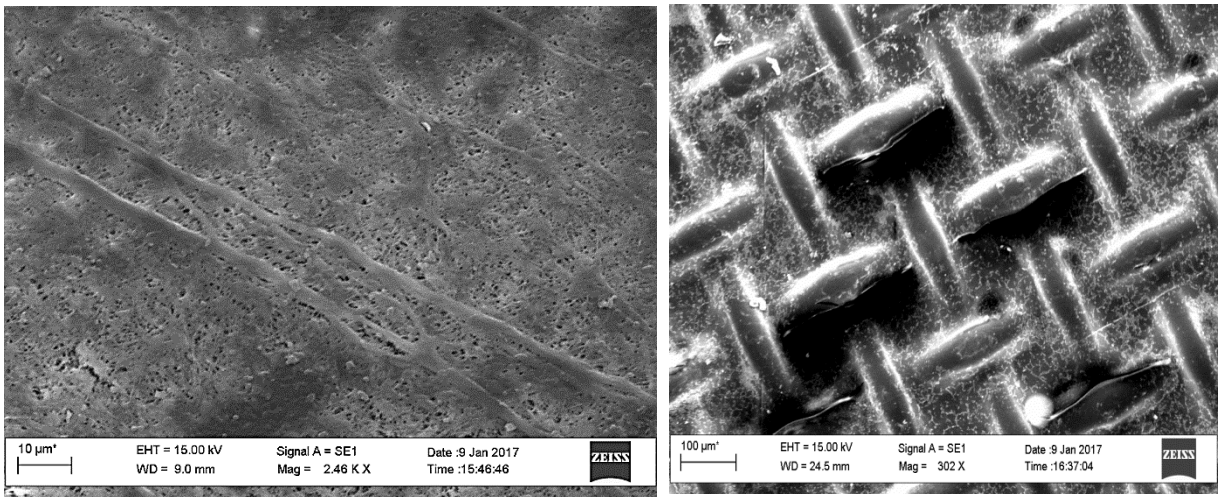


(b)

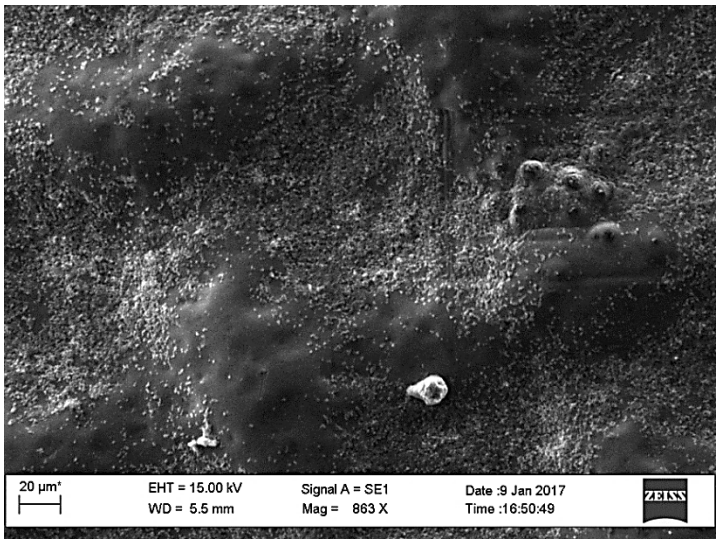


(c)

Figure 5.5 SEM image when TEAB was used as a draw solute after acidic cleaning (a) AL-FS MD (b) AL-FS FO (c) SL-DS FO



(a) (b)

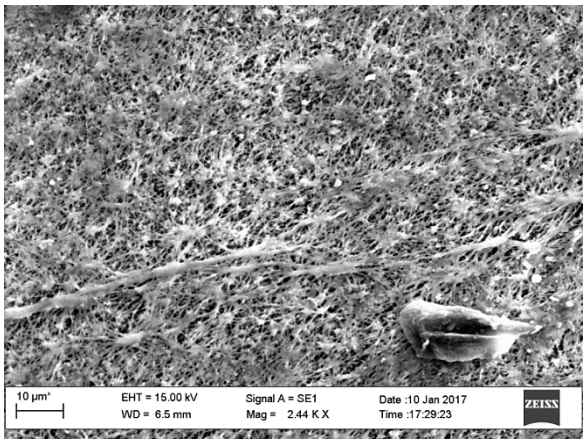


(c)

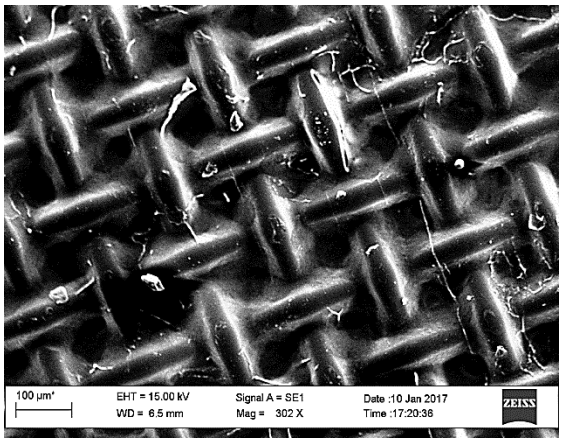
Figure 5.6 SEM image when TEAB was used as a draw solute after basic cleaning (a) AL-FS MD (b) AL-FS FO (c) SL-DS FO

5.3.4. Membrane Cleaning-PDAC Draw Solution

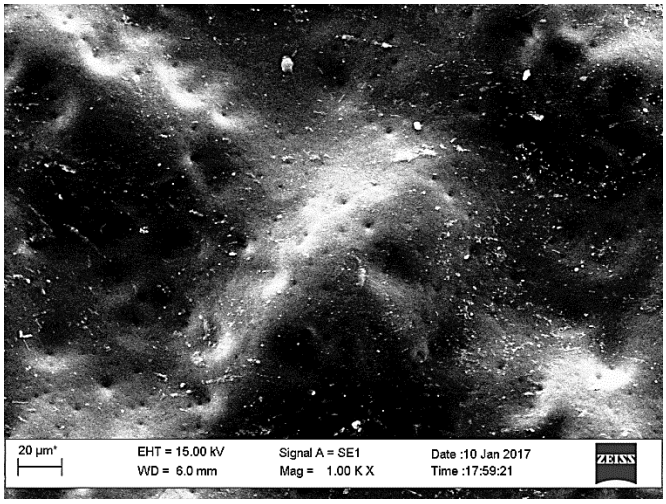
The results of basic cleaning treatment for the membranes when used with PDAC as draw solute are shown in **Figure 5.7** and can be compared with the results of acid cleaning in **Figure 5.8**. The MD active layer and SL for the FO are cleaner when acidic solution was used for cleaning compared to other draw solutions (Figures 5.4 (c), 5.5 (a), 5.8(a)). The FO active layer shows better results with basic treatment (Figure 5.7(b) versus 5.8(c). Nevertheless, the membrane seems to have degraded during its operation and subsequent cleaning with both solutions, as it is damaged in places (one of these places is highlighted in the image with a yellow circle). Since the active layer is common to all the treatments, this could not be a result of the cleaning chemicals. HTI CTA membranes can tolerate a range of 2-11 pH but will still be affected due to acids and basis over time. Whether this is due to the nature of the draw solute or the cleaning agent is harder to infer from the current study.



(a)



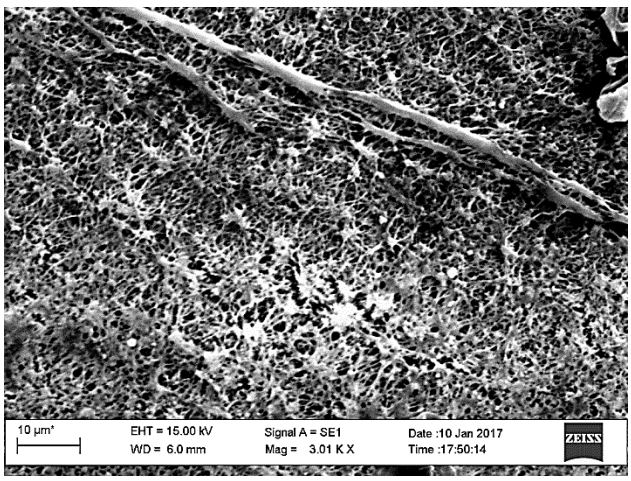
(b)



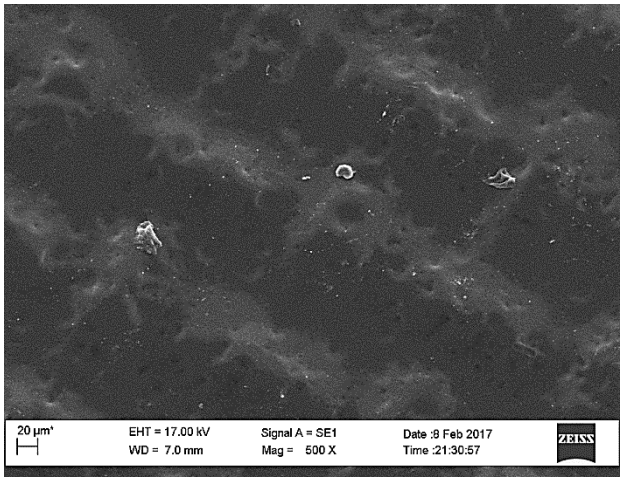
(c)

Figure 5.7 SEM image when PDAC was used as a draw solute after basic cleaning (a) AL-FS MD (b) AL-FS FO (c) SL-DS FO

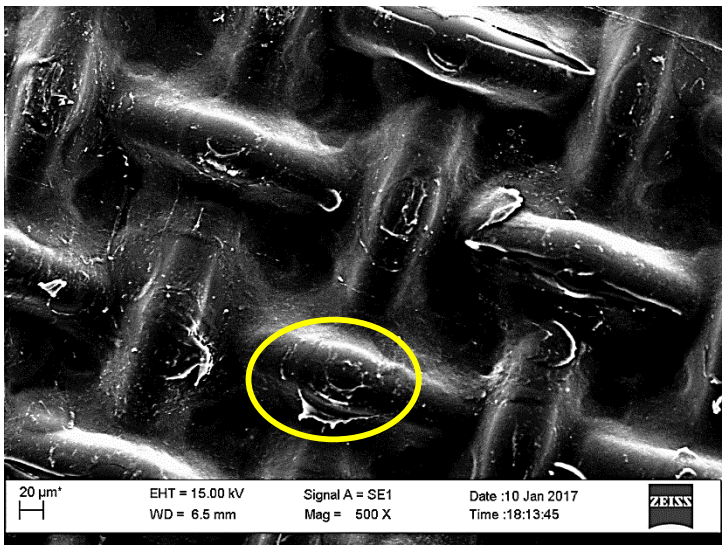
Acidic Cleaning- PDAC Draw Solution



(a)



(b)



(c)

Figure 5.8 SEM image when PDAC was used as a draw solute after acidic cleaning (a) AL-FS MD (b) SL-DS FO (c) AL-FS FO

As was also the case with NaCl, PDAC did not deposit on the membrane surface as much as TEAB (compare Figures 5.5 and 5.6 with Figures 5.7 and 5.8).

Based on the various SEM images obtained, the following recommendations can be made with regard to the best method for cleaning the membranes chemically.

Based on the various SEM images obtained, the following recommendations can be made with regard to the best method for cleaning the membranes chemically.

Table 5.1 Summary of best cleaning procedures based on SEM imaging of membranes after cleaning.

Draw solute	**FO-AL**	**FO-SL**	**MD-AL**
PDAC	Basic/Acidic cleaning	Acidic cleaning	Acidic/basic cleaning
NaCl	Basic cleaning	Acidic cleaning	Acidic/Basic cleaning
TEAB	Acidic	Acidic	Acidic/Basic cleaning

As the FOMBR-MD hybrid for 0.25M TEAB in Figure 5.2 showed a steady flux decline, it was studied for a longer period. The flux for 0.25M TEAB was measured over a period of seven days with daily cleaning in place, and is shown in **Table 5.2.**

Table 5.2 FO and MD flux for TEAB in the FOMBR-MD hybrid

Day	**MD (LMH)**		**FO (LMH)**	
	Average at hour 1	**Average at 24 hours**	**Average at hour 1**	**Average at 24 hours**
1	5.5	4.2	2	1.9
2	4	3.1	2.2	1
3	3	2.4	3	2.5

4	3.2	3	2.5	1.8
5	3	2.8	2.8	1.9
6	3	2.6	2.2	2.1
7	5	4.1	2.4	2

The results showed that the fluxes are recoverable and stable when the FOMBR-MD hybrid is run over extended periods of time and regular (in this case daily) chemical cleaning is applied.

5.4 Conclusions

The following conclusions can be drawn from the current study of membrane fouling and cleaning for the FO-MBR hybrid process for wastewater recovery and recycle:

- The fouling tendency of an FO and MD membrane in the presence of a simple inorganic draw solution like NaCl (that shows high osmotic pressure) is low, despite being able to yield a very high flux (7-8LMH at 0.5M) in FO.
- For NaCl as a draw solute in FO and as a feed for regeneration in MD, basic cleaning was deemed fit to treat the FO-AL side faced with biological feed. The FO-SL side showed better cleaning with acidic solution while both acidic and basic cleaning worked well for the MD AL.
- Unlike NaCl, TEAB showed a greater decline in flux and a greater residual foulant deposition on its surface after cleaning the membrane. The feed side (AL) of the FO membrane became more fouled, and more bacteria were observed attached to it.

- The acidic cleaning solution out-performed the basic cleaning solution for both the AL and SL membrane surfaces when TEAB was used as draw solute. While the acidic cleaning of the FO membrane was observed to be more effective than with basic cleaning, the MD membrane was observed to clean equally well with both acidic and basic cleaning solutions.
- The PDAC draw solute showed the lowest flux of all for FO, but unlike the other two draw solutes its FO and MD flux is more steady and stable, and a negligible decline in flux was observed for PDAC. However, because the MD flux was almost double that for FO, and the draw solute was thus concentrating more by MD than it was diluting by FO, a slight increase in flux was observed after several days
- Having a larger molecular size than TEAB, PDAC was expected to cause more concentration polarization and fouling in the FO membrane. However, the membrane observed under SEM after cleaning showed that the clean membranes are comparable to that when using NaCl as draw solute. It can therefore be inferred that the medium molecular size compounds with higher flux cause more fouling than the larger molecular compounds with relatively lower flux. This might also be explained by the lower flux generated by the high molecular weight leading to lower fouling and vice versa. The larger molecule is also less able to occupy all the available adsorption sites on the membrane. Acid cleaning was always shown to be suitable and preferable for treating the FO membrane support layer, while in some cases basic cleaning was preferable for the FO membrane active layer. For the MD membrane (feed side), both acidic and basic cleaning were equally effective.

Chapter 6

Conclusions and Recommendations for Future Work

6.1 Summary of Work Done

The overall aim of the current work was to perform a practical, lab-scale study involving thorough experimental work to examine the component parts and integrated operation of a continuous and feasible FOMBR-MD hybrid system for the treatment and recycle of wastewater, using novel and existing draw solutions to achieve stable and acceptable fluxes. This was investigated by comparing organic (surfactants and polyelectrolytes) and inorganic draw solutes using two different membranes (HTI and NF) in a live membrane bioreactor (MBR) for performance comparison. Synthetic municipal wastewater was selected as a feed, and *Bacillus subtilis* species was inoculated in the solution and grown overnight for development of a monoculture bioreactor. DI water was used as feed for control. Conventional inorganic salts (NaCl, Na_3PO_4) were tested against the surfactants (TEAB, SDS) and polyelectrolytes (PDAC, PGBE) as novel draw solutes. Osmotic pressure, flux, toxicity, reverse solute transport and viscosity were observed for the draw solutions. The study was then extended to investigate the integration of a Membrane Distillation (MD) unit with the Forward Osmosis (FO) unit as a means of recovering clean water from the latter and regenerating the draw solution. In this hybrid system, the diluted draw solution was fed to the MD unit. This hybrid setup was used to run a continuous FOMBR-MD system to study the flux, reverse transport of solute, and their toxicity. To conclude the study, acidic and basic cleaning solutions were employed for both FO and MD membranes for different draw solutions followed by observation using SEM. For basic cleaning,

0.5mM EDTA was used with 0.5g/l NaOH. For acidic cleaning, 2% HNO_3 and 2% H_3PO_4 was used for cleaning the membrane.

6.2 Conclusions

It was found that NF membranes when used in the FO-MBR yield a higher flux. The initial fluxes were higher for the NF membrane than the HTI FO membrane in FO-MBR because the NF was a single layer membrane with higher pore size and water permeability than that of the HTI FO membrane. With the NF membrane, as the feed was changed from DI water to monoculture synthetic wastewater, a decline in flux was observed over several hours. The decrease in Flux for CTA membrane was; TEAB (28.5 %), Na_3PO_4 (44.8 %), PGBE (18.9%), NaCl (38%), PDAC (27%), SDS (13%), While the decrease in flux for NF with the change in feed was; PDAC (57%), TEAB (41 %), PGBE (20.4%), SDS (12.5%). Measurements of reverse solute transport were also made; the RST values for the NF membrane were only slightly higher than for the HTI-FO membrane, and in either case led to a low consequent toxicity to the microbial consortium. In the absence of a reconcentration system in place after 24 hours of operation, the highest RST was observed for NaCl (9.33 GMH) and the lowest for higher molecular weight draw solutes (PGBE: 1.2 GMH), both for the CTA FO membrane, and similar results were observed for the NF membrane. Draw solutes that exhibited highest viscosities also showed lower fluxes ($\geq$ 2cP for SDS and PDAC), while draw solutes that exhibited lower viscosities, showed highest flux (e.g. NaCl: 1.2cP). NF membranes are therefore recommended for further investigation in the FOMBR-MD process. Although the observed RST values were not toxic for the bacteria under observation, long-term accumulation of draw solute in a water and wastewater treatment plant using FO can be an issue requiring further investigation.

When the FO-MD hybrid was set in place and allowed continuous system operation with regeneration of the draw solution, the flux achieved was more stable and steady as compared to when FO when run on its own. A temperature difference as low as 15°C (Feed: 20°C; Permeate: 35°C) was used and a CFV of 0.17m/s was finalised to achieve better performance. A more balanced FO-MD hybrid system was observed for NaCl (Figure 4.6), as it gave a high flux for FO and the overall fluxes for FO and MD seemed to balance such that the draw solution remained at the same concentration. A steady decline in flux was still observed (although much lower than that compared to FO run on its own), however, which was attributed to both membrane fouling, and RST leading to the presence of draw solute in the feed. In the case of TEAB (Figure 4.7) and PDAC (Figure 4.8), however, the fluxes for FO were initially lower than those for MD, leading to a gradual concentration of the draw solution being fed to the MD. The more concentrated draw solution did not cause an increase in the FO flux ; the increase in feed concentration due to RST was likely to be small, and it was concluded that fouling must play a role. For the case of PDAC, the fluxes were both low and thus the dynamics of draw concentration were less apparent.

Overall, it was shown that the FO-MD hybrid can be used in combination with the draw solutes studied to ensure long term operation and clean water production, provided that balanced systems (FO/MD) with high fluxes are achieved. In this regard, control of the MD flux (perhaps by regulation of the feed temperature) is expected to be more important for the larger molecular weight solutes due to their poorer flux performance per unit concentration. That said, an FOMBR-MD system can always be expected to evolve to a state in which FO and MD fluxes are balanced, since greater MD flux leads to greater draw concentration and thence FO flux, and vice versa. The final flux is necessarily lower in the case of poor flux performers, such as the PDAC.

Acid cleaning was shown to be suitable for treating the FO membrane support layer. Basic cleaning was sometimes preferable for the FO membrane active layer, while for the MD membrane feed side both acidic and basic cleaning worked equally and adequately. For TEAB, which was the draw solute studied with the greatest tendency to foul, it was shown that a continuously operated FOMBR-MD system can be run for extended periods of time (several days) and with relatively constant and stable flux on the order of 4-5 LMH, provided that regular membrane cleaning was performed.

Overall, for nearly all draw solutes, the highest reverse (FO) and forward solute (MD) transport was seen to occur during the first two days and the following days showed a lower reverse solute transport. The RST was lowest for the high molecular weight draw solutes. The forward solute transport across the MD membrane to the permeate as observed via electrical conductivity was very low, suggesting that the water is fit for reuse (including for potable purposes after appropriate further treatment) or environmental discharge. Similar trends were observed for FOMBR-MD hybrid and high quality permeate was achieved (>99% rejection of solute).

It is recommended that when high flux is important and salinity or solute build-up issues are not important, low molecular weight, inorganic salts are used as draw solutes. On the other hand, when flux is less important and toxicity issues due to salinity build-up are critical, higher molecular weight organic or poly-electrolytic solutes are used.

The overall aim of this work, which was to perform an engineering-oriented study of the component parts and integrated operation of a continuous and feasible FOMBR-MD system, was deemed a success in the sense that such a system was installed and run over the longer term. Nevertheless, key questions remain and key deficiencies in

the experimental procedure must be addressed, and these points are discussed below.

6.3 Recommendations for Future Work

Due to the lab health and safety regulations, real wastewater was not permitted for the current research project and therefore municipal synthetic wastewater with a monoculture was established to mimic the reality. This is not the best alternative to wastewater from treatment plant; the author has previously worked with wastewater and understands well that the operational issues and their scale will be yet greater with real wastewater. It is recommended that future studies incorporate real wastewater; this will likely have an effect on membrane fouling, toxicity, FO flux and RST, and so on.

A key limitation of the current work is that it has been run using a continuous, closed-loop batch system. This presents a number of questions with respect to its applicability to a full-scale, engineered system. In the FO process, reverse solute transport can be expected to lead to a non-steady state accumulation of draw solute in the MBR tank; a fully continuous system is to be preferred, in which fresh wastewater is fed and spent sludge (containing retained draw solute) is removed from the tank, and make-up draw solute is introduced to the draw tank, allowing a closed material balance. The long-term accumulation of draw solute in the MBR tank will have implications for microbial toxicity, fouling and FO flux stability. In the MD regeneration loop, the forward solute transport to the permeate appears to be minimal; however, solutes introduced in the wastewater feed can forward transport across the FO membrane and again build-up in the MD feed loop, causing gradual loss of the vapour pressure driving force in the latter.

The lower temperatures needed as well as the lower temperature differences required for FO-MD in the lab made it easy to operate, but less control was possible during long-term study. For example, changes in the weather were able to affect the temperature of the system; this was partly because it was impossible to immerse the whole process or at least the entirety of the flow loops in the water bath or chiller (the establishment of a submerged membrane system was attempted, but this could not be achieved). Indeed, the temperature of the FO feed was mostly not controlled because of the limited size of the chiller bath and the priority for temperature control of the permeate.

It was also realised that control of the MD feed temperature was more important for those draw solutes with higher molecular weight which exhibited a poorer FO flux performance. Greater temperature control is therefore necessary. An alternative might be to place the whole system in a sealed tent in which air temperature is controlled.

For temperature polarization, temperature sensors were placed close to the membrane and in the main supply. Values were observed in person, but automatic monitoring overnight was not possible because of lack of the sensors required. Similarly, simultaneous temperature control in all three streams was not achieved; in addition to the limitations mentioned above, the author did not have access to the many sensors, controllers and actuators required. Again, future work should consider including these components.

A direct osmotic pressure measuring device was fabricated and developed during the project, but could not be made to perform correctly because of a leak in the system. Such a device would nevertheless be desirable, since osmotic pressure is a key

parameter; in many cases (e.g. SDS), the freezing point depression method was not suitable because of a limited solute solubility at low temperature.

Reverse solute transport values would be difficult or practically impossible to calculate with municipal wastewater as feed when using the analytical facilities available for this study, because of the presence of several other species. Nevertheless, such measurements will be essential in the future.

Table 6.1 Draw solution RST loss in FOMBR-MD hybrid (see also Appendix I)

Draw solute	Total Draw solute (KG) for 500L feed	RST[c] (FO-MD bench scale hybrid after 24 hours (GMH)	Total RST/day in grammes (RST*24*Membrane area) (kg)	Percentage loss in one day (%)	Cost of RST loss/day (£)
NaCl (1M)	29.2	0.22	0.327	1.12	0.1[a] 8[b]
TEAB (0.5M)	52.5	0.268	0.398	0.75	0.12[a] 34.6[b]
PDAC (0.5M)	40.4	0.148	0.220	0.54	0.3[a] 5.9[b]

[a:] cost assumed is that of industrial-grade material [b]:cost assumed is that of lab grade material. Economy of manufacturing scale means the industrial cost would be much lower than the lab-scale so these latter figures are extremely pessimistic. [c] See section 4.3.4, Figure 4.9 (these figures are much smaller than those observed in section 3.3.3)

With the help of the research literature and values obtained from the bench-scale process, a pilot-scale FOMBR-MD Hybrid for small community provision is briefly designed for future application and this is presented in Appendix I. Using the RST

values obtained from the FO-MD hybrid, the RST loss and the material cost incurred/day was calculated and is presented in Table 6.1. It can be observed from this Table that there is a significant amount of RST; as mentioned above, the associated material cost and other issues like long term salinity in the case of NaCl and toxicity in the case of TEAB during very long-term operations of the hybrid systems will need to be taken into account.

The next important consideration for FO-MD hybrid process is the level of flux of FO and MD (and finding a balance between the two systems by suitable control, as discussed elsewhere). For examples, in Table 4 in appendix I it can be observed that the membrane requirement for the PDAC draw solution is approximately 290 modules of 2.5m^2 surface area, which is very high and will lead to a high capital costs, due to the very low flux values of PDAC in FO compared to that for regeneration with MD. In the current study, the same concentration of draw solutions were used for FO throughout, in order to allow a meaningful comparison. Their use at a higher concentration would yield a correspondingly higher flux. It is advised for future research on this system to focus on using draw solutions at a concentration where similar fluxes between FO and MD can initially be produced; the system should then proceed in a balance fashion as discussed previously. Nevertheless, this might cause other problems to arise from the increased RST, toxicity, and fouling. The alternative would be to control MD feed temperature, but this would imply lower fluxes.

The research objectives of the current study were intentionally broad, as the objectives were ambitious. Nevertheless, with the successful establishment and optimisation of the FO-MD process in the lab, more focused research studies can and should be performed in the future.

Appendix I

FOMBR-MD Hybrid Scale up

The overall aim of this study was to perform an engineering-oriented study to examine the component parts and integrated operation of a continuously operated MBR FO-MD hybrid system for the treatment and recycle of wastewater. By and large, this was achieved. However, the focus of the current study was on a continuously run closed-loop, batch process at the lab-scale; due to limited resources and time, it was not possible to consider all the issues related to scale-up to a full-size, open-loop and continuous system, nor to monitor and control those factors which would play an important role. Although current economic and technical uncertainties are such that the hybrid process is not yet recommended for very large-scale wastewater treatment plants, such as those required to serve a population on the order of tens of thousands, scaling up for the installation of a niche, small-scale treatment plant is more feasible, and is briefly considered in the following design exercise.

A small housing society of 150 people is considered for the currently recommended installation, with a water consumption and wastewater generation of 150L/person/day.

The wastewater treatment plant will comprise of an equalisation tank, followed by primary treatment (coarse filtration, and flocculation). FO membranes will be installed in the bioreactor tank as secondary treatment, and this will be followed by an MD installation in the re-generation tank as tertiary treatment. A schematic for the process flowsheet is given in Figure 1, and an outline design for the secondary and tertiary treatment processes are given below.

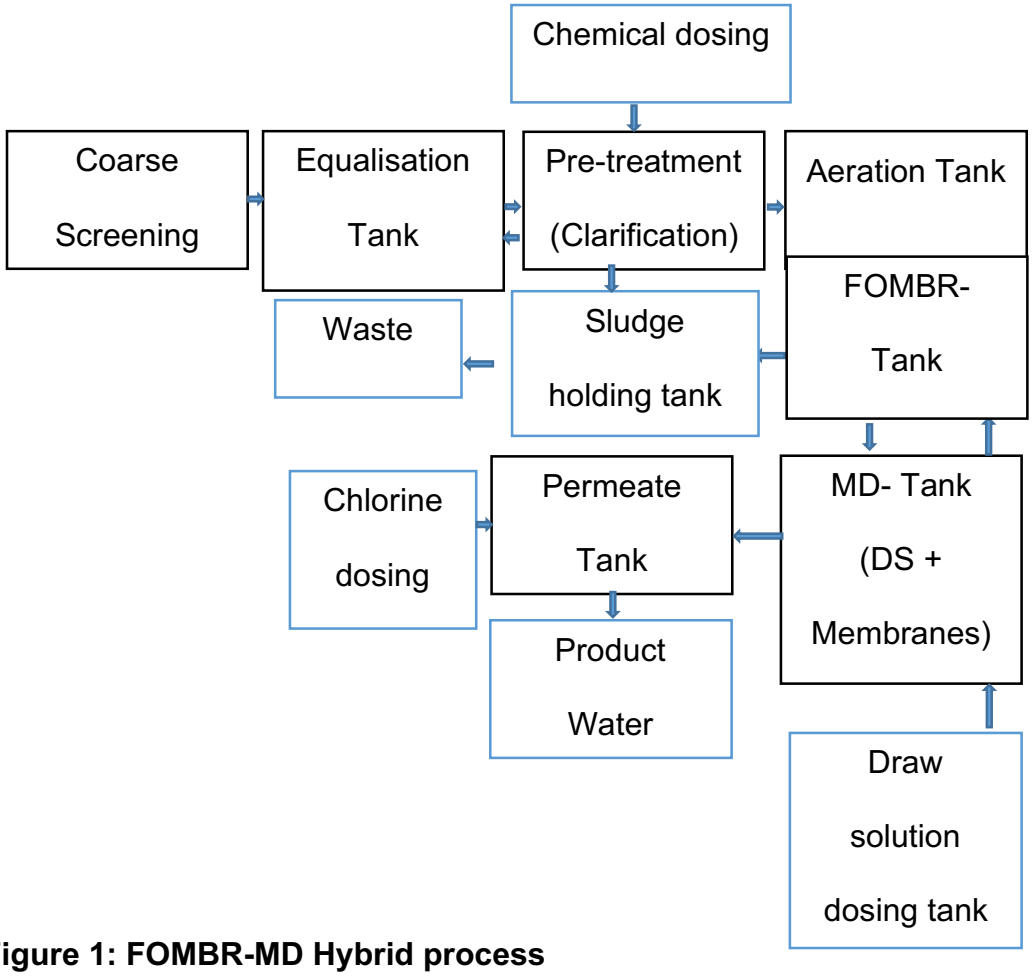


Figure 1: FOMBR-MD Hybrid process

The following design specifications are assumed:

Total Service Population: 150 people equivalent

Water consumption: 150L/day/person equivalent

Total water production/ day = 22.5 m^3/day

Plant operation time: 24hours/day

<u>Forward Osmosis Membrane Bioreactor</u>

Flux Achieved with NaCl (1M) = 15 LMH (a ball-park estimate; see below).

Total Flux per day = 15 LMH * 24 h = 360 LMD (i.e. litres per m^2 per day).

We will assume the application of a commercial HF membrane provided by Aquaporin (Table 1). For this product, 2.3 m^2 is the specified surface area of the membrane module; minimum FO flux 15 LMH.

Table 1: Aquaporin* commercial FO membrane specification (FO-mode, 1M NaCl Draw Solution)

	m^2	Mm	L/h	LMH	g/L
HFFO2	2.3	0.2	>34.5	>15	<0.20

*provided by supplier

Thus, the number of modules required = 22,500 L per Day / (360 LMD *2.3 m^2) = 27 modules/elements. These modules will be connected in parallel.

Total flow rate F: 0.938 m^3/h or 938 Litres per hour

Total membrane surface area = 2.3 * 27 = 62.1 m^2

*FO-aeration and MBR Tank**

Calculation for FO-MBR Tank

Influent flow (Q): 22.5m^3/day

Influent BOD (B0): 350 mg/L

Effluent BOD (B): 0.8 mg/L

Assuming:

Yield Coefficient (Y) = 0.6

Decay rate (Kd) = 0.06 d^{-1}

MLSS (X) = 4000 mg/L

Activated Sludge MLSS (Xw) = 10,000 mg/L

SRT = 10 days

V= (10*22.5*0.6)/4 [(0.35-0.0008)/ (1+0.06*10)]

V= 135/4 (0.349/1.6) = 7.08m^3

Assume Depth = 2m

Therefore, Area = 7.08/2= 3.54m^2 (Length: 1.88m, Width: 1.88m)

HRT = V/Q_0 = (7.08m^3 *24)/ 22.5 m^3d^{-1} = 7.5h

Volume of wasted sludge = (7.08 m^3*4)/(10*10) = 0.283m^3 per day

Thus HRT= 7.5 h and SRT= 10 days

Reactor volume = F X HRT = 7.04m^3 (Depth: 2m, length: 1.88m, width: 1.88m)

Draw Solute Consumption

According to Figure 4.9, the loss of NaCl draw solute is 0.2 GMH or 0.2 X 24 X 62.1 = 0.3 kg per day or 0.013kg/m^3 water produced. Assuming industrial grade NaCl, this costs a half less than pence per m^3 water produced (see Table 6.1 for all draw solutes).

Membrane Distillation

We assume the average MD flux achieved is 7 LMH (from Figure 4.3, a ball-park estimate of flux for the diluted NaCl draw solution is 7 LMH).

Total MD Flux per day = 7 * 24 = 168 LMD

By mass balance at steady-state operation, the total water drawn by FO is equal to the water regenerated by MD = 22,500 Litres per Day.

We assume the installation of a DCMD membrane distillation (Membrane solutions, China) unit with a membrane area per module of 2.5 m^2.

Number of modules required = 22,500 Litres per Day / (168 LMD * 2.5 m^2) = 54 modules. These modules will operate on the diluted draw solution and be connected in parallel.

Performance:

A performance comparison between the proposed FOMBR-MD plant and an existing MBR plant can now be made.

Table 2: Performance comparison of FO-MD hybrid with MBR plant

Parameters	**Varsseveld MBR Plant, Netherlands**		**FO-MD hybrid**	
Average BOD [mg/L]	Influent: 306	Effluent: 0.8	Influent: 350	Effluent: <0.3
Average COD [mg/L]	Influent: 752	Effluent: 25	Influent: 500	Effluent: <20
Removal Efficiency BOD	99.7%		> 99%	
Removal Efficiency COD	96%		>99%	
Monthly Average Flowrate [m^3]	132,054		750	
Monthly Average Energy Consumption [kWh]	110,486		1650-3900 (without or with waste heat)	
Specific energy consumption kWh/m^3	0.84		FO: 0.23 kWh/m^3 (Jackson, 2014) MD: 0.01-2 kWh/m^3 (with thermal or waste heat) MD: 5-9 kWh/ m^3 (without waste heat)	

		Total: 2.2-5.2 kWh/m^3
Cost of Energy for Operation (kWh/m^3 * £)	0.84*2.90 = 2.5p/m3.	Waste heat: 0.23*2.90pence= 0.6p pence/ m^3 Higher grade heat: 9.23*2.90= £2.7/m^3

The comparison reveals that the specific energy requirement for treating wastewater is higher for the FOMBR-MD system than the conventional MBR, unless we can utilize a free source of waste heat e.g. that derived from the condenser of a power generation cycle. On the other hand, the generation of clean water using the FO system will cost a half pence per m^3 in draw solutes; however, the MBR system will not produce clean water and this can be set off against the sale value of the clean water. The value of this water will obviously be much higher in water scarce regions; in developed countries with low water stress, such as the UK, the sale value for clean water provision (and the cost of wastewater treatment) is on the order of £1.00 per m^3. So that this cost for the draw is easily adsorbed, A further example of a wastewater treatment plant in a Jordan refugee camp is quoted below, where the candidate worked over summer 2017. The FOMB-MD performance and specific energy consumption compares favourably to this case, especially when waste heat is available for the MD regeneration process (0.23 versus 5.4 kWh/m^3). Nevertheless, the greater capital cost of membrane installation must also be considered at the outset of the project.

Table 3: Wastewater treatment plant in Za'atari refugee camp, Jordan (Internship, July 2017)

Parameters	Za'atari MBR Plant, Jordan	
Average BOD [mg/L]	Influent: 2047	Effluent: 29.5
Average COD [mg/L]	Influent: 3596	Effluent: 58.4
Removal Efficiency BOD	98.3%	
Removal Efficiency COD	98.2%	
Monthly Average Flowrate [m^3]	14887	
Monthly Average Energy Consumption [kWh]	80840	
Specific Energy Consumption [kWh/m^3]	5.43	

In the table below, similar figures are calculated for the other draw solutes.

Table 4: Membrane modules required for other draw solutions

Draw solution		Flux (LMH)	LMD	Modules required	Total membrane surface area (m^2)
PDAC	FO	1.4	33.6	290	670
	MD	5	120	75	187
TEAB	FO	5.6	134.4	73	168
	MD	7	168	53.57	133.9

Table 5: Cost of Components (for NaCl) and other Draw solutes.

Other		MD	FO	Cost (£)
1	Piping	15-100 ft		500
2	Membrane modules (total)	57	27	2000
3	Pipe fittings and PH probe, power gauges etc	-	-	3000
4	Civil investment and manpower	-	-	varying
5	TEAB	-	-	300 /Ton (Alibaba)
6	NaCl	-	-	300 /Ton (Alibaba)
7	PDAC	-	-	1350 /Ton (Alibaba)
8	EDTA	-	-	1500 /Ton (Alibaba)
9	NaOH	-	-	150 / Ton (Alibaba)
10	HNO_3	-	-	200 / Ton (Alibaba)
11	H_3PO_4	-	-	500 /Ton (Alibaba)
12	Chlorine	-	-	700 /Ton (Alibaba)

A rough estimation for power consumption to calculate the operational cost incurred is presented in Table 6

Table 6: Auxiliary Equipment list and estimated power consumption (for Table 2)

S.no	Description	FO-MD Hybrid System		Total Power consumption KW
		MD	FO	
1	Inlet Pump	-	1	1.2
2	Mixers and diffusers	-	1	1.5
3	Recirculation Pump		1	1.5
4	Chlorine Dosing	1		0.01
5	Sludge Pump (MBR waste)	-	1	0.75
6	Boiler	1	-	1.2
7	Chiller	1	1	2.4

Appendix II

FOMBR- MD bench-scale setup: installation cost

The following tables specify the equipment, materials and suppliers utilized for the lab-scale process developed in this project.

Table 1: FO chemical cost, equipment cost, and supplier list

S.NO	Instrument	Supplier	Cost
1	Weighing Balance	VWR	£654
2	Data Logger	VWR	£126
3	Pipes	Cole Parmer	
	Norprene #17		£30
	Norprene #25		£30
4	Draw solutes	Sigma Aldrich	
	NaCl (1 KG)		£24.90
	Na_3PO_4 (500g)		£100
	TEAB (1 KG)		£87
	PDAC (1L)		£27.20
	SDS (100 g)		£99.50
5	Membranes	HTI	
	Basic FO kit (CTA)		£145
	Basic FO kit (TFC)		£145
6	Pump	Cole Parmer Longer Pumps (2 single head one 2 head pump)	£1000 £2500

Membrane Distillation:

Table 2: MD Equipment cost and supplier list

S.No	Equipment	Supplier	Cost
1	Balance Data logger	VWR	£654 £126
2	1 double head pump Tubing	Longer pump	$700 $(190$shipping cost) $100-200 (£670)
3	3 flow meters	Cole parmer	£150
4	Buckets (30L)	Ampulla	£24
5	Thermostat	Amazon	£11
6	Chiller and water bath	In the lab	
7	Membrane Cell	In workshop	
8	Membrane	a. MSPTFE260322B-Hydrophobic PTFE laminated membrane pore size 0.22 µm (260*300mm) b. MSPTFE260010B-Hydrophobic PTFE laminated membrane pore size 0.1 µm (260*300mm)	£200 £200

Appendix III

List of Journal Articles and Conference Presentations by the Author

Articles Accepted

Nawaz, M.S., **Parveen, F.**, Gadelha, G., Khan, S. J., Wang, R., Hankins, N.P. 2016. Reverse solute transport, microbial toxicity, membrane cleaning and flux of regenerated draw in the FO-MBR using a micellar draw solution. *Desalination,* 391: 105-111 (IF: 3.756)

Note: The candidate had carried out the toxicity studies in this paper (not included in this thesis after revision)

Articles Submitted

Parveen, F. Hankins, N. P. Performance Comparison of Nanofiltration (NF) and Commercial Forward Osmosis (FO) Membranes against Novel Draw Solutions in a Forward Osmosis Membrane Bioreactor (FO-MBR). *Journal of Water Process Engineering*. (May 2018)

Ready for submission

Parveen, F. and Hankins, N. P. Integration of Forward Osmosis and Membrane Distillation Units for Regeneration of Novel Draw Solutions and Water Reclamation, Environmental Science and Technology (June 2018)

In preparation:

Parveen, F. and Hankins, N. P. Feasibility of using co-polymers as novel draw solutions in Forward osmosis membrane bioreactors (FO-MBRs) for *Journal of Water Process Engineering.*

Oral Presentation

Parveen, F.* and Hankins, N. P. Integration of Forward Osmosis and Membrane Distillation Units for Regeneration of Novel Draw Solutions and Water Reclamation,1st International Conference on Sustainable Water Processing, Sitges, Spain, September 11-14th, 2016

Invited lecture

Parveen, F*. & Hankins, N. P. Integration of Forward Osmosis and Membrane Distillation Units for Regeneration of Novel Draw Solutions and Water Reclamation, Indo-UK workshop on "Nano-Biomaterials for Water Purification", Kottayam, Kerala, India, December 12-16th, 2016

Keynote lectures

Parveen, F. Tang, C., Hankins, N. P*. Performance Comparison of Nanofiltration (NF) and Commercial Forward Osmosis (FO) Membranes against Novel Draw Solutions in a Forward Osmosis Membrane Bioreactor (FO-MBR), Engineering with Membranes 2015, Beijing China, March 6-10th, 2015

Nawaz, M.S., **Parveen, F.**, Gadelha, G., Khan, S. J., Wang, R., Hankins, N.P*. 2015. Membrane Fouling and Microbial Toxicity in the Forward Osmosis Membrane

Bioreactor using Micellar Draw Solutions. 2nd International Conference on Desalination Using Membrane Technology, Singapore, 26-29 July 2015

Poster

Parveen, F.* and Hankins, N. P. 2015. Performance Evaluation of Nanofiltration and Commercial Forward Osmosis (FO) Membrane for Forward Osmosis Membrane Bioreactor (FO-MBR), IWA UK Young Water Professionals Conference, April 13-15th, 2015

*** Presenter**

Others:

Jul – Aug 2017 Intern- UNICEF WASH section, Amman Jordan

Responsibilities: Za'atari Refugee camp wastewater treatment plant performance evaluation and improvement recommendation

Mar 2016 Thought for food summit, Pitch competition, Zurich, Switzerland.

Business plan competition for food production. Our team called 'oxmosis' was the only team from the UK in the Top 10.

Business idea: Using forward osmosis for wastewater treatment using fertiliser as draw solution, followed by direct use of draw water for fertigation.

References

Abdelrasoul, A., Doan, H., & Lohi, A. 2013. Mass Transfer - Advances in Sustainable Energy and Environment Oriented Numerical Modeling. Intech Open Access Publisher, 195

Achilli, A., Cath, T. Y., and Childress, A. E. 2010. Selection of inorganic-based draw solutions for forward osmosis applications. Journal of Membrane Science, 364(1-2): 233-241

Achilli, A., Cath, T.Y., Marchand, E.A., Childress, A.E. 2009. The forward osmosis membrane bioreactor: a low fouling alternative to MBR processes. Desalination, 239:10–21

Adham, S., Oppenheimer, J., Liu, L., and Kumar, M. 2009. Dewatering Reverse Osmosis concentrate from water reuse applications using Forward Osmosis, Water Reuse Foundation.

Adham, S., Oppenheimer, J., Liu, L., Kumar, M.2007. Dewatering reverse osmosis concentrate from water reuse applications using forward osmosis. Water Reuse Foundation Research Report

Aimar, P. Howell, J.A., Turner, M.1989. Effects of concentration boundary layer development on the flux limitations in ultrafiltration, Chemical Engineering Research and Design, 67(3): 255–261.

Al-Amoudi, A. S.2010. Factors affecting natural organic matter (NOM) and scaling fouling in NF membranes: A review. Desalination, 259(1-3): 1-10

Alejo, T., Arruebo, M., Carcelen, V., Mosalvo, V. M., Sebastian, V. 2017. Advances in draw solutes for forward osmosis: Hybrid organic-inorganic nanoparticles and conventional solutes. Chemical Engineering Journal, 309: 738–752

Alkhudhiri, A., Darwish, N., Hilal, N. 2012. Membrane distillation: A comprehensive review. Desalination, 287:2-18

Alsvik, L. I. and Hagg, M. 2013. Pressure Retarded Osmosis and Forward Osmosis Membranes. Materials and Methods. Polymers, 5:303-327.

Altaee, A., Miller, G. J., Zaragoza, G., Sahrif, A. O. 2017. Energy efficiency of RO and FO-RO system for high salinity seawater treatment. Clean technologies and Environmental policy, 19(1): 77-91

Alturki, A., McDonald, J., Khan, S. J., Hai, F. I,Price, W. E., Nghiem, E. D. 2012. Performance of a novel osmotic membrane bioreactor (OMBR) system: flux stability and removal of trace organics. Bioresource Technology, 113: 201-206

Amin, M.M., Heidari, M., Momeni, S. A., Ebrahimi, H. 2016. Performance evaluation of membrane bioreactor for treating industrial wastewater: A case study in Isfahan Mourchekhurt industrial estate. International Journal of Environmental Health Engineering, 5:12

Amini, M., Jahanshahi, M., Rahimpour, A. 2013.Synthesis of novel thin film nanocomposite (TFN) forward osmosis membranes using functionalized multi-walled carbon nanotubes. Journal of Membrane Science, 435: 233-241

Amos, D. A., Markels, J. H., Lynn, S. B & Radke, C. J. (1998). Osmotic Pressure and Interparticle Interactions in Ionic Micellar Surfactant Solutions. Journal of Physical Chemistry, 102:2793-2753

Bai, H., Liu, Z., Sun, D.D. 2011. Highly water soluble and recovered dextran coated Fe3O4 magnetic nanoparticles for brackish water desalination. Separation and Purification Technology, 81:392–399

Batchelder, G.W. 1965. Process for the Demineralization of Water, US Patent, 3171799.

Bhausaheb, L., Pangarkar, M. G. Sane, M. G. 2011. Reverse Osmosis and Membrane Distillation for Desalination of Groundwater: A Review. ISRN Materials Science, Article ID 523124, doi:10.5402/2011/52312

Blandin, G.,Gautier, C., Toran, M. S., Monclus, H., Rodriguez-Roda, Ignasi., Comas, J. 2018. Retrofitting membrane bioreactor (MBR) into osmotic membrane bioreactor (OMBR): a pilot scale study. Chemical Engineering Journal, https://doi.org/10.1016/j.cej.2018.01.103

Boubakri, A., Bouchrit, R., Hafiane, Bouguecha, S. A. 2014. Fluoride removal from aqueous solution by direct contact membrane distillation: theoretical and experimental studies. Environmental Science and Pollution Research. 21(17):10493-10501

Boubakri, A., Hafiane, A. and Bouguecha, S.A.T. 2014b. Direct contact membrane ditillation: capability to desalt draw water. Arabian Journal of Chemistry, http://dx.doi.org/10.1016/j.arabjc.2014.01.010

Bowden, K.S., Achilli, A. , Childress. A.E. 2012. Organic ionic salt draw solutions for osmotic membrane bioreactors. Bioresource Technology, 122: 207-216

Bowles, B. L., & Miller, A. J. 1993. Antibotulinal properties of selected aromatic and aliphatic aldehydes. Journal of Food Protection, 56:788-794.

Bowles, B. L., Sackitey, S. K., Williams, A. C. 1995. Inhibitory effects of flavor compounds on Staphylococcus aureus WRRC B124. Journal of Food Safety, 15:337-347.

Brul, S. & Coote, P. 1999. Preservative agents in foods: mode of action and microbial resistance mechanisms. International Journal of Food Microbiology, 50:1-17.

Bui, N.-N., McCutcheon, J. R. 2013.Hydrophilic nanofibers as new supports for thin film composite membranes for engineered osmosis. Environmental Science and Technology, 47: 1761-1769

Camacho, L.M., Dumee, L., Zhang, J., Li, J., Duke, M., Gomez, J. & Grey, S. 2013. Advances in Membrane Distillation for Water Desalination and Purification Applications. Water, 5:94-196

Cannon J, Kim D, Maruyama S, et al. (2012). Influence of ion size and charge on osmosis. Journal of Physical Chemistry B, 116:4206–4211. doi:10.1021/jp2113363

Carmignani, G., Sitkiewitz, S. & Webley, J.W.2012. Recovery of Retrograde Soluble Solute for Forward Osmosis Water Treatment, WO 2012/148864.

Cath, T. Y., Gormly,S., Beaudry, E.G., Flynn, M.T., Adams, V.D., Childress A.E. 2005. Membrane Contactor Processes for Wastewater Reclamation in Space Part I. Direct Osmotic Concentration as Pretreatment for Reverse Osmosis. Journal of Membrane Science, 257(1-2):85-98.

Cath, T.Y., Hancock, N.T., Lundin, C.D., HoppeJones, C. Drewes, J.E. 2010. A multi-barrier osmotic dilution process for simultaneous desalination and purification of impaired water, Journal of Membrane Science, 362:417–426.

Chang, H., Wang, G. Chen, Y., Li, C., Chang, C. 2010. Modeling and optimization of a solar driven membrane distillation desalination system. Renewable Energy, 35(12): 2714-2722

Chekli, L., Sherub, P., Kim, S. E., Kim, J., Choi, J. Y., Choi, J., Kim, S., Kim, J. H., Hong, S., Sohn, J., Shon, H. K. 2016. A comprehensive review of hybrid forward osmosis systems: Performance, applications and future prospects. Journal of Membrane Science, 497 (430-449)

Chemical Rubber Co., Handbook of Chemistry and Physics, 50th edition, Cleveland, Ohio, 1970

Chen, L., Gu, Y.S., Cao, C.Q., Zhang, J., Ng, J.W., Tang, C.Y. (2014). Performance of a submerged anaerobic membrane bioreactor with forward osmosis membrane for low-strength wastewater treatment. Water Resource, 50: 114-123

Cheng,T., Han, C.,Hwang, K., Ho, C., & Cooper, W. J. 2010. Influence of Feed Composition on Distillate Flux and Membrane Fouling in Direct Contact Membrane Distillation, Separation Science and Technology, 45:7, 967-974, DOI:10.1080/01496391003666908

Choi, Y. J., Choi, J. S., Oh, H. J., Lee, S., Yang, D. R. and Kim, J. H. (2009). Toward a combined system of forward osmosis and reverse osmosis for seawater desalination. Desalination, 247(1-3): 239-246.

Chou, S., Shi, L., Wang, R.,Tang, C.Y., Qiu, C., Fane, A. G .2010. Characteristics and potential application of a novel forward osmosis hollow fiber membrane. Desalination, 261:365-372

Chung, T., Lui, L., Wan, C. F., Cui, Y., Amy, G. 2015. What is next for forward osmosis (FO) and pressure retarded osmosis (PRO). Separation and Purification Technology. 156(2): 856-860

Coday, B. D. Xu, P., Beaudry, E. G., Herron, J., Lampi, K., Hancock, N. T. and Cath, T. Y. 2014. The sweet spot of forward osmosis: Treatment of produced water, drilling wastewater, and other complex and difficult liquid streams. Desalination, 33:23-35.

Cornelissen, E.R., Harmsen, D., Beerendonk, E.F. , Qin, J.J., Oo, H., de Korte, K.F., Kappelhof, J.W.M.N. 2011. The innovative Osmotic Membrane Bioreactor (OMBR) for reuse of wastewater. Water Science and Technology, 63: 1557-1565

Cornelissen, E.R., Harmsen, D., de Korte, K.F., Ruiken, C.J.,Qin, J.J., Oo, H., Wessels, L.P. 2008. Membrane fouling and process performance of forward osmosis membranes on activated sludge. Journal of Membrane Science, 319 (1-2):158-168

Costa, R., Pereira, J. L., Gomes, J., Goncalves, F., Hunkeler, D., Rasteiro, M. G. 2014. The effects of acrylamide polyelectrolytes on aquatic organisms: Relating toxicity to chain architecture. Chemosphere, 112:177-184

Cui, Y., Wang, H., Wang, H., Chung, T.-S. 2013.Micro-morphology and formation of layer-by-layer membranes and their performance in osmotically driven processes

Daniels, F. H., Nedev, N.D., Cataldo, T., Leonardo, E. F. & Cortell, S.(1988). The use of polyelectrolytes as osmotic agents for peritoneal dialysis. Kidney International. 33:925-929

Darton, T., Annunziata, U., Pisano, F.D.V., Gallego, S. 2004. Membrane autopsy helps to provide solutions to operational problems. Desalination, 167:239-245

Dey, P., Izake, E.L.2015. Magnetic nanoparticles boosting the osmotic efficiency of a polymeric FO draw agent: effect of polymer conformation. Desalination, 373:79–85

Dufour, V., Stahl, M., Baysse, C. 2015. The antibacterial properties of isothiocyanates. Microbiology, 161, 229-243

Dumée, L., Lee, J., Sears, K., Tardy, B., Duke, M., Gray, S. 2013.Fabrication of thin film composite poly(amide)-carbon-nanotube supported membranes for enhanced performance in osmotically driven desalination systems. Journal of Membrane Science, 427:422–430

Duong, P.H.H., Zuo, J., Chung, T.-S. 2013. Highly crosslinked layer-by-layer polyelectrolyte FO membranes: understanding effects of salt concentration and deposition time on FO performance. Journal of Membrane Science, 427: 411-421

EL-Abbasi, A., Hafidi, A., Khayet, M. & Gracia-Payo, M. C. 2013. Integrated direct contact membrane distillation for olive mill wastewater treatment. Desalination, 323:31-38

El-Bourawi, M.S., Ding, Z., Ma, R., Khayet, M. 2006. A framework for better understanding membrane distillation separation process Journal of Membrane Science, 285, 4–29

El-Fadel, M., Hashisho, J. 2014. A comparative examination of MBR and SBR performance for the treatment of high-strength landfill leachate. Journal of the Air & Waste Management Association, 64(9): 1073-1084

Emadzadeh, D. , Lau, W.J. , Ismail, A.F. 2013.Synthesis of thin film nanocomposite forward osmosis membrane with enhancement in water flux without sacrificing salt rejection. Desalination, 330: 90-99

Environmental Protection Agency. 2003. Membrane filtration guide manual. Washington DC: Allgeier, S.

Ettouney, H.M. , El-Dessouky, H.T., Faibish, R.S., Gowin, P.2002. Evaluating the economics of desalination, Chemical Engineering Progress, 98 (12):32–40

Ettouney, H.M. , El-Dessouky, H.T., Faibish, R.S., Gowin, P.2002. Evaluating the economics of desalination, Chemical Engineering Progress, 98 (12):32–40

Fam, W., Phuntsho ,S., Lee, J. H. & Shon, H. K. 2013.Performance comparison of thin-film composite forward osmosis membranes, Desalination and Water Treatment, 51(31-33):6274-6280

Field, R. 2010. Fundamentals of fouling. Peinemann,K.V., Nunes, S. P. (Eds.), Membranes for Water Treatment, Wiley-VCH Verlag GmbH & Co. KGaA, Weinheim,1–24

Field, R. W. & Pearce, G. K. 2011. Critical, sustainable and threshold fluxes for membrane filtration with water industry applications. Advances in Interface Colloid and Science, 164: (38-44).

Frank, B.S. 1972. Desalination of Sea Water, US Patent 3670897

Franken, A.C.M.,Nolton, J.A.M., Mulder, M.H.V.,Bargeman, D., Smolders, C.A. 1987. Wetting criteria for the applicability of membrane distillation. Journal of Membrane Science, 33 (3): 315–328

Franken, A.C.M.,Nolton, J.A.M., Mulder, M.H.V.,Bargeman, D., Smolders, C.A. 1987. Wetting criteria for the applicability of membrane distillation. Journal of Membrane Science, 33 (3): 315–328

Gadelha, G. A. F., and Hankins, N. P. 2011. Assessment of draw-solution performance in combination with assymetric membranes for forward osmosis. IDAWC, Perth, Australia

Gai, J. & Zhang, X. 2015. Single-layer graphene membranes for super-excellent brine separation in forward osmosis. RSC Advances. 5: 68109-68116 (DOI: 10.1039/C5RA09512C)

Gai, J.G., Gong, X.L.2014. Zero internal concentration polarization of membrane: Functionalized graphene. Journal of Material Chemistry, 2:425–429.

Ge, Q., Ling, M., Tung, T., -S. 2013. Draw solutions for forward osmosis processes: Developments, challenges, and prospects for the future. Journal of Membrane Science, 442:225-237

Ge, Q., Su, J., Chung, T.-S. , Amy, G.2011. Hydrophilic superparamagnetic nanoparticles: synthesis, characterization, and performance in forward osmosis processes. Industrial and Engineering Chemistry Research, 50: 382–388

Ge, Q., Wang, P., Wan, C., and Chung, T.-S. 2012. Polyelectrolyte-Promoted Forward Osmosis–Membrane Distillation (FO–MD) Hybrid Process for Dye Wastewater Treatment. Environmental science and technology, 46(11): 62366243

Ge, Q.C., Fu, F.J., Chung, T.S.2014. Ferric and cobaltous hydroacid complexes for forward osmosis (FO) processes. Water Research, 58: 230–238

Gill, A. O. & Holley, R. A. 2004. Mechanisms of Bactericidal Action of Cinnamaldehyde against Listeria monocytogenes and of Eugenol against L. monocytogenes and Lactobacillus sakei. Applied Environmental Microbiology, 70(10): 5750-5755

Gonotec GmbH, Instruction Manual for Osmomat 030 Freezing Point Osmometer, 1996, Page 2.

Gryta, M., Karakulski, K., Morawski, A.W.2001. Purification of oily wastewater by hybrid UF/MD, Water Research, 35 (15):3665–3669

Gryta, M., Tomaszewska, M. & Karakulski, K. 2006. Wastewater treatment by membrane distillation. Desalination, 198(1-3): 67-73

Gryta, M.2005. Long-term performance of membrane distillation process. Journal of Membrane Science, 265 (1–2):153–159

Gryta, M.2005. Long-term performance of membrane distillation process. Journal of Membrane Science, 265 (1–2):153–159

Gryta, M.2005. Long-term performance of membrane distillation process. Journal of Membrane Science, 265:153–159

Gryta, M. 2008. Fouling in direct contact membrane distillation. Journal of Membrane Science, 325 (1): 383-394

Gryta, M. 2012. Effectiveness of water desalination by membrane distillation process. Membranes, 2: 415-429

Gryta, M. Tomaszewska, M., Karakulski, K.2006. Wastewater treatment by membrane distillation, Desalination, 198:67–73

Gu, Y.S., Chen, L., Ng, J.W., Lee, C., Chang, V.W.C., Tang, C.Y. 2015.Development of anaerobic osmotic membrane bioreactor for low-strength wastewater treatment at mesophilic condition. Journal of Membrane Science, 490: 197-208

Guglielmi G., Andreottola G.2010. Selection and Design of Membrane Bior, Handbook of Environmental Engineering reactors in Environmental Bioengineering, in Environmental Biotechnology. Wang L.K., Ivanov V., Tay J.-H., Hung Y.-T., editors. Volume 10. Humana Press; New York, NY, USA: pp. 439–514.

Gunko, S., Verbych, S.,Bryk,M.,Hilal,M. 2006. Concentration of apple juice using direct contact membrane distillation. Desalination, 190 (1–3):117–124

Guo, C.X., Zhao, D., Zhao, Q., Wang, P., Lu, X.2014. Na+-functionalized carbon quantum dots: a new draw solute in forward osmosis for seawater desalination. Chemical Communications, 50:7318–7321

Gupta, V. K., Ali, I., Saleh, T.A., Nayak, A. and Agarwal, S. 2012. Chemical treatment technologies for waste-water recycling—an overview. Royal Society of Chemistry Advances, 2: 6380-6388

Han, J., Cho, Y.H. , Kong, H., Han, S., Park, H.B. 2013.Preparation and characterization of novel acetylated cellulose ether (ACE) membranes for desalination applications. Journal of Membrane Science, 428: 533-545

Hancock, N.T. & Cath. T.Y. 2009 .Solute coupled diffusion in osmotically driven membrane processes, Environmental Science and Technology, 43: 6769–6775.

Harwood, C. R., and S. M. Cutting. 1990. Chemically defined growth media and supplements, p. 548. In C. R. Harwood and S. M. Cutting (ed.), Molecular biological methods for Bacillus. Wiley, Chichester, United Kingdom.

Helander, I. M., Alakomi, H. L., Latva-Kala, K., Mattila-Sandholm, T., Pol, L., Smid, E. J., Gorris, L. G. M., von Wright, A. 1998. Characterization of the action of selected

essential oil components on Gram-negative bacteria. Journal of Agriculture Food Chemistry, 46:3590-3595.

Hickenbottom, K. L. and Cath, T. Y. 2014. Sustainable operation of Membrane distillation for enhancement of mineral recovery from hypersaline solutions. Journal of Membrane Science, 454:426-435

Hickenbottom, K. L. and Cath, T. Y. 2014. Sustainable operation of Membrane distillation for enhancement of mineral recovery from hypersaline solutions. Journal of Membrane Science, 454:426-435

Holloway, R. W., Maltos, R., Vaneeste, J. & Cath, T. Y. 2015. Mixed draw solutions for improved forward osmosis performance. Journal of Membrane Science, 491: 121-131

Hough, W.T. 1970. Process for Extracting Solvent from a Solution, US Patent 3532621

Hoyer, M., Haseneder, R. &Repke, J.2016. Development of a hybrid water treatment process using forward osmosis with thermal regeneration of a surfactant draw solution. Desalination and water Treatment, 57:59 (28670-28683)

Hsu, S.T., Cheng, K.T., Chiou, J.S.2002. Seawater desalination by direct contact membrane distillation. Desalination, 143 (3):279–287

Huang, L. , McCutcheon, J.R. 2014.Hydrophilic nylon 6,6 nanofibers supported thin film composite membranes for engineered osmosis. Journal of Membrane Science, 457:162-169

Huang, M. H. Chen, Y. S. Huang, C. H. Sun, P. Z. Crittenden, J. 2015.Rejection and adsorption of trace pharmaceuticals by coating a forward osmosis membrane with TiO2. Chemical Engineering Journal, 279:904– 911

Hunag, L., Lee, D., Lai, J. 2015b. Forward osmosis membrane bioreactor for wastewater treatment with phosphorus recovery. Bioresource Technology, 198: 418-423

Hwang, H. J., He, K., Grey, S., Zhang, J. & Moon, S. L. 2011. Direct contact membrane distillation (DCMD): Experimental study on the commercial PTFE membrane and modelling. Journal of Membrane Science. 371(1-2):90-98

Jin, X., Tang, C. Y., Gu. Y, She, Q., Qi, Saren. 2011. Boric Acid Permeation in Forward Osmosis Membrane Processes: Modeling, Experiments, and Implications. Environmental Science and Technology. 45 (6): 2323–2330

Jun, B. M., Nguyen, T. P. N., Ahn, S. H., Kim., I.C. & Kwon, Y. N. 2015. The application of polyethyleneimine draw solution in a combined forward osmosis/nanofiltration system, Journal of Applied polymer science, 132(27), DOI: 10.1002/app.42198

Karakulski, K., Gryta, M., Morawski, A. 2002. Membrane processes used for potable water quality improvement, Desalination, 145:315–319

Karakulski, K. , Gryta, M. 2005. Water demineralisation by NF/MD integrated processes, Desalination, 177 :109–119

Kavanaugh, N.L., Ribbeck, K.2012. Selected antimicrobial essential oils eradicate Pseudomonas spp. and Staphylococcus aureus biofilms. Applied Environmental Microbiology.78(11):4057–4061.

Kesieme, U. K., Milne, N., Aral, H., Cheng, C. Y., Duke, M. 2013. Economic analysis of desalination technologies in the context of carbon pricing, and opportunities for membrane distillation. Desalination, 323: 66–74

Kessler, J.O., Moody, C.D. 1976.Drinking water from sea water by forward osmosis, Desalination, 18:297–306.

Kessler, J.O., Moody, C.D. 1976.Drinking water from sea water by forward osmosis. Desalination, 18:297–306.

Kezia, K., Lee, J., Weeks, M. and Kentish, S. 2015. Direct contact membrane distillation for concentration of saline dairy effluent. Water Research, 81:167-177

Khan, S. J., Parveen, F., Ahmed, Aman., Hashmi, I. and Hankins, N. 2013. Performance evaluation and bacterial characterization of FO-MBR. Bioresource Technology, 141:2-7

Khayet, M., Matsuura, T.2001. Preparation and characterization of polyvinylidene fluoride membranes for membrane distillation. Industrial and Engineering Chemistry Research ,40 (24):5710–5718

Khayet, M., Matsuura T. 2011. Membrane distillation principles and applications, Elservier B.V., ch. 10, pp. 254-268.

Khorshidi, B., Bhinder,A., Thundat, T., Pernitsky, D., Sadrzadeh, M. 2016. Developing high throughput thin film composite polyamide membranes for forward osmosis treatment of SAGD produced water, Journal of Membrane Science, http://dx.doi.org/10.1016/j.memsci.2016.03.052

Kim, B., Gwak, G., Hong, S. 2017. Review on methodology for determining forward osmosis (FO) membrane characteristics: Water permeability (A), solute permeability (B), and structural parameter (S). Desalination, 422: 5-16

Kook, S., Swetha, C. D., Lee, J., Lee, C., Fane, T., Kim, I. S. 2018. Forward Osmosis Membranes under Null-Pressure Condition: Do Hydraulic and Osmotic Pressures

Have Identical Nature?. Environmental Science and Technology, 52 (6): 3556-3566Amin

Kullab, A., Martin, A. 2011. Membrane distillation and applications for water purification in thermal cogeneration plants. Separation and Purification Technology, 76(3):231-237

Kurokawa, H., Sawa, T.1996. Heat recovery characteristics of membrane distillation. Heat transfer-Japanese Research, 25:135–150

Kwan, S.E., Bar-Zeev, E., Elimelech, M. 2015. Biofouling in forward osmosis and reverse osmosis: measurements and mechanisms. Journal of Membrane Science, 493:703–708.

Law, J. Y. & Mohammad, A. W. 2017. Assessing the forward osmosis performances using CTA membrane: effect of solution volume ratio and type of draw solute. Jurnal Teknologi. 79(5):47-52

Lay, W.C.L., Zhang, J.S., Tang, C.Y. Wang, R. Liu, Y., Fane, A.G. 2012. Analysis of salt accumulation in a forward osmosis system. Separation Science and Technology, 47: 1837-1848

Lay, W.C.L., Zhang, Q., Zhang, J., McDougald, D., Tang, C., Wang, R., Liu, Y., Fane, A.G. 2011.Study of integration of forward osmosis and biological process: membrane performance under elevated salt environment, Desalination, 283:123–130.

Lay, W.C.L., Zhang, Q., Zhang, J., McDougald, D., Tang, C., Wang, R., Liu, Y., Fane A.G.2012. Effect of pharmaceuticals on the performance of a novel osmotic membrane bioreactor (OMBR), Separation Science and Technology, 47:543–554.

Le-Clech ,P., Chen, V., Fane, T.A.G.2006. Fouling in membrane bioreactors used in wastewater treatment. Journal of Membrane Science, 284:17–53. doi: 10.1016/j.memsci.2006.08.019

Lechunga, M., Fernandez-serrano, M., Jurado, E., Nunez-Olea, J. & Rios, F. 2016. Acute toxicity of anionic and non-ionic surfactants to aquatic organisms. Ecotoxicology and Environmental Safety, 125:1-8

Lee, J.-Y. ,Qi, S. , Liu, X. , Li, Y. , Huo, F. ,Tang , C.Y.2014. Synthesis and characterization of silica gel–polyacrylonitrile mixed matrix forward osmosis membranes based on layer-by-layer assembly. Separartion and Purification Technology, 124: 207-216

Lee, S. 2004. Microbial Safety of Pickled Fruits and Vegetables and Hurdle Technology. Internetional Journal of Food Safety, 4: 21–32

Lee K.L., Baker R.W., Lonsdale H.K.1981. Membranes for power generation by pressure-retarded osmosis, Journal of Membrane Science, 8(2): 141-171

Li, D., Yan, Y. S., Wang, H. T. Recent advances in polymer and polymer composite membranes for reverse and forward osmosis processes Progress in Polymer Science. 2016, 61, 104– 155

Li, D., Zhang, X., Yao, J., Simon, G.P., Wang, H. 2011. Stimuli-responsive polymer hydrogels as a new class of draw agent for forward osmosis desalination. Chemical Communications, 47:1710–1712

Li, F., Sun, M. L., Cheng, Q. X., Tian, Q., Ma, C. Y., Huang, M. H. Characterization and antifouling performance of cellulose triacetate forward osmosis membranes modified with graphene oxide Desalination. Water Treat. 2017, 62, 32– 42

Li, J., Liu, Q., Liu, Y., Xie, J. 2017. Development of electro-active forward osmosis membranes to remove phenolic compounds and reject salts. Environmental science: Water Research and Technology, 3:139-146

Li, L. Liu, X., Li, H. 2017. A review of forward osmosis membrane fouling: types, research methods and future prospects. Environmental Technology Reviews, 6:1

Li, Z.Y., Yangali-Quintanilla, V., Valladares-Linares, R., Amy,G.2012 . Flux patterns and membrane fouling propensity during desalination of seawater by forward osmosis. Water Research, 46:195–204.

Ling, M. M., and Chung, T.-S. 2011. Desalination process using super hydrophilic nanoparticles via forward osmosis integrated with ultrafiltration regeneration. Desalination, 278:194-202.

Ling, M.M., Chung, T.S., Lu, X. 2011. Facile synthesis of thermosensitive magnetic nanoparticles as ‘‘smart’’ draw solutes in forward osmosis. Chemical Communication, 47:10788–10790

Liu, B., Yu, J., Li, D., Lv, D., Zhang, J. 2015. Research advance on draw solution in forward osmosis process. International Conference on Advances in Energy and Environmental Science, 898-902

Liu, H. & Wang, J. 2013. Treatment of radioactive wastewater using Direct contact membrane distillation. Journal of Hazardous waste, 261:307-315

Liu, X.,Ng, H.Y. 2014.Double-blade casting technique for optimizing substrate membrane in thin-film composite forward osmosis membrane fabrication. Journal of Membrane Science, 469 :112-126

Liu, X. , Qi, S. , Li, Y. , Yang, L., Cao, B., Tang, C.Y. 2013.Synthesis and characterization of novel antibacterial silver nanocomposite nanofiltration and forward osmosis membranes based on layer-by-layer assembly. Water Research, 47: 3081-3092

Liu, Y. & Mi, B.2012. Combined fouling of forward osmosis membranes: synergistic foulant interaction and direct observation of fouling layer formation. Journal of Membrane Science, 407-408: 136-144

Liu, Y., Mi, B. 2012. Combined fouling of forward osmosis membranes: synergistic foulant interaction and direct observation of fouling layer formation. Journal of Membrane Sciences, 407: 136-144

Loeb, S., Titelman, L.,Korngold, E.,Freiman.J. 1997. Effect of porous support fabric on osmosis through a Loeb–Sourirajan type asymmetric membrane. Journal of Membrane Science, 129 :243-249

Loeb, S. 2002. Large-scalepower production by pressure-retarded osmosis using river water and seawater passing through spiral modules. Desalination,143:115–122.

Loeb. S. 1975. Osmotic powerplants. Science, 189:654–655.

Loeb. S. 1975. Osmotic powerplants. Science,189:654–655.

Lokare, O. R., Tavakkoli, S., Wadekar,S., Khanna, V., Vidic., R. D. 2017. Fouling in direct contact membrane distillation of produced water from unconventional gas extraction. Journal of Membrane Science, 524:493-501

Long, Q., Qi, G., Wang, Y. 2016. Evaluation of Renewable Gluconate Salts as Draw Solutes in Forward Osmosis Process. Sustainable Chemistry and Engineering, 4:85-93

Long, Q., Shen, L., Chen, R., Huang, J., Xiong, S., Wang, Y. 2016. Synthesis and Application of Organic Phosphonate Salts as Draw Solutes in Forward Osmosis for Oil–Water Separation. Environmental Science and Technology, 50 (21): 12022-12029

Long, Q., Wang, Y. 2015. Novel carboxyethyl amine sodium salts as draw solutes with superior forward osmosis performance. AIChe Journal, 62 (4): 1226-1235

Long, Q., Wang, Y. 2015. Novel carboxyethyl amine sodium salts as draw solutes with superior forward osmosis performance. AIChe Journal, 62 (4): 1226-1235

Lorhemen, O. T., Hamza, R. A. & Tay, J. H. 2018. Membrane Bioreactor (MBR) Technology for Wastewater Treatment and Reclamation: Membrane Fouling. Membranes (Basel). 6(2):33, doi: 10.3390/membranes6020033

Luo, L., Wang, P. , Zhang, S., Han, G. , Chung, T.-S. 2014. Novel thin-film composite tri-bore hollow fiber membrane fabrication for forward osmosis. Journal of Membrane Science, 461: 28-38

Lutchmiah, K., Verliefdea, A. R. D., Roest, K., Rietveld, L. C. & Cornelissen, E. R. 2014. Forward osmosis for application in wastewater treatment: a review. Water Research, 58: 179–197

Ma, N., Wei, J., Qi, S., Zhao, Y., Gao, Y., Tang, C.Y. 2013.Nanocomposite substrates for controlling internal concentration polarization in forward osmosis membranes. Journal of Membrane Science, 441:54-62

Mallevialle, J., Odendall, P.E., and Wiesner, M.R. 1996. Water treatment membrane processes. McGraw-Hill, New York

Martinetti, C. R., Childress, A. E., and Cath, T. Y. 2009. High recovery of concentrated RO brines using forward osmosis and membrane distillation. Journal of Membrane Science, 331:31-39.

MartinezDiez, L. &Vaquez-Gonalez. 1999. Temperature and concentration polarization in membrane distillation of aqueous salt solutions. Journal of Membrane Science, 156:265-273

McCutcheon, J.R., Elimelech, M. 2007. Modelling water flux in forward osmosis: Implications for improved membrane design. American Institute of Chemical Engineers Journal, 53(7):1736-1744

McCutcheon, J.R., McGinnis, R.L., Elimelech, M. 2005.A novel ammonia-carbon dioxide forward (direct) osmosis desalination process. Desalination, 174:1-11.

McCutcheon, J. R., McGinnis, R. L. and Elimelech, M., 2006. Desalination by ammonia-carbon dioxide forward osmosis: Influence of draw and feed solution concentrations on process performance. Journal of Membrane Science, 278: 114-123.

McGinnis, R.L. 2002. Osmotic Desalination Process, US Patent, 6391205 B1.

Meng, F., Zhang, S., Oh, Y., Zhou, Z., Shin, H., Chae, S. 2017. Fouling in membrane bioreactors: An updated review. Water Research, 114:151-180

Mi, B., Elimelech, M. 2010. Organic fouling of forward osmosis membranes: fouling reversibility and cleaning without chemical reagents. Journal of Membrane Science, 348(1):337-345

Mishra, T., Srivastava, R. K. 2015. Selection of inorganic-based fertilizers in forward osmosis for water desalination. International Journal of Environment, 4(2):319-329

Morrow, C. P., McGaughey, A. L., Hiibel, S. R., Childress, A. E. 2018. Submerged or sidestream? The influence of module configuration on fouling and salinity in osmotic membrane bioreactors. Journal of Membrane Sciences, 548: 583-593

Motsa, M.M., Mamba, B.B., D'Haese, A., Hoek, E. M. V.,Verliefde, A. R. D.2014 . Organic fouling in forward osmosis membranes: the role of feed solution chemistry and membrane structural properties. Journal of Membrane Science, 460:99–109.

Na, Y., Yang, S., Lee, S.2014. Evaluation of citrate-coated magnetic nanoparticles as draw solute for forward osmosis. Desalination, 347: 34–42

Naidu, G., Jeong, S., Choi, Y. & vigneswaran, S. 2017. Membrane distillation for wastewater reverse osmosis concentrates treatment with water reuse potential. Journal of Membrane Science, 524:556-525

Nawaz,M.S., Gadelha, G., Khan, S. J. and Hankins, N. 2013. Microbial toxicity effects of reverse transported draw solute in the forward osmosis membrane bioreactor (FO-MBR). Journal of Membrane Sciences, 429:323-329.

Nawaz, M.S., Parveen, F., Gadelha, G., Khan, S. J., Wang, R. & Hankins, N.P. (2016). Reverse solute transport, microbial toxicity, membrane cleaning and flux of regenerated draw in the FO-MBR using a micellar draw solution. Desalination, Volume 391, Pages 105-111

Neff, R.A. 1964. Solvent Extractor, US Patent, 3130156.

Nguyen, H.T., Chen, S.S., Nguyen, N.C., Ngo, H.H. , Guo, W.S. , Li, C.W.2015. Exploring an innovative surfactant and phosphate-based draw solution for forward osmosis desalination. Journal of Membrane science, 489:212–219

Nguyen, H.T., Chen, S.S., Nguyen, N.C., Ngo, H.H., Guo, W.S. , Li, C.W.2015. Exploring an innovative surfactant and phosphate-based draw solution for forward osmosis desalination. Journal of Membrane science, 489:212–219

Nguyen, N. C., Chen, S., Nguyen, H. T., Chen, Y., Ngo, H. H., Guo, W., Ray, S. S., Chang, H. & Le, Q. H. (2017). Applicability of an integrated moving sponge biocarrier-osmotic membrane bioreactor MD system for saline wastewater treatment using highly salt-tolerant microorganisms. Separation and Purification Technology, In press, Corrected proof.

Nguyen,Q., Lee, S. 2015. Fouling analysis and control in a DCMD process for SWRO brine. Desalination, 367, 21-27

Noh, M., Mok, Y., Lee, S., Kim, H.,Lee, S. H., Jin, G. W., Seo, J. H.,. Koo, H., Parka, T. H., Lee, Y. 2012.Novel lower critical solution temperature phase transition materials effectively control osmosis by mild temperature changes. Chemical Communications, 48 :3845-3847

Ong, R.C., Chung, T-S., de Wit, J.S., Helmer, B.J. 2015. Novel cellulose ester substrates for high performance flat-sheet thin-film composite (TFC) forward osmosis (FO) membranes. Journal of Membrane Science, 473: 63–71.

Ong, R.C. ,Chung, T.-S. Helmer, B.J. , de Wit, J.S. 2012.Novel cellulose esters for forward osmosis membranes. Industrial and Engineering Chemistry Research, 51: 16135-16145

Ooi, L. S., Li, Y., Kam, S. L. , Wang, H., Wong, E. Y., Ooi, V. E. 2006. Antimicrobial activities of cinnamon oil and cinnamaldehyde from the Chinese medicinal herb Cinnamomum cassia Blume. The American Journal of Chinese Medicine, 34(3):511-522

Ou, R., Wang, Y., Wang, H. & Xu, T., 2013. Thermo-sensitive polyelectrolytes as draw solutions in forward osmosis process. Desalination. 318:48-55

Ou, R., Wang, Y., Wang, H., Xu, T. 2013. Thermo-sensitive polyelectrolytes as draw solutions in forward osmosis process. Desalination, 318: 48-55

Palvic, Z., Vidakovic-Cifrek, Z. & Puntaric, D. 2005. Toxicity of surfactants to green microalgae Pseudokirchneriella subcapitata and Scenedesmus subspicatus and to marine diatoms Phaeodactylum tricornutum and Skeletonema costatum. Chemosphere, 61(8):1061-1068

Petrotos, K.B., Quantick, P., Petropakis, H. 1998. A study of the direct osmotic concentration of tomato juice in tubular membrane—module configuration. I. The effect of certain basic process parameters on the process performance, Journal of Membrane Science, 150: 99–110.

Phillip, W.A., Yong, J.S., Elimelech, M.2010. Reverse draw solute permeation in forward osmosis: Modelling and experiments. Environmental Science Technology, 44: 5170–5176.

Phuntsho, S,Shon, H. K., Hong, S.K.,Lee, S.Y., Vigneswaran, S. 2011.A novel low energy fertilizer driven forward osmosis desalination for direct fertigation: evaluating the performance of fertilizer draw solutions. Journal of Membrane Science, 375:172-181

Puguan, J.M.C. , Kim, H.-S., Lee, K.-J. , Kim, H. 2014.Low internal concentration polarization in forward osmosis membranes with hydrophilic crosslinked PVA nanofibers as porous support layer. Desalination, 336 :24-31

Qin, D., Liu, S., Sun, D. D., Song, X., Bai, H. 2015. A new nanocomposite forward osmosis membrane custom-designed for treating shale gas wastewater. Scientific Reports, 5, 14530

Qin,J.J., Kekre, K.A., Oo, M.H., Tao, G.H., Lay, C.L., Lew, C.H., Cornelissen, E.R., Ruiken, C.J. (2010). Preliminary study of osmotic membrane bioreactor: effects of draw solution on water flux and air scouring on fouling. Water Science and Technology, 62: 1353-1360

Qiu, C., Setiawan, L., Wang, R. , Tang, C.Y. , Fane, A.G.2012. High performance flat sheet forward osmosis membrane with an NF-like selective layer on a woven fabric embedded substrate. Desalination, 287:266–270

Qiu, G. L., Ting, Y.P. 2014. Direct phosphorus recovery from municipal wastewater via osmotic membrane bioreactor (OMBR) for wastewater treatment. Bioresource Technology, 170: 221-229

Qiu, G.L. Ting, Y.P. 2013. Osmotic membrane bioreactor for wastewater treatment and the effect of salt accumulation on system performance and microbial community dynamics. Bioresource Technology, 150: 287-297

Qtaishat, M., Mastuura, T., Kruczek, B., Khayet, M. 2008. Heat and mass transfer analysis in direct contact membrane distillation. Desalination, 219: 272-292

Qtaishat, M. R. & Banat, F. 2013. Desalination by solar powered membrane distillation systems. Desalination, 308: 186-197

Qu, D., Sun, D., Wang, H., Yun, Y.2013. Experimental study of ammonia removal from water by modified direct contact membrane distillation. Desalination, 326: 135-140.

Rashid, K. T. & Rahman, S. B. A. 2016. Ehancement of the Flux of PVDF-Co-HFP Hollow Fiber membranes for Direct Contact Membrane Distillation Applications. ARPN Journal of Engineering and Applied Sciences. 11:2189-2192

Rebello, S., Asok, A.K., Mundayoor, S., Jisha, M. S. 2014. Surfactants: toxicity, remediation and green surfactants. Environmental Chemistry Letters, 12: 275-287

Ren, J., McCutcheon, J, R. 2014. A new commercial thin film composite membrane for forward osmosis. Desalination, 343:187-193

Reyes, M., Borras, L., Seco, A., Ferrer, J. 2015. Identification and quantification of microbial populations in activated sludge and anaerobic digestion processes. Environmental Technology. 36(1): 45- 53.

Roach, J. D., Al-Abdulmalek, A., Al-Naama, A. and Haji, M. 2014. Use of micellar draws solutions as draw agents in forward osmosis. Journal of Surfactant and Detergents, 17:1241-1248

Saren, Q., Qiu, C.Q., Tang, C.Y.2011. Synthesis and characterization of novel forward osmosis membranes based on layer-by-layer assembly, Environmental Science and Technology, 45:5201-5208

Schofield, R.W.,Fane, A. G., Fell, C. J.D., Macoun, R. 1990. Factors affecting flux in membrane distillation. Desalination, 77: 279–294

Schofield, R.W., Fane, A.G., Fell, C.J.D.1987. Heat and mass transfer in membrane distillation. Journal of Membrane Science, 33 (3):299–313

Setiawan, L. , Wang, R. , Shi, L. , Li, K. ,Fane, A.G. 2010.Novel dual-layer hollow fiber membranes applied for forward osmosis process. Journal of Membrane Science, 421–422 :238-246

Setiawan, L. , Wang, R. ,Tan, S. , Shi, L. ,Fane, A.G. 2013.Fabrication of poly(amide-imide)-polyethersulfone dual layer hollow fiber membranes applied in forward osmosis by combined polyelectrolyte cross-linking and depositions. Desalination, 312: 99-106

Shen, M., Keten, S. & Lueptow, R.M. 2016. Dynamics of water and solute transport in polymeric reverse osmosis membranes via molecular dynamics simulations. Journal of Membrane Science, 506 :95-108.

Shi, L. ,Chou, S.R. ,Wang, R. ,Fang, W.X. , Tang, C.Y. ,Fane, A.G. 2011.Effect of substrate structure on the performance of thin-film composite forward osmosis hollow fiber membranes. Journal of Membrane Science, 382:116-123

Shirazi, M.M.A., Kargari, A., Shirazi, M.J.A.2012. Direct contact membrane distillation for seawater desalination. Desalination and Water Treatment, 49: 368-375.

Shirazi, M.M.A., Kargari, A., Shirazi, M.J.A.2012. Direct contact membrane distillation for seawater desalination. Desalination and Water Treatment, 49: 368-375.

Shirazi, S., Lin, C.-J., Chen, D.2010. Inorganic fouling of pressure-driven membrane processes -A critical review. Desalination, 250 (1): 236–248

Soroush, A. 2015. Development of Antimicrobial Thin Film Composite Forward Osmosis Membranes by Using Silver Nanoparticles and Graphene Oxide Nanosheets, Concordia University, Montreal, Canada.

Srisurichan, S., Jiraratananon, R., Fane, A.G.2006. Mass transfer mechanisms and transport resistances in direct contact membrane distillation process. Journal of Membrane Science, 277 (1–2): 186–194

Srisurichan,S. Jiraratananon, R. Fane, A.G.2005. Humic acid fouling in the membrane distillation. Desalination, 174 :63–72

Stillman, D., Krupp,L., La, Y.-H.2014. Mesh-reinforced thin film composite membranes for forward osmosis applications: the structure–performance relationship

Stone, M. L., Rae, C., Stewart, F. F., and Wilson, A. D. 2013a. Switchable polarity solvents as draw solutes for forward osmosis. Desalination, 312, 124-129.

Stone, M. L., Wilson, A. D., Harrup, M. K., Stewart, F. 2013. An initial study of hexavalent phosphazene salts as draw solutes in forward osmosis. Desalination, 312: 130-136

Su, J., Ong, R.C., Wang, P., Chung, T.S., Helmer, B.J., De Wit, J.S. 2013. Advanced FO membranes from newly synthesized CAP polymer for wastewater reclamation through an integrated FO–MD hybrid system. American Institute of Chemical Engineers, 59: 1245-1254

Su, J. C., Chung, T. S., Helmer, B. J.,de Wit, J. S.2012. Enhanced double-skinned FO membranes with inner dense layer for wastewater treatment and macromolecule recycle using sucrose as draw solute. Journal of Membrane Science, 396:92-100

Sukitpaneenit, P., Chung, T.-S. 2012.High performance thin-film composite forward osmosis hollow fiber membranes with macrovoid-free and highly porous structure for sustainable water production. Environmental Science and Technology, 46:7358-7365

Tan, C. H., and Ng, H. Y. 2010. A novel hybrid forward osmosis –nanofiltration (FO-NF) process for seawater desalination: Draw solution selection and system configuration.Desalination and Water Treatment, 13, 356–361.

Tchobanoglous, G., Burton, F. L., Stensel, H. D. 2014. Wastewater engineering: treatment and resource recovery, 5th edn. Metcalf and Eddy Inc., McGraw-Hill, New York

Tijing, L.D., Yun, C.W., Choi, J.S., Lee, S., Kim, S., Shon, H. K.2015. Fouling and its control in membrane distillation—a review. Journal of Membrane Science, 475:215–244.

Tiraferri, A. , Yip, N.Y. ,Phillip, W.A., Schiffman, J.D. , Elimelech. M. 2011.Relating performance of thin-film composite forward osmosis membranes to support layer formation and structure. Journal of Membrane Science, 367:340-352

Trung, N. Q., Nhan, L. V., Thao, P. T. P., Giang, T. 2017. Novel draw solutes of iron complexes easier recovery in FO process. Journal of water reuse and Desalination, In press

UN-Water, FAO, 2007. Coping with water scarcity. Challenge of the twenty-first century. UN-Water, FAO/Publication

Uragami, T. 2017. Science and Technology of Separation Membranes, 2 Volume Set. Japan: Wiley.

Us'yarov. O. G. 2004. Critical micellization concentration of ionic surfactants: Comparison of theoretical and experimental results. Colloid Journal, 66:612–616

Valente, A. J. M., Burrows, H.D., Polishchuk, A. Y., Domingues, C. P., Borges, O.M. F., Eusebio, M.E.S., Maria, T.M.R., Lobo, V.M.M. & Monkman, A.P. 2005. Permeation of sodium dodecyl sulfate through polyaniline-modified cellulose acetate membranes. Polymer, 46 (16): 5918-5928.

Vilakati, G.D., Wong, M.C.Y., Hoek, E.M.V., Mamba, B.B. 2014.Relating thin film composite membrane performance to support membrane morphology fabricated using lignin additive. Journal of Membrane Science, 469 :216-224

Wachinski, A.M. 2013. Membrane processes for water reuse. McGraw-Hill, New York

Wak, G., Jung, B., Han, S. & Hong, S. 2015. Evaluation of poly (aspartic acid sodium salt) as a draw solute for forward osmosis. Water Research, 80:294-305

Wallberg, O. Jonsson, A., Wickstrom, P. 2001. Membrane cleaning — a case study in a sulphite pulp mill bleach plant. Desalination, 141(3): 259-268

Wallace, M., Cui, Z., Hankins, N.P. 2008. A thermodynamic benchmark for assessing an emergency drinking water device based on forward osmosis. Desalination, 227: 34-45

Wang, K.Y., Chung, T.-S., Amy, G.2011. Developing thin-film-composite forward osmosis membranes on the PES/SPSf substrate through interfacial polymerization. American Institute of Chemical Engineers, 53(3):770-781

Wang, K.Y., Chung, T.-S., Qin, J.-J. 2007. Polybenzimidazole (PBI) nanofiltration hollow fiber membranes applied in forward osmosis process. Journal of Membrane Science, 300:6–12

Wang, K.Y., Chung, T.S., Ong. R. C. 2010. Double-Skinned Forward Osmosis Membranes for Reducing Internal Concentration Polarization within the Porous Sublayer. Industrial and Engineering Chemistry Research, 49:4824-4831

Wang, K. Y., Teoh, M. M., Nugroho, A., Chung, T. 2011. Integrated forward osmosis–membrane distillation (FO–MD) hybrid system for the concentration of protein solutions. Chemical Engineering Science, 66(11): 2421-2430

Wang, P., Cui, Y., Ge, Q., Tew, T. F., Chung, T. 2015. Evaluation of hydroacid complex in the forward osmosis–membrane distillation (FO–MD) system for desalination. Journal of Membrane Science. Journal of Membrane Science, 494: 1-7

Wang, X., Chang, V.W.C., Tang, C.Y. 2016. Osmotic membrane bioreactor (OMBR) technology for wastewater treatment and reclamation: Advances, challenges, and prospects for the future. Journal of Membrane Science, 504:113–132

Wang, X.H., Chen, Y., Yuan, B., Li, X.F., Ren, Y.P. 2014. Impacts of sludge retention time on sludge characteristics and membrane fouling in a submerged osmotic membrane bioreactor. Bioresource Technology, 161:340-347

Wang, X.H. Yuan, B. Chen, Y. Li, X.F., Ren, Y.P. 2014. Integration of micro-filtration into osmotic membrane bioreactors to prevent salinity build-up

Wang, Z., Zheng, J., Tang, J., Wang, X., Wu, Z. 2016. A pilot-scale forward osmosis membrane system for concentrating low-strength municipal wastewater: performance and implications. Scientific Reports 6, Article number: 21653

Widjojo, N. ,Chung, T.-S. , Weber, M. ,Maletzko, C. ,Warzelhan, V. 2013. A sulfonated polyphenylenesulfone (sPPSU) as the supporting substrate in thin film composite (TFC) membranes with enhanced performance for forward osmosis (FO). Chem. Engineering Journal, 220 :15-23

Wu, C.-Y.,Chen, S.-S., Zhang, D.-Z.,Kobayashi, J. 2017.Hg removal and the effects of coexisting metals in forward osmosis and membrane distillation. Water Science and Technology, DOI: 10.2166/wst.2017.143

WWAP (United Nations World Water Assessment Programme). 2012.Report on the development of water resources in the world 2012. Worldwide evaluation of water (WWAP) program, UNESCO

Xie, M., Nghiem, L.D., Price, W. E. and Elimelech, M. 2013. A forward osmosis-Membrane distillation hybrid process for direct sewer mining: system performance and limitation. Environmental Science and Technology, 47:13486-13493

Xie, M., Nghiem, L.D., Price, W. E. and Elimelech, M. 2013. A forward osmosis-Membrane distillation hybrid process for direct sewer mining: system performance and limitation. Environmental Science and Technology, 47:13486-13493

Xie, M., Nghiem, L.N., Price, W.E., Elimelech, M. 2014.Toward resource recovery from wastewater: extraction of phosphorus from digested sludge using a hybrid forward osmosis–membrane distillation process. Environmental Science and Technology Letters, 1:191-195

Xie, M., Price, W. E., Nghiem, L. D. & Elimelech, M. 2013. Effects of feed and draw solution temperature and transmembrane temperature difference on the rejection of trace organic contaminants by forward osmosis. Journal of Membrane Science, 438 57-64.

Xu, Y., Peng, X., Tamg, C. Y., Fu, Q. S. and Nie, S. 2010. Effect of draw solution concentration and operating conditions on forward osmosis and pressure retarded osmosis performance in a spiral wound module. Journal of Membrane Science, 348(1-2): 298-309

Yaeli, J. 1992. Method and apparatus for processing liquid solutions of suspensions particularly useful in the desalination of saline water, US patent, 5098575

Yang, H.-M., Seo, B.-K., Lee, K.-W., Moon, J.-K.2014. Hyperbranched polyglycerol-coated magnetic nanoparticles as draw solute in forward osmosis. Asian Journal of Chemistry, 26: 4031–4034

Yang, Q., Wang, K.Y., Chung, T. S. 2009. Dual-Layer Hollow Fibers with Enhanced Flux As Novel Forward Osmosis Membranes for Water Production. Environmental Science and Technology, 43:2800-2805

Yasukawa, M., Tanka, Y., Takahashi, T., Shibuya, M., Mishima, S., Matsuyama, H. (2015). Effect of Molecular Weight of Draw Solute on Water Permeation in Forward Osmosis Process. Industrial and Engineering chemistry research. 54, 8239−8246

Yen, S. K., Mehnas Haja, N. F., Su, M., Wang, K. Y. & Chung, T.-S.2010.Study of draw solutes using 2-methylimidazole-basedcompounds in forward osmosis. Journal of Membrane Science, 364, 242–252.

Yip, N. Y. & Elimelech, M. 2011. Performance Limiting Effects in Power Generation from Salinity Gradients by Pressure Retarded Osmosis. Enviroenmental Science and Technology, 45(23):10273-10282

Yong, J. S., Phillip, W. A., Elimelech, M. 2012. Coupled reverse draw solute permeation and water flux in forward osmosis with neutral draw solutes. Journal of Membrane Science, 392-393: 9-17

You, S., Tang,C., Yu, C., Wang, X., Zhang,J., Han,J. Gan, Y., Ren, N. 2013. Forward Osmosis with a Novel Thin-Film Inorganic Membrane. Environmental Science and Technology, 47 (15), 8733-8742.

Yu, C., Wang, Y., Lang, X., Fan, S. 2016. A Method for Seawater Desalination via Squeezing Ionic Hydrogels. Environmental Science and Technology, 50(23): 13024-13031

Yu, X., Yang, H., Lei, H., Shapiro, A.2013. Experimental evaluation on concentrating cooling tower blowdown water by direct contact membrane distillation. Desalination, 323:134-141.

Yun, Y., Wang, J., Ma, R. & Fane, A.G. 2011. Effects of channel spacers on direct contact membrane distillation. Desalination and Water Treatment, 34:63-69

Zauner, P. and Zha, F. 2011. Method of cleaning membranes. US 20110056522 A1.

Zeng, Y., Qiu, L., Wang, K., Yao, J., Li, D., Simon, G. P., Wang, R., Wang, H. 2013. Singificantly enhances water flux in forward osmosis desalination with polymer graphene composite hydrogels as draws agents. Royal Society of Chemistry, 3, 887-894

Zhang, J.S., Loong, W.L.C., Chou, S.R., Tang, C.Y., Wang, R., Fane, A.G. (2012). Membrane biofouling and scaling in forward osmosis membrane bioreactor

Zhang, X. Tian,J. Ren,Z.,Shi,W., Zhang,Z., Xu,Y., Gao,S., Cui, F. 2016. High performance thin-film composite (TFC) forward osmosis (FO) membrane fabricated on novel hydrophilic disulfonated poly(arylene ether sulfone) multiblock copolymer/polysulfone substrate. Journal of Membrane Science, 520:529–539

Zhao, D.L., Wang, P., Zhao, Q.P., Chen, N.P., Lu, X.M.2014. Thermoresponsive copolymer-based draw solution for seawater desalination in a combined process of forward osmosis and membrane distillation. Desalination, 348:26–32

Zhao, D.L., Wang, P., Zhao, Q.P., Chen, N.P., Lu, X.M.2014. Thermoresponsive copolymer-based draw solution for seawater desalination in a combined process of forward osmosis and membrane distillation. Desalination, 348:26–32

Zhao, P., Gao, B., Xu, S., Kong, J., Ma, D., Shon, H. K., Yue, Q. & Liu, P. 2015. Polyelectrolyte-promoted forward osmosis process for dye wastewater treatment – Exploring the feasibility of using polyacrylamide as draw solute. Chemical Engineering Journal, 264:32-38

Zhao, S., Zou, L., Mulcahy, D. 2012. Brackish water desalination by a hybrid forward osmosis–nanofiltration system using divalent draw solute. Desalination, 284: 175-181

Zhao, S. Hunag, K., Lin, H. 2015. Impregnated Membranes for Water Purification Using Forward Osmosis. Industrial and Engineering Chemistry Research, 54(49):12354-12366

Zhong, P., Fu, X., Chung, T. S. 2013. Development of Thin-Film Composite forward Osmosis Hollow Fiber Membranes Using Direct Sulfonated Polyphenylenesulfone (sPPSU) as Membrane Substrates. Environmental Science Technology, 47 (13):7430–7436

Zhou, A., Luo, H., Wang, Q., Chen, L., Zhang, T.C., Tao, T.2015. Magnetic thermoresponsive ionic nanogels as novel draw agents in forward osmosis. RSC Advances, 5:15359–15365

Zolotarev, P.P., Ugrozov, V. V., Volkina, I. B., Nikulin, V.M.1994.Treatment of waste water for removing heavy metals by membrane distillation. Journal of Hazardous Material, 37 (1):77–82